Dottorato di Ricerca Internazionale

"INSECT SCIENCE AND BIOTECHNOLOGY"

XXIV ciclo

Settore Disciplinare BIO 09

MECHANISMS INVOLVED IN THE ABSORPTION OF BIOINSECTICIDES AND STRATEGIES TO ENHANCE THEIR PASSAGE THROUGH THE INSECT MIDGUT

Tesi di dottorato di:
Ilaria CASTELLI

Coordinatore del dottorato:
Prof. Francesco PENNACCHIO
Università di Napoli "Federico II"

Docenti guida:
Prof.ssa Barbara GIORDANA
Dott.ssa Morena CASARTELLI
Università degli Studi di Milano

Dott.ssa Mylène OGLIASTRO
Université Montpellier 2

Anno Accademico 2010-2011

Introduction

1.1 The need of new strategies for pest control

Reducing crop losses due to pests is essential to increasing food security, poverty reduction and sustainable agricultural development (Van Huis and Meerman, 1997; Oerke *et al*., 1994). There are estimated to be around 67000 different crop pest species, including plant pathogens, weeds, invertebrates and some vertebrate species and together they cause about a 40% reduction in the world's crop yield.

Since the introduction of DDT in the 1940s, chemical pesticides continue to be the main form of pest control recommended by extension agents and used in much of the developing world (Casida and Quistad, 1998). Fast acting, cheap to produce, relatively easy to deliver and highly potent, chemical insecticides have been viewed with extreme optimism. Alongside advances in plant varieties, mechanization, irrigation and crop nutrition, they have helped increase crop yields by nearly 70% in Europe and 100% in the USA (Pretty, 2008). However, the use of synthetic pesticides is becoming significantly more difficult owing to a number of interacting factors. The injudicious use of broad spectrum pesticides can damage human health and the environment and can result in management failure through pest resurgence, secondary pest problems or the development of heritable resistance (Van Emden *et al*., 2004). Worldwide, over 500 species of arthropod pests have resistance to one or more insecticides (Hajek, 2004). Furthermore, pesticide products based on chemistry, such as DDT or other chlorinated insecticides, are being withdrawn because of new health and safety legislation. Therefore, it is essential to develop new strategies alternative to chemical pesticides and to help make crop protection more sustainable. Many experts promote Integrate Pest Management (IPM) as the best way and

the EU has placed it centrally within its 2009 Sustainable Use Directive on pesticides (European Parliament). According to the U.S. Environmental Protection Agency, the IPM is an effective and environmentally sensitive approach to pest management that relies on a combination of commonsense practices. IPM programs use current, comprehensive information on the life cycles of pests and their interaction with the environment. This information, in combination with available pest control methods, is used to manage pest damage by the most economical means, and with the least possible hazard to people, property, and the environment. An analysis of 62 IPM research and development projects in 26 countries, covering over 5 million farm households, showed that IPM leads to substantial reductions in pesticide applications (Pretty, 2008).

Biopesticides are a particular group of crop protection tools used in IPM. The term biopesticides describes a large number of control techniques, including the application of microbial organisms (e.g., a bacterium, fungus, virus or protozoan), or natural products derived from fungi, plants, insects, viruses and natural antagonists of insects. Marrone (2007) has estimated the biopesticides sector to have a 5 year compound annual growth rate of 16% (compared with 3% for synthetic pesticides), which is expected to produce a global market of $10 billion by 2017. Key factors in this growth include a larger overall investment in biopesticide research and development, a more established application of IPM concepts, and increased area under organic production. Nevertheless, biopesticides represented only about 2.5% of the overall pesticides market (Bailey, *et al*., 2010). In comparison to chemical counterparts, biopestides are often slow acting, and have narrow host specificity and poor longevity in the field. Some of these characteristics are positive as well as negative qualities. The rapid environmental degradation of biopesticides obliges to a more frequent application, but also reduces pest resistance development. The high specificity of biopesticides often requires application of several types of pesticides to control all major pest species involved in a particular agricultural setting, but also eliminates harm infliction to non target organisms (Whetstone and Hammock, 2007). Moreover, very often, these compounds have been prohibitively expensive for use in developing countries where sophisticated IPM systems are also difficult to implement. To increase utilization of bioinsecticides, it is necessary to improve the knowledge and the

technologies to overcome the limitations of their slow action and narrow host specificity, and to increase toxicity and rate of delivery.

In most cases, the biological alternatives to chemical pesticides are peptidic or proteinaceous in nature that have haemocoelic targets and therefore must pass undegraded the gut barrier in sufficient amount to exert their activity. Then, for an effective oral delivery of this class it will be crucial to characterize the molecular mechanisms mediating their absorption by the insect gut and to develop strategies to facilitate their passage through the midgut barrier. Molecules can reach the haemocoel either through the cellular pathway, crossing the two polarized plasma membranes of the epithelial cells, or through the paracellular pathway, along the aqueous channels formed by the lateral membranes of two adjacent cells and the junctional complexes, according to their physico-chemical and biological properties.

The research work performed during my PhD course fits in this scenario. I characterized the strategies adopted by *Junonia coenia* densovirus, a parvovirus lethal for the larval stages of several insect pest species, to cross the midgut barrier of the lepidopteran pest *Spodoptera frugiperda*. Moreover, I showed that a medium chain fatty acid, known to modulate the paracellular permeability in mammalian epithelia, is effective also on lepidopteran midgut and I started the characterization of the intracellular pathway activated by this molecule leading to the modulation of this permeation route. Finally, I investigated possible strategies to increase the protein permeation through the plasma membrane of lepidopteran midgut cells: the use of Cell Penetrating Peptides as a delivery system and the manipulation of the transcellular mechanism involved in the protein absorption (transcytosis) have been considered.

1.2 The midgut epithelium of lepidopteran larvae

In insect, like in mammals, the intestinal epithelium is one of the main interfaces between the body and the external environment. In lepidopteran larvae, it is an important site for both nutrient absorption and in ionic and water regulation (Dow, 1986).

The digestive system of an insect is usually a long straight tube running from the mouth to the anus, it is often divided into the foregut, the midgut and the hindgut. The primary function of the foregut is to begin the breakdown of food particles and transport them to the next region, the midgut. The midgut is the major area of digestion and absorption. Undigested food particles then pass into the third region, the hindgut that functions in water and solute reabsorption and waste elimination.

Midgut epithelium, formed by a folded epithelial cell monolayer, can be divided in three different regions: the anterior, the middle and the posterior. They have different morphology, degree of folding and color. The three regions have also different distribution of digestive enzyme (Terra and Ferreira, 1994) and transport proteins for the absorption of amino acids (Giordana *et al*., 1998; Casartelli *et al*., 2001). Midgut epithelium rests on a basement lamina with which are associated tracheae, tracheoles, an inner layer of circular muscles and an outer layer of longitudinal muscles (Anderson *et al*., 1966).

Midgut is composed by three main cell types: goblet, columnar, stem cells (Cioffi, 1979; Baldwin and Hakim, 1991), and by some endocrine cells. Goblet cells (figure 1.1) are typical of lepidopteran larvae and have a peculiar shape, with a basally located nucleus and a cavity lined by an apical plasma membrane forming numerous microvilli. A vacuolar-type proton ATPase coupled to a $K^+/2H^+$ antiporter is expressed in the apical membranes lining goblet cells large cavity (Wieczorek *et al*., 1989). The electrogenic activity of the V-ATPase generates a large transapical electrical potential difference, cell interior negative, with values ranging between 140 and 240 mV (Dow and Peacock, 1989; Moffett and Koch, 1992). The cooperative activity of the V-ATPase and of the $K^+/2H^+$ antiporter is responsible for the passive re-entry of the protons into the goblet cell cytoplasm following the large electrochemical gradient, and for the active secretion of K^+ into the midgut lumen. The V-ATPase is also responsible for the high alkaline pH present in the midgut lumen. (Dow, 1992). Columnar cells (figure 1.1) have an almost cylindrical shape with a central nucleus, an apical thick brush border and deep infoldings of the basal plasma membrane (Cioffi, 1979; Baldwin and Hakim, 1991). This cell type is involved in nutrient digestion (Terra and Ferreira, 1994) and absorption, columnar cells perform a remarkable net absorption of amino acids by K^+-dependent transport systems located in their apical membrane

(Giordana *et al*., 1982, 1998; Leonardi *et al*., 1998; Casartelli *et al*., 2001). Columnar cells are the most numerous in 5:1 ratio with the goblet cells (Baldwin and Hakim, 1991).

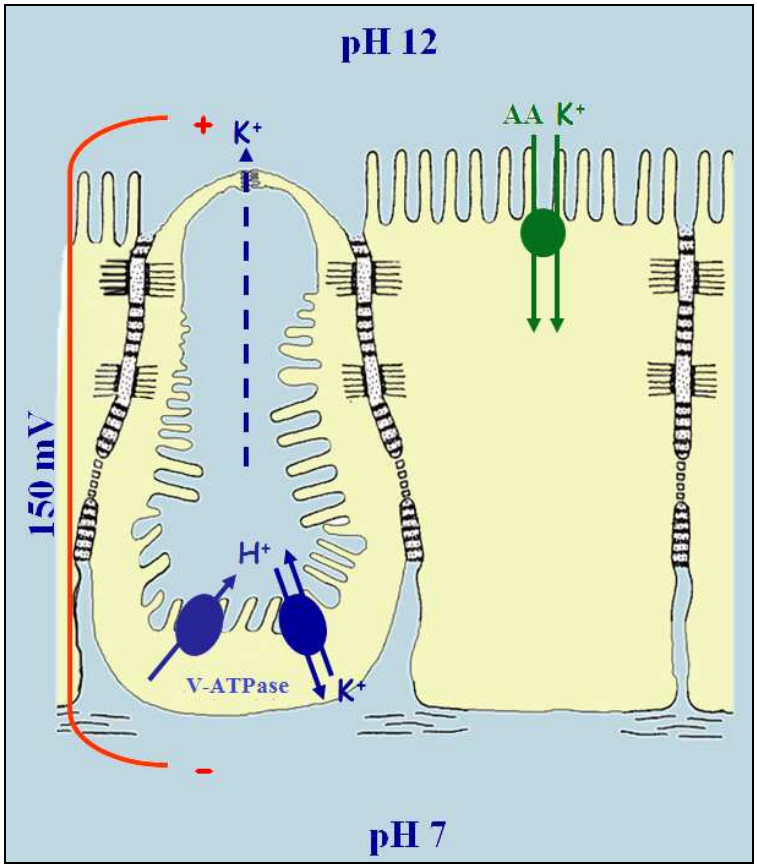

Figure 1.1: schematic representation of goblet and columnar cells. V-H^+-ATPase, $K^+/2H^+$ antiporter, K^+-dependent symporter for amino acid are indicated.

The small stem cells, roughly conical or spindle shaped with a large nucleus, are located at the base of the epithelium (Turbeck, 1974; Baldwin and Hakim, 1991): they are the only cell type that undergoes mitosis (Loeb and Hakim, 1996). In lepidopteran larval midgut stem cells repair the damaged midgut by replacement (Loeb *et al.,* 2001), maintaining the tissue functional integrity (Spies *et al*., 1985). In addition, it has been demonstrated that these cells, normally present as single cells during the larval feeding periods, proliferate extensively before each moult, forming large nests, or "nidi", and then intercalate between

the mature cells of the intestinal monolayer, differentiating, following appropriate stimuli, into mature columnar and goblet cells during the moult (Wigglesworth, 1972).

In insect midgut epithelium, like in vertebrates, the cells are connected together by junctional structures. These structure can be classified in terms of functional in:

- occluding junction: seal cells together in an epithelium in a way that prevents even small molecules from leaking from one side of the sheet to the other. They are known as tight junctions (TJ) in vertebrates and septate junctions (SJ) in invertebrates;
- anchoring junction: mechanically attach cells (and their cytoskeletons) to their neighbors or to the extracellular matrix (adherent junctions, desmosomes, hemidesmosomes and focal adhesions).
- communicating junctions: mediate the passage of chemical or electrical signals from one interacting cell to its partner.

In vertebrate epithelia, the closure of the intercellular space is achieved by the tight junction (figure 1.2.A), which acts as a permeability barrier for the paracellular pathway. In insect the septate junction is able to fulfill a similar function (Noirot and Noirot-Timothèe, 1998).

In insects, two types of septate junctions have been identified: the pleated type junctions (PSJ) (figure 1.2.B) and the smooth type (SSJ) (figure 1.2.C) (Flower and Filshie, 1975; Noirot and Noirot-Timothèe, 1998). In both types of junctions, intercellular space is divided by regular septa of about 15 nm. The PSJ are mainly associated with epithelia of ectodermal origin as epidermis and trachea, while SSJ are associated with epithelia of endodermal origin, such as gut epithelium and Malpighian tubules. In both cases the junction is extensive, encircling the whole cell.

In vertebrate epithelia the adherent junctions (zonula adherens) forms a girdle around the cell just basal to the tight junction. In contrast, this junction is, in insects, always placed at the most apical party of the junctional complex. The adherent junction is a characteristic feature of most insect epithelia, more precisely those in which a PSJ is also present. When the septate junction is of the smooth type, the adherent junction is replaced by several punctae adherentes.

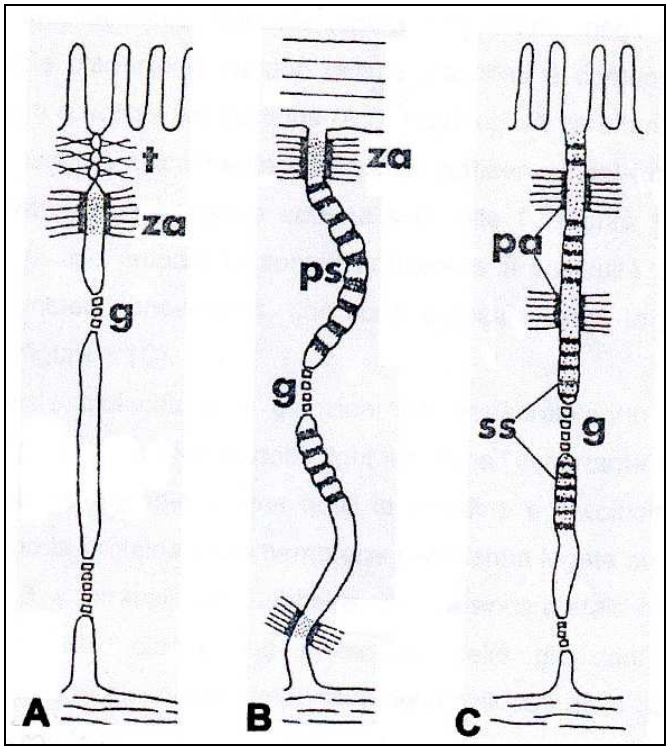

Figure 1.2: junctional complexes in monolayered epithelia. **A**: vertebrates tight junction (t); **B**: insects pleated septate junction (ps); **C**: insect smooth septate junction (ss). za, zonula adherens; g, gap junction; pa, punctae adherentes. (Noirot and Noirot-Timothèe, 1998, modified).

Although no systematic attempt has yet been made to characterize the molecular components of the SJ, molecular genetic analysis of several developmentally interesting genes has led to the discovery of SJ components homologous to those present in the tight junction of vertebrates, some of which play a key role in determining the structural and functional properties of SJ (Tepass *et al*., 2001; Behr *et al*., 2003).

SJ-associated proteins Coracle, Neurexin IV and Nervana 2 form a single, highly interdependent core complex that plays a role in formation of the morphological SJ and in maintaining epithelial polarity (Oshima and Fehon, 2011). Discs large protein (Dlg) is the prototypic member of a growing family of proteins collectively termed membrane associated guanylate kinase homologs (MAGUKs). They are localized on the cytoplasmic face of the septate junction and are required for septate junction structure, cell polarity, and proliferation control in *Drosophila* epithelia (Woods *et al*., 1996). In Drosophila, *pyd*

gene encodes a protein that is similar to the mammalian ZO-1 protein, the first identified tight junction component. Although PYD/ZO-1 was originally described as a SJ component, subsequent studies indicate that one isoform is localized apical to the SJ, while another seems more broadly distributed in the apical region of the cell. The Baz/Par-3 complex have mammalian homologues that reside in the tight junction and is essential for tight junction assembly (Tepass *et al*., 2001). Analysis of vertebrate tight junctions has identified two other types of proteins that seem to be integral to the tight junction, the occludins and the claudins. The *Drosophila* genome does not contain any convincing occludin homologues. In contrast, there are at least two possible claudin-like genes in the genomic sequence, the Megatrachea (Mega) (Behr *et al*., 2003) and the Sinuous (Sinu) (Wu *et al*., 2004). Both these proteins have a transepithelial barrier function.

In vertebrates, the intestinal tract is characterized by a luminal surface border of microvilli, which serve to increase the surface area of the absorptive membrane of the gut. The structure of these microvilli is maintained by a core of actin filaments which are held in place by various ancillary proteins (Bement and Mooseker, 1996) attached to the plasma membrane and which are tethered at their base by insertion into a ‘‘terminal web’’ of cytoskeletal fibers that lies parallel to the luminal surface. The acto-myosin perijunctional ring inserts into the lateral borders of the cell’s plasma membrane via a series of special proteins which terminate in either adherent junctions or occluding junctions.

Lane and Flores (1988) demonstrated, in insect, that elements of the cytoskeletal system insert into the cytoplasmic face of septate junctions and in particular actin-like filaments, are associated with the membranes where septate junctions are located. It has also been suggested that the actin filaments, abundantly present in microvilli and in the portion of the cytoplasm immediately below, from here descend deep into the cell running parallel to each other. The filaments tend to lean towards the lateral membrane, making contact with it at the level of aligned intramembranous particles (IMPs) that serve as serial anchorage points for the septa in the opposing plasma membranes (Kukulies e Komnick, 1983). The use of an actin depolymerizer, cytochalasin D, leads to disorganization of the intramembrane components of septate junctions. These data suggest that a primary role

of septate junctions could be to maintain intercellular cohesion and hence tissue integrity (Lane and Flores, 1988).

The presence of myosin associated with actin in the cytoskeleton is still not entirely clear: a myosin-like protein was identified in *Manduca sexta* (Bonfanti *et al*., 1992), but nothing is yet known about how this protein interacts with actin.

1.3 Mechanism of proteins absorption and strategies to enhance their passage through the transcellular route

The insect gut carries out some of the most vital functions as nutrition and solute and water balance of the organism. As a result of this function, the absorptive epithelial cells have evolved two specialized plasma membrane domains with distinct proteins and lipids composition (Simons and Fuller, 1985). The specificity of these two domains is maintained by the junctions, which are also a fence between neighboring cells. Ions and solutes can cross this selective barrier following the transcellular or the paracellular pathways (figure 1.3).

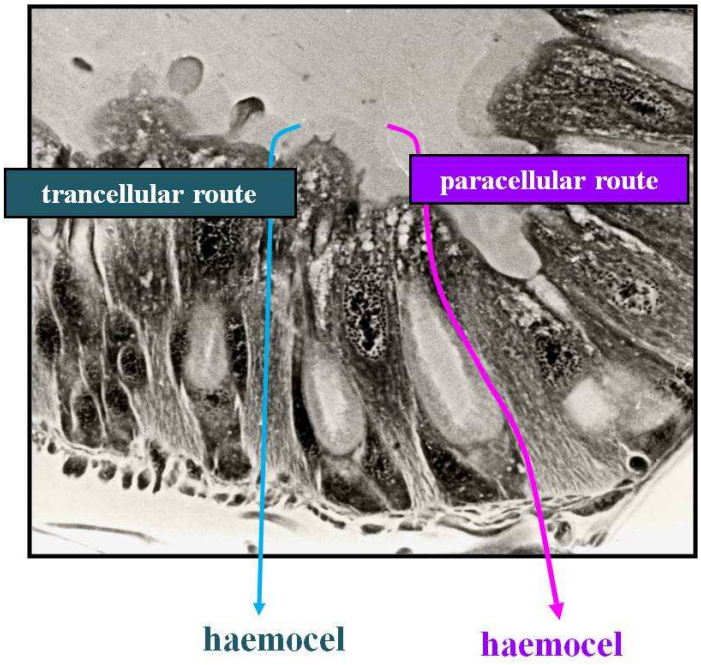

Figure 1.3: schematic representation of the transcellular (blue arrow) and the paracellular (pink arrow) pathways in the midgut of lepidopteran larvae.

The passage through the paracellular route, that is the watery channel interposed between two adjacent cells, is finely regulated by the junctions and depends on their permeability (paragraph 1.4). The passage through the transcellular pathway implies the crossing of the apical and basolateral membranes. The transcellular movement of ions and small molecules through a cell, is accomplished by the differential distribution of membrane transporters/carriers on opposite sides of a cell. In mammalian epithelia it has been demonstrated that proteins can be transported through the transcellular pathway. The mechanism involved is transcytosis, a complex sequence of intracellular events that exploits the membrane traffic involved in endocytosis and extocytosis at the apical and basal poles of the cell (Tuma and Hubbard, 2003).

Transcytosis has been extensively studied in mammals (reviewed by Apodaca, 2001; Tuma and Hubbard, 2003). Following the first suggestions by Palade (1953) on the possible occurrence of transcytosis, several subsequent studies have addressed the functional bases of this transport process. Now, it is known that transcytosis is an active process, regulated by specific internal signals that guide the internalization and transport of the macromolecules within the cytoplasm, from one pole of the cell plasma membrane to the other one. In detail the process implies:

- internalization of the macromolecules by a specific endocytic mechanism at one pole of the cell plasma membrane;
- the vesicles containing the protein are transported in the cell cytoplasm and, following a complex sequence of intracellular events, fuse with specific cell compartments;
- the protein is released by exocytosis in the extracellular milieu of the opposite plasma membrane domain.

1.3.1 Protein endocytosis and intracellular trafficking of endocytic vesicles

The plasma membrane is a dynamic structure that regulates the entry and the exit of all solutes. In endocytosis, the material to be internalized is surrounded by an area of plasma membrane, which then buds off inside the cell to form a vesicle containing the ingested material. The endocytic processes are classified in two different categories, phagocytosis and pinocytosis, depending on the size of the endocytic vesicles, the nature of the cargo and the mechanism of vesicle formation (figure 1.4).

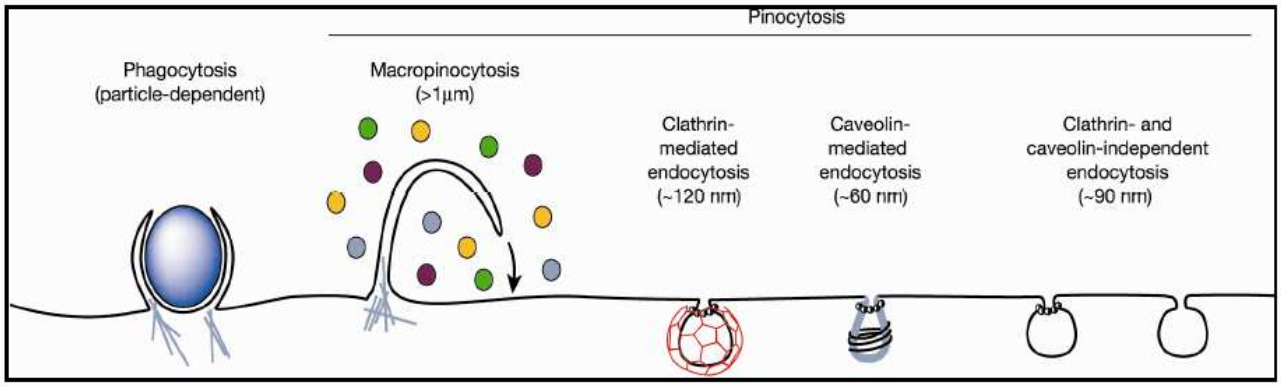

Figure 1.4: multiple portals of entry into the mammalian cell. The endocytic pathways differ with regard to the size of the endocytic vesicle, the nature of the cargo (ligands, receptors and lipids) and the mechanism of vesicle formation. (Conner and Schmid, 2003)

Phagocytosis is the uptake of large particles and pinocytosis is the uptake of fluid and solutes (Conner and Schmid, 2003). Phagocytosis is an active and highly regulated process involving specific receptors and signaling cascades mediated by Rho-family GTPases. Phagocytosis is involved in the acquisition of nutrients for some cells, and, in the immune system, it is the major mechanism used to remove pathogens and cell debris. Bacteria, dead tissue cells, and small mineral particles are all examples of objects that may be phagocytosed. When phagocytosis occurs, the cell creates membrane protrusions that surround the particle to be internalized, and then fuse forming vesicles that are released into the cytoplasm.

Pinocytosis is a process well studied in mammals that includes the internalization of solutes by a non-specific binding to the cell membrane (fluid-phase) or by specific high-affinity receptors concentrated into specialised membrane invaginations. Pinocytosis is divided in four different classes: macropinocytosis, clathrin-mediated endocytosis, caveolae mediated endocytosis and clathrin- and caveolae-independent endocytosis (Conner and Schmid, 2003).

Macropinocytosis is a form of endocytosis that accompanies cell surface ruffling. Because macropinosomes are relatively large (diameter > 1 μm), they provide an efficient route for non-selective endocytosis of solute macromolecules. This route is activated by the signalling cascades mediated by Rho-family GTPases. Because the ruffling that leads to macropinocytosis is regulated, it has been exploited by some pathogenic bacteria as a novel route for entry into cells (Swanson and Watts, 1995). This is also an endocytic mechanism used by HIV-1 virus to infect macrophages (Marechal *et al*., 2001).

Clathrin-mediated endocytosis (CME) (McMahon and Boucrot, 2011) is the most characterized endocytic process and involves the concentration of high-affinity transmembrane receptors and their bound ligands into “coated pits” on the plasma membrane. Clathrin-mediated endocytosis is driven by a cycle of assembly and disassembly of clathrin-coated vesicles (CCVs): the clathrin coat is assembled on the cytoplasmic face of the plasma membrane, where generates pits that invaginate and pinch off, becoming CCVs (Marsh and McMahon, 1999). The formation of CCV is then a multi-step process that requires the sequential function of more than fifty different proteins. The major protein classes that mediate the formation of a CCV are: the adaptors that select the transmembrane cargo proteins and link the cargo to the polymerization of the clathrin coat, the scission factors such as the GTPase dynamin and its binding partners that couple to force generating events such as actin polymerization, and auxilin and Hsc70 that facilitate the uncoating of the endocytic vesicle. Central to the formation of CCVs is clathrin itself. Clathrin is composed by a 180 kDa protein called clathrin heavy chain (CHC), which is associated to a 25 kDa protein called clathrin light chain (CLC). The assembly unit of the clathrin coat is the triskelion, composed of three copies of the clathrin-heavy chain (CHC) linked at their C-termini through a trimerization domain. When triskelia assemble into a

clathrin coat, the legs interdigitate to form a lattice of open hexagonal and pentagonal faces with a trimerization domain at each vertex and numerous weak contacts between leg segments stabilizing the lattice (Wakeham *et al*., 2003). Destabilization of the lattice needed for coat disassembly following release of CCVs from the membrane is likely to be strongly influenced by disruption of this interaction (Fotin *et al*., 2004). Triskelia do not bind directly to membranes and thus other factors are needed to recruit clathrin and to stabilize its interaction with the membrane. These factors are collectively known as adaptors, and many proteins that fulfill this role have been identified (Traub *et al*., 2003). In the case of CME, one key adaptor is adaptor protein 2 (AP-2), a multi-subunit complex composed of two large subunits, α- and β2-adaptin and two smaller subunits, μ2-and σ2-adaptin (Ritter *et al*., 2004). A fundamental protein for most of the endocytic processes, CME included, is dynamin, an atypically large GTPase, which is thought to self assemble creating a spiral around the "necks" of the budding coated pits (Conner and Schmid, 2003). Although there are many studies on this protein in different animal models, its exact function is still controversial (Mettlen *et al*., 2009). One hypothesis suggests that dynamin, triggered by GTP binding, assembles at the necks of invaginated coated pits causing constriction. It was proposed that subsequent assembly-stimulated GTP hydrolysis causes a concerted conformational change to generate force required for membrane fission (Hinshaw *et al*., 1995; Warnock *et al*., 1996). The second is that it functions, like other GTPase, as a regulatory molecule in the formation of endocytic vesicles (Sever *et al*., 1999). Caveolae have been recognized as abundant and morphologically characteristic structures at the surface of many mammalian cell types. The shape and structural organisation of caveolae are conferred by caveolin, a 22 kDa dimeric protein that binds colesterol, inserts as a loop into the inner leaflet of the plasma membrane and self-associates to form a striated caveolin coat on the surface of the membrane invaginations (Lajoie and Nabi, 2010; Sandvig *et al*., 2011). The mammalian caveolin gene family consists of caveolin-1, -2, and -3. Caveolin-1 is present in two alternatively spliced isoforms (α and β). Caveolin-2 is often coexpressed and associated with caveolin-1 in the same type of cell/tissue, with particularly high levels in adipocytes (Scherer *et al*., 1996; 1997), and caveolin-3 is expressed predominantly in skeletal and cardiac muscles (Way and Parton, 1995).

The term lipid rafts refers to putative membrane microdomains with a different composition respect to surrounding regions of the membrane. They are involved in clathrin- and caveolae-independent endocytosis (Lajoie and Nabi, 2010). It is thought that lipid rafts are enriched in cholesterol, glycosphingolipids, sphingomyelin, phospholipids with long, unsaturated acyl chains, glycosylphosphatidylinositol (GPI)-linked proteins and at least some membrane-spanning proteins (Simons and van Meer, 1988; Simons and Ikonen, 1997; Brown, 1998; Simons and Toomre, 2000). A functional role for rafts has been invoked in a diverse array of cellular processes, the common theme being that rafts could provide sites of local enrichment of molecules that need to interact with each other or to be transported to the same place in the cell (Simons and Ikonen, 1997).

Once internalised, the macromolecule inside the endocytic vesicle can follow different fates (figure 1.5): it can be delivered at the opposite plasma membrane domain (transcytosis), recycled to the same plasma membrane where the endocytosis had occurred or it can be delivered to lysosomes for intracellular degradation (Apodaca, 2001).

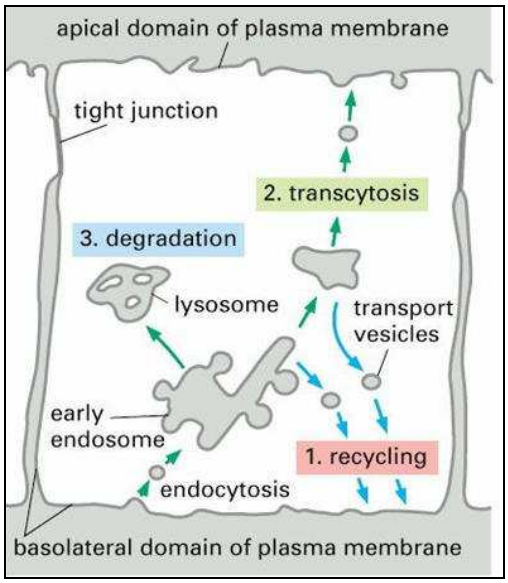

Figure 1.5: schematic representation of the intracellular pathways followed by endocytic vesicles formed at the basolateral side of the epithelial cell (http://molbiol4masters.org/Co_and_Post_Translational_Events5-ellular_Protein_ Traffic.htm)

Their intracellular pathways are independent of the endocytic mechanism by which they were endocytosed. Protein internalisation by polarised epithelial cells can occur at either the apical or the basolateral membranes and the intracellular pathways involved can be different at one membrane domain or at the other (Apodaca, 2001; Mostov *et al*., 2000).

Proteins endocytosed from the apical or basolateral membrane first reach the apical (AEE) or basolateral early endosomes (BEE), respectively. Most of the apically internalised vesicles are delivered to the apical recycling endosomes (ARE) for the recycling to the apical membrane or are transcytosed through the basolateral membrane; only a small amount is delivered to late endosomes (LE) and then degraded in lysosomes. Apical recycling proteins are delivered from the AEE to the ARE or to the common endosome (CE) before their ultimate release from the apical pole of the cell. Vesicles internalised at the basolateral membrane are primarily delivered to late endosomes and lysosomes or can be destined to the CE. From CE, molecules can be recycled to the basolateral membrane or sent to the ARE and then exocytosed at the apical plasma membrane domain (Apodaca, 2001).

The molecular mechanisms by which this traffic is regulated to ensure both the fidelity and efficiency of transport is a significant focus of research (Hutagalung and Novick, 2011). Cellular organelles in the exocytic and endocytic pathways have a distinctive spatial distribution and communicate through an elaborate system of vesiculo-tubular transport. Rab proteins and their effectors coordinate consecutive stages of transport, such as vesicle formation, vesicle and organelle motility, and tethering of vesicles to their target compartment (Zerial and McBride, 2001). Rabs constitute the largest family of small Ras-like GTPases with 11 identified in yeast and more than 60 members in humans that can be classified in several phylogenetic and functional groups (Pereira-Leal and Seabra, 2001; Seabra *et al*., 2002). There are numerous Rabs associated with endosomal traffic, and the most active site of localization is the early endosome. Most early endocytic steps rely on Rab5, which mediates fusion of endocytic vesicles to form the early endosome. Traffic can be directed towards the lysosome for degradation, which relies on action of Rab7, or to various recycling compartments to return factors to the plasma membrane. Rab15 directs

membrane traffic from the early endosome to the recycling endosome. Rab4 and Rab11 regulate fast and slow endocytic recycling, respectively (Hutagalung and Novick, 2011).
Another important player in endocytic trafficking is the cytoskeleton, the cytoskeletal elements involved are microtubules and actin filaments. Actin plays a role in internalization at both cell surfaces. Microtubules and actin are required for efficient transcytosis and delivery of proteins to late endosomes and lysosomes. Microtubules are also important in apical recycling pathways and, in some polarized cell types, basolateral recycling requires actin (Apodaca, 2001).

1.3.2 The movement of proteins across the insect midgut epithelium

The movement of intact proteins across the digestive system of insects was shown in a number of different orders (reviewed by Jeffers and Roe, 2008). Protein movement was observed for both normal dietary and xenobiotic proteins, which suggest that the mechanism for transfer is not substrate specific. One of the first study in this field, published by Wigglesworth in 1943, demonstrated that a small amount of ingested haemoglobin was internalised by the gut of *Rhodnius prolixus* and released into the haemolymph. From this first work, several studies performed *in vivo* demonstrated that proteins are able to cross undegraded the gut barrier, but only recently the mechanism involved in this process has been described. Functional experiments were performed in my laboratory under *in vitro* controlled experimental conditions, to detect the mechanism of albumin and horseradish peroxidase transport across the intestinal barrier of *Bombyx mori* larvae. Casartelli *et al*. (2005) demonstrated that in the midgut isolated and perfused *in vitro*, albumin can be transported from the lumen to the haemolymph through the transcellular pathway by transcytosis. The occurrence of this absorption pathway is corroborated by several evidences. First, fluorescein isothiocyanate (FITC)-albumin was localized inside the midgut columnar cells and was not detected in the paracellular space. The flux of the protein is a saturable process, and incubation of the midgut at 4 °C caused a

drastic inhibition of the flux, a clear indication that an energy-dependent process was involved in the protein transport. In a following study (Casartelli *et al*., 2007), the mechanism of horseradish peroxidase (HRP) transport through the isolated midgut was identified. The results confirmed that the key mechanism for proteins absorption in lepidopteran midgut was transcytosis. More recently, the mechanism involved in albumin internalization in columnar cells was characterized. It was demonstrated that the uptake was clathrin-dependent and mediated by a megalin-like multiligand receptor homologous to that present in many absorptive epithelia of mammals (Casartelli *et al*., 2008). The insect megalin-like receptor, which considerably increases the transepithelial transport of the bound protein, recognizes also insulin, transferring, and the polybasic drug gentamicin (Casartelli, unpublished data). Therefore, it might act as a scavenger receptor, like its mammalian homolog (Christensen and Birn, 2002).

This novel information sheds light on the functional mechanisms of protein absorption in the insect midgut and provides new opportunities for developing new molecular strategies to increase the permeation through the midgut epithelium of orally delivered proteins.

1.3.3 Strategies to enhance the passage of protein through the transcellular route

Most of bioinsecticides have haemocoelic targets and must pass undegraded the gut barrier and in sufficient amount to exert their activity. One of the major problems to face when using orally administered bioinsecticidal proteins with a cytosolic or haemocoelic target is their delivery across the cell membrane of the gut epithelium and their translocation across the cell layer lining the digestive system.

A recent approach to increase proteins and peptides passage through the insect gut has been the use of *Galantus nivalis* agglutinin (GNA), a mannose-specific lectin. GNA is one of the most closely studied plant lectins, mainly because it was the first plant lectin shown to be toxic against Hemiptera and the protein is easy to purify (Shi *et al*., 1994; Hilder *et al*., 1995). The group of prof. Gatehouse demonstrated that GNA can be also utilized as a

delivery system to transport a linked peptide to the haemolymph of lepidopteran larvae. They first demonstrated that a fusion protein GNA-allatostatin was able to reach undegraded the haemolymph of the tomato moth, *Lacanobia oleracea*, at variance to allatostatin alone (Fitches *et al*., 2002). An analogous result was obtained with a fusion protein between GNA and an insecticidal spider venom toxin (Segestria florentina toxin 1, SFI1). When this fusion protein was fed to larvae of *Lacanobia oleracea*, 100% mortality was observed 6 days after the administration. The mortality was drastically reduced when larvae were fed with GNA or SFI1 separately (Fitches *et al*., 2004). In 2006, it was produced a fusion protein with GNA and a lepidopteran specific toxin (ButalT) from the red scorpion (*Mesobuthus tamulus*). By western blotting, the intact fusion protein was detected in the haemolymph of tomato moth larvae (*Lacanobia oleracea*) after feeding. Interestingly, it has been claimed that the scorpion toxin, ButalT, is lepidopteran-specific, but the fusion protein may have a wider range of toxicity. In fact, when the fusion protein was fed to *Nilaparvata lugens* (Homoptera), larval mortality was significantly higher than with GNA alone (Trung *et al*., 2006). Recently, feeding bioassays demonstrated the potential use of the ButaIT/GNA fusion protein as an orally active insecticide against lepidopteran, dipteran and coleopteran pests (Fitches *et al*., 2010).

PEGylation is an alternative effective method to improve the delivery and stability of therapeutic molecules in the human internal environment and, more recently, through the intestinal barrier (Youn *et al*., 2006). This technology involves the covalent binding of poly-
98 ethylene glycol (PEG) to active macromolecules, like normally a drugs or therapeutic proteins, to improve their water solubility and resistence to hydrolisis, and to reduce renal excretion and antigenicity (Bailon and Won, 2009; Kang *et al*., 2009; Ryan *et al*., 2008). It produces alterations in the physiochemical properties including changes in conformation, electrostatic binding, hydrophobicity etc. Jeffers and Roe (2008) reported that a similar approach enhanced the passage of human insulin across the insect gut, and induced its accumulation into the haemolymph, as well as of bioinsecticide molecules. PEGylated insect hormone trypsin modulating oostatic factor (TMOF) fed to *Heliothis virescens* larvae accumulated in the insect haemolymph, and caused a tenfold increase of TMOF toxicity to mosquito larvae (Jeffers and Roe, 2008). This is a promising methodology that needs to be

further refined before it can be profitably used as a strategy to enhance uptake and permeation of biopesticides by insect gut.

Another strategy to enhance the permeation of bioactive macromolecules through the insect gut is the use of analogs resistant to peptidase attack. Nachman *et al*. (2002) observed a higher delivery rate through the insect gut and an unaltered biological activity of peptidase-resistant neuropeptides analogs, compared to their natural counterparts. The authors suggest that the chemical modification of the native neuropeptides performed to confer peptidase resistance increased the survival time in the digestive tract and, therefore, their penetration across the gut wall.

While a variety of transporters currently exist for membrane impermeable cargo translocation, cell penetrating peptides (CPPs) have become one of the most popular and efficient techniques for achieving intracellular access. Extensive studies performed in mammalian cells identified a number of peptides that posses the intriguing ability to cross the cell membrane entering in the cell. These peptides can act as delivery vectors because they can translocate a variety of cargo molecules attached to them. A wide range of biomolecules such as antigenic peptides, antisense oligonucleotides, full-length proteins, nanoparticles or liposomes have been delivered by this way (Richard *et al*., 2003). In addition, this highly efficient translocation capacity has been observed in a variety of cell lines with minimal toxicity, overcoming challenges often faced with other delivery methods (Nagahara *et al*., 1998).

CPPs are also called protein transduction domains (PTDs) or membrane transduction peptides (MTPs). Generally, CPPs are cationic or amphipathic peptides which consist of up to 30 amino acid residues. Cationic CPPs are characterized by the presence in their sequence of clusters of arginine and lysine residues (Patel *et al*., 2007). Amphipathic CPPs, unlike the cationic ones, are characterized by a highly hydrophobic C-terminus and a mainly hydrophilic N-terminus containing lysine and/or arginine residues. These peptides adopt a α-helix conformation in aqueous solution at pH 7 (Fernàndez-Carneado *et al.,* 2004). The presence of the guanidine group in cationic CPPs is thought to mediate their internalization into the cell through the formation of bidentate hydrogen bonds with the anionic groups on the membrane (Patel *et al*., 2007). On the contrary, it seems to be

necessary for amphipathic CPPs internalization the presence of the hydrophilic and hydrophobic regions inside the α-helical structure of the peptides (Patel *et al*., 2007).

Within the last two decades the number of peptides included in the CPPs family has considerably increased (Fonseca *et al*., 2009). Some of them, named protein derived CPPs, are the minimal effective amino acid sequence of the parent translocation protein, like the Tat peptide, derived from the HIV-1 Tat protein, and Penetratin peptide derived from the Antennapedia homeodomain. Alternatively peptide may be *de novo* designed, like the oligoarginine peptide, based on structure activity relationship of the known CPPs (Hansen *et al*., 2008).

Among the cell penetrating peptides, the arginine-rich cell penetrating peptides have been the most widely studied (El-Sayed *et al*., 2009). The Tat protein is an 86 amino acid long protein that is released by HIV infected cells and is an essential regulatory gene for HIV replication (Jeang *et al*., 1999). In 1997, Vives *et al*. found that a 11-amino acid sequence, Tat (47–57), now known as Tat peptide or Tat PTD, can not only enter cells but can efficiently translocate linked macromolecules like proteins (Fawell *et al*., 1994), nucleic acids (Chiu *et al*., 2004) or small therapeutic molecules (Musacchio *et al*., 2011).

The mechanism of CPPs entry into the cell is still controversial. In some instances, transmembrane translocation appears to be mediated by endocytosis, but translocation of a wide range of CPPs has been observed also when endocytosis was inhibited (Futaki *et al*., 2007; Patel *et al*., 2007; Zorko and Langel, 2005; Schmidt *et al*., 2010).

Although it remains difficult to establish a general scheme for CPP uptake mechanism, there is a consensus that the first contacts between the CPPs and the cell surface take place through electrostatic interactions with proteoglycans, in particular it has been demonstrated that heparin sulphates are involved in this interaction. Duchardt *et al*. (2009) showed that heparinase treatment of human cervical carcinoma cell line HeLa reduced membrane binding and uptake of the peptide Tat, demonstrating the relevance of heparan sulfate binding for the function of the Tat peptide as a CPP.

Moreover, the cellular uptake pathway is driven by several parameters including the nature and secondary structure of the CPP; its ability to interact with cell surface and

membrane lipid components; the nature and type of the cargo; and the cell system under investigation and its membrane composition.

The mechanism of internalization should also govern the intracellular processing and final fate of the CPP and of its cargo. If the CPP is transduced directly into the cytoplasm, it could interact with its cytoplasmic target, be imported to the nucleus, be degraded by cytoplasmic proteases or be redirected out of the cell either intact or after degradation. On the other hand, if it is internalized by endocytosis, it could be targeted for lysosomal degradation, may be able to escape lysosomal degradation and enter the cytoplasm and possibly the nucleus, or be taken to the Golgi apparatus or the endoplasmic reticulum, or transcytosed out of the cell. As for internalization, the intracellular pathway followed will be highly governed by several factors including the type of CPP, the type of cargo attached, the nature of linkage between the cargo and the CPP, and the cell system under investigation (Patel *et al*.,2007).

1.4 Permeability of the paracellular pathway and its modulation

The paracellular route across the intestinal tight junction (TJ) is a crucial path for drug delivery in mammals (Salama *et al*., 2006; Deli, 2009) because it lacks proteolytic enzymes and its permeability can be modulated by various enhancers, allowing the passage of large peptides (Cano-Cebrian *et al*., 2005; Deli, 2009). While the permeability of the tight junctions of vertebrates has been extensively characterized, few studies have been performed to clarify the functional properties of the septate junction (SJ) in insect and its role in the permeation of ions and small organic molecules. In the larval rectal epithelium of *Aeshna cyanea*, lanthanum ions (La^{3+}) were unable to cross the entire length of the pleated SJ, suggesting a strictly occlusive role for this junction (Kukulies and Komnick, 1983). The septate junctions of an epidermal cell line (UMBGE-4) derived from the cockroach *Blatella germanica* were extensively permeated by lanthanum, although a partial resistance to the complete diffusion of the molecule across the cell layer was observed also in this experimental model (Reise Sousa *et al*., 1993). Conversely, a

significant permeation of large molecules was observed in the gut of *Schistocerca gregaria*, where smooth SJ allowed the passage of a molecule as large as inulin (Zhu *et al*., 2001). Skaer *et al*. (1987) demonstrated that the SJ of the upper Malpighian tubules of *Rhodnius* are readily permeable to a wide variety of substances differing in molecular size, shape and charge. The authors propose two possible explanations for the high permeability of insect SJ. First, the septa are not solid structures spanning the intercellular space but are fenestrated, permitting the passage of molecules through them (Hand and Gobel, 1972; Staehelin, 1974). Second, the septa might be arranged so as to reduce the path length. For example, if, instead of running horizontally round the cells, the septa are pitched at an angle to the horizontal plane, then the paracellular path length would be very considerably reduced (figure 1.6) (Skaer *et al*., 1987).

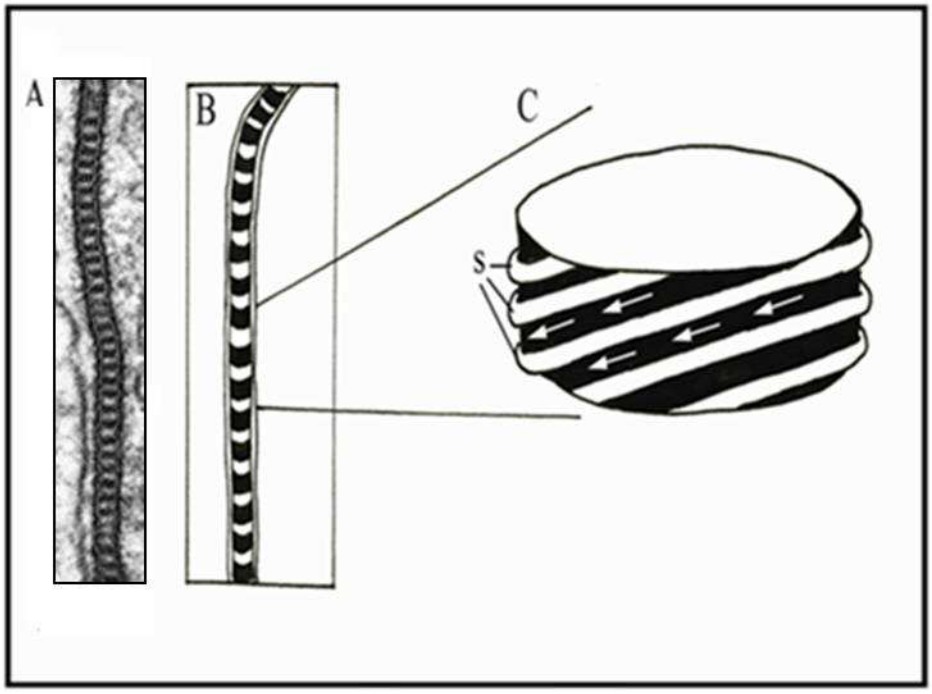

Figura 1.6: diagram of a single upper Malpighian tubule cell showing the septa of the junction tilted at an angle to the horizontal plane. The effect of even quite a shallow tilt is a very considerable reduction in the paracellular path length (Skaer *et al*., 1987, modified).
A: electron microscope images of SJ
B: schematic representation of septate junction
C: enlargement of the schematic representation, showing the septa (s)

In our laboratory a characterization *in vitro* of the paracellular pathway was performed in lepidopteran larval midgut. It was found that it was cation selective and that small organic molecules and peptides, like proctolin and fluorescein, crossed the epithelium exclusively by this route (Fiandra *et al*., 2009).

One of the most sensitive parameter to evaluate the intestinal barrier function is transepithelial electrical resistance (TER). TER is the result of the paracellular resistance or shunt resistance (R_{sh}) and the cellular resistance (R_c) in parallel (figure 1.7). The R_{sh} represents the resistance of the paracellular pathway to the passive permeation of ions and charged molecules. The R_c describes the cellular membranes resistance to ions that in lepidopteran larval midgut is dominated by the electromotive force (E_c) generated by the activity of the V-ATPase. TER can be easily determined by measuring the variation of transepithelial voltage (V_t) induced by constant transepithelial current pulses. According to the theoretical model and the experimental data discussed by Pannabecker *et al*. (1992) for *Aedes aegypti* Malpighian tubules, in those epithelia that are characterized by a highly active electrogenic pump, the inhibition of E_c causes a large increase of R_c, and in this condition the TER value approaches that of R_{sh}. Therefore, an inhibition of the dominant active transcellular transport, obtained by blocking V-ATPase activity, will allow an estimation of midgut R_{sh}. The proton pump can be inhibited by simply removing K^+ from the incubation solutions (Fiandra *et al*., 2006). The possibility to measure R_{sh} values is particularly useful to evaluate the effect of molecules able to modulate the permeability of this route. With this approach, in our laboratory, it has been demonstrated that in lepidopteran larval midgut the paracellular permeability was modulated by cAMP and/or a fine regulation of cytosolic Ca^{2+} concentration (Fiandra *et al*., 2006), two intracellular messengers known to be effective also on tight junction permeability (Perez *et al*., 1997).

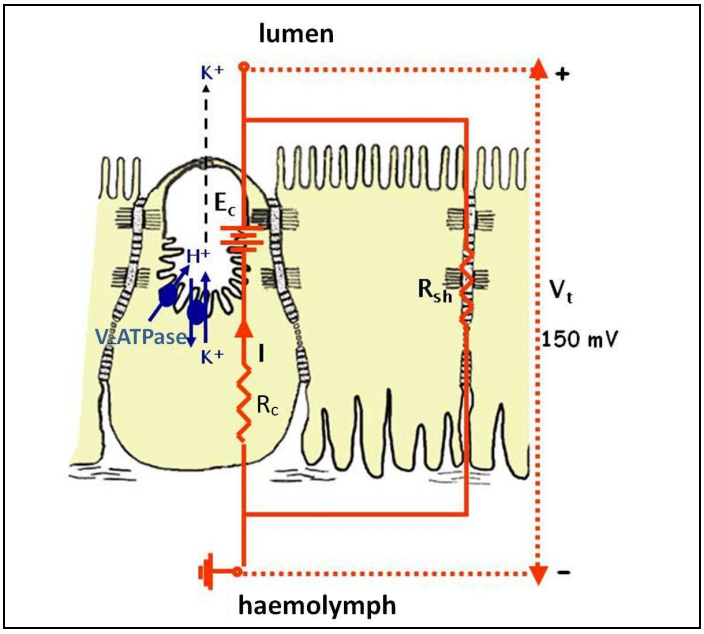

Figure 1.7:"electrical equivalent circuit of transepithelial electrolytes". The components of the circuit are : E_c, cell electromotive force determined by the V-ATPase and $2H^+/K^+$ antiport activity; I, loop current; R_c, cellular resistance represented by apical and basolateral cell membrane; $R_{sh.}$ paracellular resistance or Shunt resistance; V_t, transepithelial voltage.

It has been demonstrated that different categories of molecules are effective in modulating the permeability of the paracellular pathway in mammalian intestine. Among these chitosan and derivates and medium chain fatty acids (MCFAs) should be mentioned (Cano-Cebriàn *et al*., 2005).

Chitosan is produced by deacetylation of chitin and is a linear polysaccharide composed of randomly distributed β-(1-4)-linked D-glucosamine (deacetylated unit) and N-acetyl-D-glucosamine (acetylated unit). It has been shown that the effect of these polymers on the modulation of the permeability of the intestinal barrier depends on their ability to induce a structural reorganization of membrane proteins (Schipper *et al*., 1996; Smith *et al*., 2004).

Medium chain fatty acids (MCFA) are among the most extensively studied modulators of TJ. Fatty acid chains differ by length and are often categorized as short, medium, or long. MCFA are fatty acids with aliphatic tails of 6–12 carbons, which can form medium-chain triglycerides. Lindmark *et al*. (1995) studied the effects of the sodium salts of three MCFAs, C8 (caprylate), C10 (caprate) and C12 (laurate), on the permeability of the hydrophilic

marker molecule mannitol in monolayers of Caco-2. They demonstrated that all the three molecules enhanced the permeability of mannitol in a dose-dependent manner, even though C12 was the most effective. On the contrary, studies *in vivo* have shown the following order of effectiveness in changing the permeability of the paracellular route: C10 > C12 > C8 (Ishizawa *et al*., 1987; Sasaki *et al*., 2003). This result, coupled with the fact that the C10 is currently the only salt of fatty acid included in a pharmaceutical preparation (Takahashi *et al*., 1994), make C10 the most studied compound in this area. It has been demonstrated that C10 causes an increase of the transepithelial permeability to ions, described as a decrease of the paracellular electrical resistance (Sakai *et al*., 1997; Chao *et al*., 1999; Kamm *et al*., 2000). In addition, studies with Caco-2 cells demonstrated that C10 increases significantly and in dose- and time-dependent manner the transepithelial passage of low molecular weight molecules, such as mannitol, red phenol, sodium fluorescein and polyethylene glycol (Anderberg *et al*., 1993, Lindmark *et al*., 1995, Sakai *et al*., 1997, Chao *et al*., 1999), markers of the paracellular route, but also the passage of high molecular weight organic molecules (Kamm *et al*., 2000). C10 induces an enhanced permeability of insulin across the rat intestine (Uchiyama *et al*., 1999) and induces an increased permeability to polysucrose and the opening of the tight junctions in rat ileal mucosa (Soderholm *et al*., 1998). As regards the effect of C10 on the paracellular permeation of pharmaceutical molecules, it has been established that sodium caprate is able to increase the absorption rate constant (ka) of acamprosate in the intestine of rats (Zornoza *et al*., 2003). C10 induces also an increased permeability to epirubicin, an anthracycline drug used for chemotherapy, both in Caco-2 cell monolayer that through the ileum of rats (Chao *et al*. 1999; Kamm *et al*. 2000; Lo and Huang, 2000). Lv *et al.* (2010) have demonstrate in intestine of rat that sodium caprate significantly promotes the absorption of berberine, a plant alkaloid used in traditional Chinese medicine with wide spectrum of pharmacological actions and poor bioavailability

The local toxicity of C10 in the small intestine is one of the main concerns in relation to the use of this fatty acid in pharmaceutical products. The toxicity of C10 has been extensively studied *in vitro*. Considering that cytotoxicity depends on the concentration and duration of exposure, comparison among results obtained in experiments using different protocols

may not always be valid. A list of cytotoxicity data for C10 in Caco-2 and isolated intestinal mucosal has been recently reported by Maher *et al* (2009).

C10 exerts its effect on the paracellular permeability inducing a dilatation of the intercellular space at the level of the tight junctions (Anderberg *et al*., 1993). There is a general agreement that this molecule is able to modulate the paracellular permeability by increasing intracellular calcium concentration through the activation of phospholipase C in the plasma membrane (Lindmark *et al*. 1995, 1998; Tomita *et al.* 1995; Cano-Cebrian *et al*., 2005). The proposed signal transduction pathway is reported in figure 1.8. The increase in calcium levels is followed by phosphorylation of myosin light chains by myosin light chain kinases that causes the contraction of the perijunctional actin-myosin ring, resulting in an increased paracellular permeability.

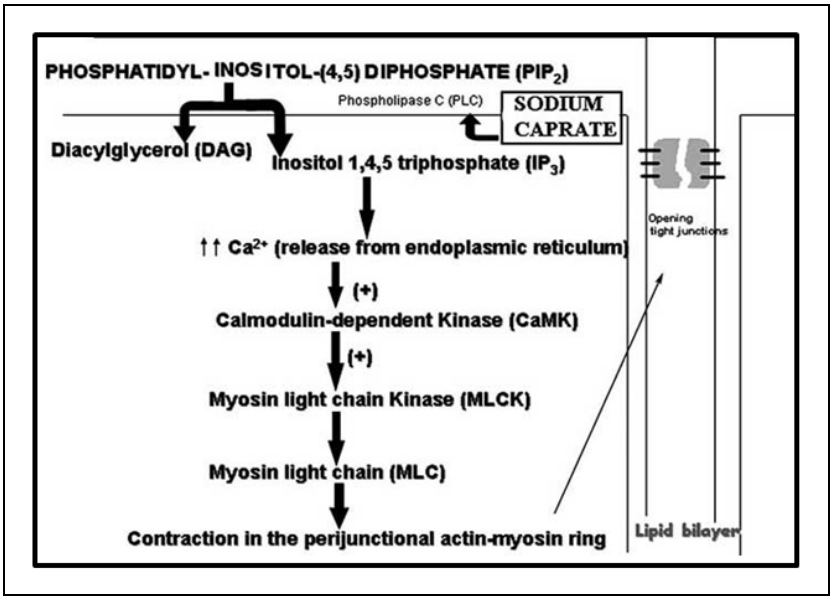

Figure 1.8: proposed mechanism of action of sodium caprate through the phospholipase-C-depentent pathway (Cano-Cebriàn *et al*., 2005)

1.5 *Junonia coenia* densovirus (*Jc*DNV)

The *Parvoviridae* family is a group that clusters small non enveloped viruses with a linear, single-strand DNA genome. It has been subdivided into two subfamilies based on their host range: *Parvovirinae* and *Densovirinae*. The *Parvovirinae* subfamily includes all the vertebrate parvoviruses, whereas *Densovirinae* are parvoviruses highly pathogenic for arthropods, mostly insects, at larval stages, including agronomical pests and insects vector-borne diseases (Bergoin and Tijssen, 2008), characteristics that make them particularly interesting as potential bioinsecticides alternative to chemical compounds (Belloncik, 1990). Two DNVs, *Sibine fusca* densovirus (*Sf*DNV) and *Casphalia extranea* densovirus (*Ce*DNV), were successfully utilized in Cote d'Ivoire and Columbia, respectively, for the control of their hosts, *C. extranea* and *S. fusca*, two major pests of oil palm industrial plantations. Similarly, a commercial formulation (Viroden) of *Aedes aegypti* densovirus (*Ae*DNV) was used for the control of *A. aegypti* larvae in different areas of the Soviet Union and a *Periplaneta fuliginosa* densovirus (*Pf*DNV) formulation is produced in China for the control of cockroaches (Bergoin and Tijssen, 2008). However, beside these few successful examples, they were never further developed in the past, due, at least in part, to the poor interest in biocontrol of developed countries. Nowadays, because of the increased insect resistance and a stronger social request to preserve the environment from chemical pesticides, the possibility of their use is reconsidered.

Characteristic of *Densovirinae* subfamily is to cause, in cells where the viral genome is replicated, hypertrophy of the nuclei, which appear electron-dense at the electron microscope (hence the name "DensoNucleosis Virus" then shortened to "densovirus", DNV). This subfamily includes four genera: Densovirus, Pefudensovirus, Iteravirus and Brevidensovirus genera. Today, more than thirty *Densovirinae* have been discovered, infecting at least 5 insect orders. They reveal a great diversity not only in genomic structures and sequences but also in the biology of infection and host range: some are monospecific, while others can infect different insect species. *Junonia coenia (Jc)* DNV (River and Longworth, 1972), discovered on the common buckeye caterpillar, is the prototype of the genus *Densovirus* (Bergoin and Tijssen, 2008). As all parvoviruses, *Jc*DNV

virions consist of a non-envepoled capsid, round and with icosahedral symmetry. The nucleocapsid is isometric and has a diameter of 20-26 nm. It consists of 60 capsomers, each a quadrilateral 'kite-shaped' wedge. Surface projections are small, surface appears rough, and with distinct spikes (figure 1.9) (Bruemmer *et al.*, 2005).

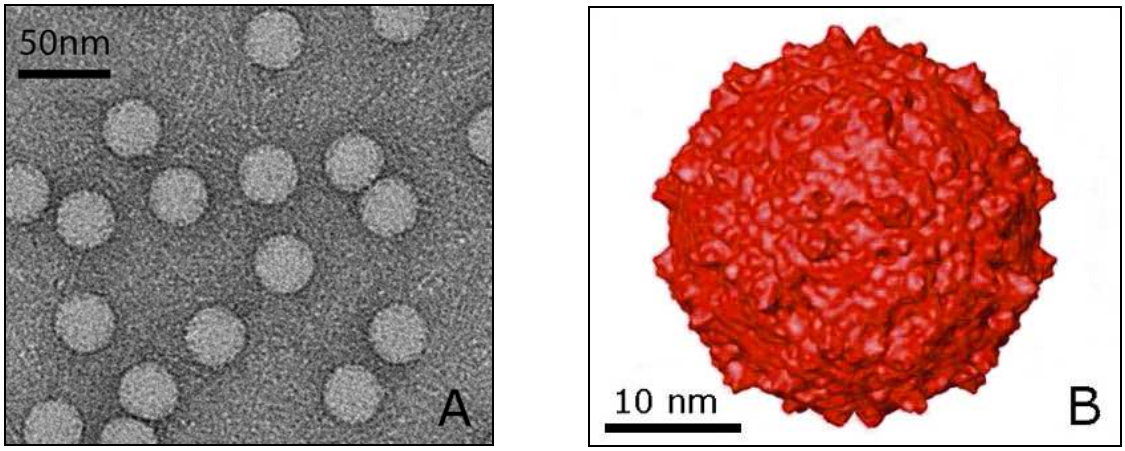

Figure 1.9: electron microscope images of native *Jc*DNV negatively stained with uranyl acetate (A) and surface representations of cryo-EM maps of native *Jc*DNV to a resolution of 17 Å (B) (Bruemmer *et al.*, 2005, modified).

The genome (6 kb) is not segmented and contains a single molecule of linear single-stranded DNA with an ambisense organization. The four structural proteins VP1, VP2, VP3, and VP4 are nested in a single large open reading frame (ORF), ORF1, located in the 5' half of one strand, whereas in the 5' half of the complementary strand ORF2, ORF3, and ORF4 encode the three nonstructural (NS) proteins NS-1, NS-2, and NS-3, respectively (Dumas *et al.*,1992.). The strands have large inverted terminal repeats (ITRs) that exceed 500 nucleotides and include the P9 and P93 viral promoters that drive the expression of VP and NS genes respectively. The four overlapping capsid polypeptides are synthesized from an unspliced 2.5-kb mRNA by a "leaky-scanning" mechanism whereby ribosomes initiate translation at the first, second, third, or fourth in-frame AUG codon. Thus, the four VPs share the same C-terminal sequence and differ only in their N-terminal region (figure 1.10). The frequency of translation initiation events at each AUG codon is very likely responsible for the different levels of expression of the four polypeptides, as reflected by the presence

of VP1, VP2, VP3, and VP4 in an approximate 1:9:9:41 ratio in the virion. Virus-like-particles (VLPs) assemble spontaneously when the individual VPs are expressed by a recombinant baculovirus, although capsid formation is much less efficient for VP1 than for VP2, VP3 or VP4 (Croizier *et al*., 2000).

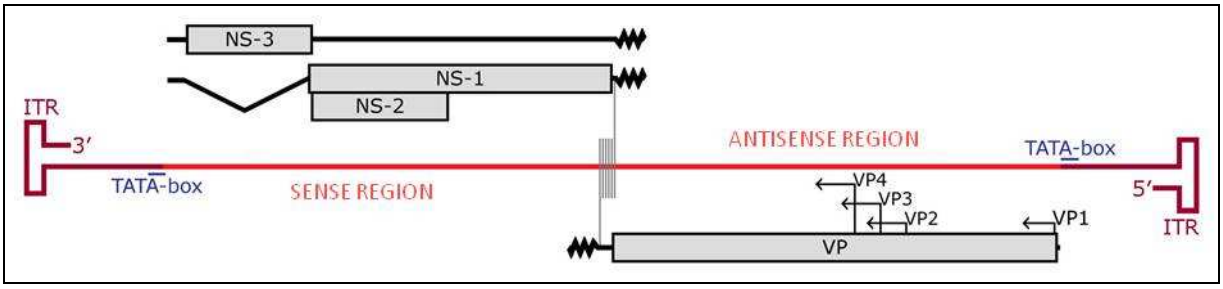

Figure 1.10: schematic representation of the structure and expression strategies of *Jc*DNVs. The genome, in red, is represented with the 5' and 3' hairpin termini, whereas transcripts from left to right (NS coding strand) are depicted above the genome and transcripts from right to left (VP coding strand) below the genome (Bergoin and Tijssen, 2008, modified).

In natural conditions, DNV infection is initiated after ingestion of viral particles. Unlike other densoviruses, *Jc*DNV does not replicate within intestinal cells, so the midgut epithelium represents a barrier that the virus has to cross to reach the host haemocoel and its target tissues (tracheae, hemocytes, visceral muscles and epidermis), where it induces cells disorganisation and oxidative stress (Mutuel *et al*, 2010).

In larvae fed with *Jc*DNV, the virus is rapidly localized at the peritrophic membrane (PM), highlighted the shielding role of this structure against microorganisms and suggesting an affinity of *Jc*DNV viral particles for some of its components, e.g. chitin (a polymer of N-acetyl-glucosamine) and/or proteins (Ogliastro, personal communication). Nevertheless, the size of the capsid theoretically allows *Jc*DNV to diffuse freely through the pore of the PM matrix (Martin *et al*., 1997), and to reach the underlying midgut cells, where columnar cells represent the specific site for absorption (Casartelli *et al*., 2001; Casartelli *et al*., 2008).

The mechanism of infection and the identification of membrane receptor responsible for the internalisation of parvoviruses are still little studied even though recent works have depicted the main events of parvovirus entry into host cells, all mediated by a wide diversity of cell surface receptors, including glycoproteins, glycans, and glycolipids, that trigger rapid clathrin-mediated endocytosis (Cotmore *et al*, 2007). For example Brown *et al.* (1993) showed that the pathogenic human parvovirus B19 replicates only in the erythoid progenitor cells and that the mechanism of uptake in these cells involved the blood-group P antigen. Canine Parvo Virus (CPV) and Feline Panleukopenia Virus (FPV) capsid bind to the transferring receptors (TfRs) of their hosts and use these receptor to infect cells (Palermo *et al*., 2003). To date no receptor has been identified for viruses belonging to the subfamily *Densovirinae*. It has been recently identified a strain of *Bombyx mori* resistant to *B. mori* densovirus type 2 (BmDNV-2). This virus, which replicates only in the midgut columnar cells and causes the death of the larva, was classified among the *Parvoviridae*, in the subfamily *Densovirina*e, but it has recently been excluded because of the peculiar features of its genome: it consists of single-stranded DNA but its size is much greater than that of other densoviruses (about 12.5 kb, instead of 6-4 kb), it is divided into two distinct macromolecules and contains the gene that encodes for its own DNA polymerase. It has been recently clarified that the resistance shown by the strain of *B. mori* is determined by a single gene that has a deletion of 6 kb; this gene was isolated, it encodes a protein with 12 transmembrane domains, belonging to a family of transporters for amino acids (Ito *et al.*, 2008). This protein, expressed only in the midgut columnar cells, is the receptor for *Bm*DNV-2.

In order to understand the early events of *Jc*DNV infection, Vendeville *et al*. (2009) have characterized the crucial endocytic events leading to the productive infection in a permissive lepidopteran cell line, *Lymantria dispar* 652 ovarian cells. They showed that *Jc*DNV infectious pathway mainly involves rapid clathrin-mediated endocytosis followed by slower traffic within early and late endocityc compartments. The infection can be inhibited by the block of late endocityc trafficking, the neutralization of the pH of the acidic organelles and the disruption of the cytoskeleton network (Vendeville *et al*., 2009). They

also demonstrated that VLPs containing only the major structural protein VP4 are able to enter *L. dispar* ovarian cells similarly to fully-virus-capsid (Vendeville *et al.*, 2009).

However how *Jc*DNV crosses the midgut epithelial cells remains an intriguing question and, since the interaction between a virus and its receptor is the first level of specificity and only few studies have been performed on the mechanism of infection of densoviruses, this field of investigation is particularly interesting.

Materials and Methods

2.1 Experimental animals

Bombyx mori eggs and the artificial diet (Cappellozza *et al*., 2005) were provided by CRA, Bee-Sericulture Research Unit (Padova, Italy). *B. mori* larvae (figure 2.1.A) were reared under controlled conditions (25 ± 1 °C, 65-70% RH, 12L:12D photoperiod).

Spodoptera frugiperda eggs were provided by "Laboratoire de Biologie Intégrative et Virologie des Insect" in Montpellier (France) and the larvae (figure 2.1.B) were reared under controlled conditions (25 ± 1 °C, 65-70% RH, 12L:12D photoperiod) on a wheat germ-based artificial diet.

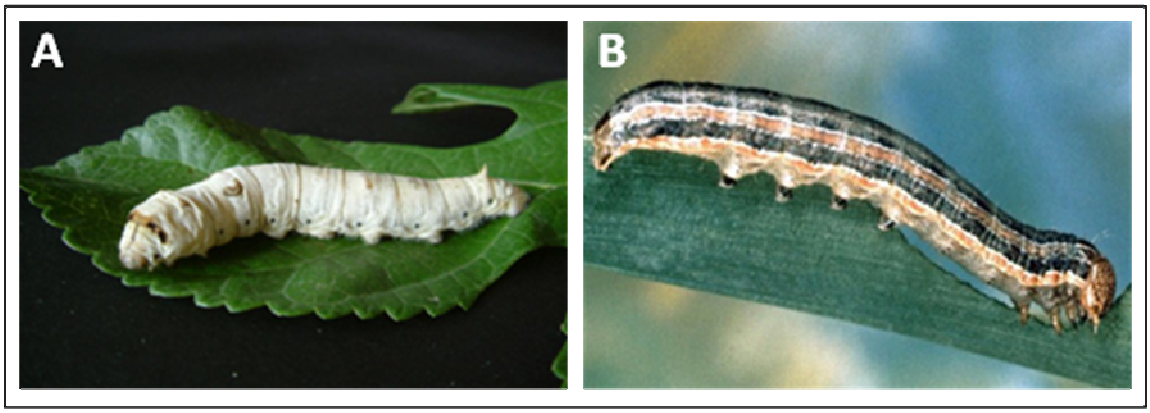

Figure 2.1: *Bombyx mori* (Lepidoptera, Bombycidae) (A) and *Spodoptera frugiperda* (Lepidoptera, Noctuidae) (B) larvae

2.2 Preparation of midgut cells in culture

B. mori larvae at the end of the IV instar, just before the IV moult, were anaesthetized with CO_2 and surface-sterilized by consecutive immersions, lasting approximately 2 min each, in the following solutions: 10% (v/v) detergent (Pharma Soap Medical); 2% (v/v) p-hydroxybenzoic acid methyl ester (Sigma), prepared from a stock solution of 15% p-hydroxybenzoic acid methyl ester (w/v) in 95% ethanol; 0.1% (v/v) sodium hypochlorite. Silkworms were cut between the second and the third pair of thoracic legs and behind the third pair of abdominal appendages to exclude the foregut and the hindgut, and the peritrophic membrane along with the enclosed intestinal contents were removed. The central part of the larva was transferred to a Petri dish containing an Insect Physiological Solution (IPS) composed of (in mM) 47 KCl, 20.5 $MgCl_2$, 20 $MgSO_4$, 4.3 K_2HPO_4, 1.1 KH_2PO_4, 1 $CaCl_2$, 88 sucrose, pH 7; modified by addition of 0.2% (v/v) gentamicin (50 mg/ml, Sigma), 0.01% (v/v) 1x antibiotic-antimycotic solution (Sigma), 0.003‰ (v/v) sodium hypochlorite. The ventral cuticle was cut longitudinally and the midgut, deprived of muscles and silk glands, was isolated. Dissected midguts were cut along the longitudinal axis and rinsed two times (10 min each) in sterile modified IPS, then two times (10 min each) in the same solution without sodium hypochlorite. Midguts were pooled into a strainer (100 µm mesh size), placed in a Petri dish containing few ml of the latter solution and left under mild agitation for 1h. In these conditions, the loosely attached stem cells migrated away from the tissue. The tissue within the sieve was discarded and the free cells in the filtrate, mostly stem cells (Cermenati *et al*., 2007), were collected and pelletted by gentle centrifugation at 400 g for 5 min. Cells were then resuspended in growth medium, composed by a mixture of 67.4% Grace's insect medium (GIBCO), 11.2% 100 mM KOH, 6.7% Fetal Bovine Serum (GIBCO), 0.5% vitamins mix (composed by, in mg/100ml: 300 riboflavin, 150 pyridoxine hydrochloride, 150 thiamine hydrochloride, 150 folic acid, 600 nicotinic acid, 600 pantothenic acid, 12 biotin, 1.2 vitamin B12), 0.018‰ Antibiotic-Antimycotic Solution 1X (Sigma), 0.1% gentamicine (50 mg/ml, Sigma). Cultured cells were supplemented with $6x10^{-8}$ M 20-hydroxyecdysone (Sigma) and 100 ng/ml α-arylphorin (purified according to Blackburn *et al*., 2004, in Insect Bio-control Laboratory, USDA,

Beltsville, MD, USA), kindly donated by Prof. R.S. Hakim, Howard University, Washington, DC, USA. All the solutions used were routinely sterilized by filtration (Nalgene, 0.2 μm pore size) prior to use. Three ml of the cell suspension in growth medium were distributed in the wells (35 mm in diameter) of six well plates. Cells, which grow and differentiate in suspension, were incubated at 25 °C, and 1 ml of medium from each well was replaced with 1 ml of fresh medium once a week.

With this experimental preparation we performed experiments to characterize the mechanism involved in Tat-eGFP uptake by columnar cells. Tat-eGFP production and purification were performed in the laboratory of Prof. R. Rao (University of Naples "Federico II").

2.3 Internalization of Tat-eGFP by columnar cells in culture

To study the mechanisms involved Tat-eGFP internalization in midgut cells of *B. mori* larvae, cultured midgut cells were pelletted by gentle centrifugation at 400 g for 5 min and resuspended in 300 μl of IPS for each experimental set up. Cells were preincubated for 30 min in the absence (control) or in the presence of the following different drugs: 100 μM 2,4-dinitrophenol (DNP), 10 mM sodium azide, 100 μM chlorpromazine and 20 μM phenylarsine oxide. If the drugs were dissolved in DMSO, control cells were incubated with a corresponding amount of solvent. In all these experiments, the cells were then incubated in the presence of 1.5 μM Tat-eGFP for 30 min. Cells were then fixed with 4% paraformaldehyde. After 3 rinses in IPS the samples were mounted in ProLong Gold antifade reagent (Invitrogen), covered with a cover-slip and then examined with a confocal microscope as described in the paragraph "Fluorescence acquisition and analysis". To avoid the contribution of unspecific binding to the cell membrane, a single optical section in a middle cell focal plane (where the nucleus was clearly evident) was acquired. Regions of interest (ROIs), precisely defining the cell cytoplasm, were drawn and the calculated mean grey values were used. Ten or more cells from at least two independent preparations were analysed for each experimental condition. The data, expressed as

arbitrary units of fluorescence intensity (8 bit acquisition), are reported as mean ± standard error. For each set of experiments Student's t Test was used for statistical analysis.

The tested drugs are effective in *B. mori* midgut cells, since they have been already successfully used to inhibit the internalization of albumin, a protein taken up by receptor-dependent clathrin-mediated endocytosis (Casartelli *et al*., 2008). Moreover, these drugs did not affect cell viability (Casartelli *et al*., 2008).

2.4 Enzymatic disaggregation of midgut tissue

5^{th} instar *B mori* larvae or 6^{th} instar *S. frugiperda* larvae were anaesthetized with CO_2 and cut between the second and the third pair of thoracic legs and behind the third pair of abdominal appendages, to exclude the foregut and the hindgut. Then, the midgut was explanted and deprived of the peritrophic membrane and intestinal contents. Midguts were then transferred in a Petri dish containing sterile IPS lacking Ca^{2+} and Mg^{2+} (47 mM KCl, 4.3 mM K_2HPO_4, 1.1 mM KH_2PO_4, 192 mM sucrose, pH 7). After two rinses in the same solution, midguts were transferred in a Petri dish containing sterile IPS lacking Ca^{2+} and Mg^{2+} with 2.5% (w/v) trypsin and left under mild agitation for 30 min. The solution was then filtered through a strainer (70 µm pore size), the tissue in the sieve was discarded and the free cells in the filtrate, mostly mature midgut cells, were collected and pelletted by gentle centrifugation at 400 g for 5 min. The supernatant was eliminated and the pellet was rinsed twice in IPS. Midgut cells obtained with this procedure were immediately used for the experiments.

2.5 Fluorescence measurements of free cytosolic Ca^{2+}

Midgut cells obtained by enzymatic disaggregation of the tissue (paragraph 2.4) were used to evaluate the effect exerted by *Junonia coenia* densovirus (*Jc*DNV) and by the medium chain fatty acid sodium caprate (C10) on intracellular calcium concentration in midgut

cells. Free cytosolic calcium was measured using the cell permeant Ca^{2+}-sensitive fluorescent dye Fluo-3 acetoxymethyl ester (Fluo-3AM) (Molecular Probes). Fluo-3AM is a fluorescent chelator excited by visible light (488 nm) and it emits green fluorescence (525 nm) when bound to calcium ions. The intensity of fluorescence depends on the free calcium concentration. Once loaded into the cell, the acetoxymethyl groups are removed by intracellular esterases and Fluo-3 can then readily combine with the free intracellular calcium ions.

Mature cells obtained by enzymatic disaggregation of the midgut tissue were pelletted by gentle centrifugation at 400 g for 5 min and resuspended in 300 µl of IPS without Ca^{2+} and Mg^{2+} for each experimental condition. Cells were incubated for 30 min in dark at 25 °C in the presence of 5 µM Fluo-3AM to allow the loading of the dye. Cells were washed three times in IPS without Ca^{2+} and Mg^{2+} to remove any dye that was non-specifically associated with the cell and then incubated for 15 min to allow the complete removal of the acetoxymethyl groups.

To assess whether *Jc*DNV causes a modulation of the cytosolic Ca^{2+} concentration, isolated cells, obtained by enzymatic disaggregation of *S. frugiperda* larval midgut, were incubated in IPS without Ca^{2+} and Mg^{2+} in the absence (control) or in the presence of *Jc*DNV (0.1 ng/µl) for 10 min. At the end of the incubation, cells were rinsed 3 times and immediately observed at the fluorescence microscope (AXIOVERT 200M equipped with AXIOcam HRm, Zeiss). For each experiment, performed in triplicate, at least 200 cells were observed and the fluorescence recorded in columnar cells was quantified. The quantification of the fluorescence intensity was performed using the software AxioVision 4.6.3 (Zeiss).

To estimate whether C10 determine the increase of cytosolic Ca^{2+} concentration, isolated cells, obtained by enzymatic disaggregation of *B. mori* larval midgut, were loaded with Fluo-3AM, as reported above, and incubated in the absence (control) or in the presence of C10 (2 mM). The cells were immediately observed for 15 min with the fluorescence microscope (AXIOVERT 200M equipped with AXIOcam HRm, Zeiss).

2.6 Measurement of SOD activity

The activity of superoxide dismutase (SOD) was measured in mature cells obtained by enzymatic disaggregation of midgut tissues (par 2.4) of *S. frugiperda*. After centrifugation at 400 g for 5 min, the pellet was resuspended in 300 µl of IPS for each experimental set up. Cells were incubated at 25 °C in the absence (control) or in the presence of *Jc*DNV (0.1 ng/µl) for 10 min. At the end of incubation, cells were diluted to 10 ml in IPS and centrifugated at 400 g for 5 min. The pellet was resuspended in a small volume (150 µl) of 100 mM mannitol, 10 mM Hepes-Tris, pH 7.2 containing proteases inhibitors (1 mM dithiothreitol, 1 mM PMSF, 0.1 mM leupeptin, 1 µM pepstatin A, 2 µg/ml aprotinin) and lysated in the eppendorf vial with a motor for pellet pestle (Sigma). Protein concentration in the lysate was determined according to Bradford (1976) with BSA as standard. SOD activity was determined as the degree of inhibition of cytochrome c reduction at 550 nm by superoxide anions generated by xanthine oxidase/hypoxanthine reaction. The concentration of the reagents was: 50 mM potassium phosphate buffer, pH 7.8, 50 µM hypoxanthine, 1.9 mU/ml xanthine oxidase and 10 µM cytochrome c. The activity is given in SOD units (1 SOD unit = 50% inhibition of the xanthine oxidase reaction).

2.7 Transcriptomic analysis

Immediately after the third moult, larvae of *S.frugiperda* were starved before infection performed individually within tissue culture plates by feeding with 1 mm^3 of diet contaminated with *Jc*DNV preparation (100 fold-LD50). Time 0 of infection was defined when contaminated food was completely eaten. Infected and non-infected (control) larvae were then fed with fresh food at 24 °C for one day or three days. Larvae were sacrificed, the midguts were isolated and mature columnar cells were obtained by enzymatic disaggregation of the tissue (paragrph 2.4). Total RNA was purified from non infected and *Jc*DNV infected cells using Trizol reagent as recommended by the manufacturer (Invitrogen). The RNA was stored at –80 °C until the use in SAGE library construction, made

by the Skuldtech (Montpellier), or the use for qPCR, performed to validate the method. Total RNA used for qPCR was DNase treated using the Turbo DNA-free kit (Ambion) and reverse transcripted by the SuperScript III RT (Invitrogen). Primers pairs were designed by Primer Express software (Applied Biosystem) on the reads sequences corresponding to the selected tags obtained from two databases, Spodobase (bioweb.ensam.inra.fr/spodobase/) and Lepido-DB (http://www.inra.fr/lepidodb). Reactions were carried out using Platinum SYBR Green qPCR Super Mix kit (Invitrogen). Fluorescent amplicons were detected using the ABI Prism 7000 apparatus (Applied Biosystem) using 96-well microtiter plates in a final volume of 25 µl under the following conditions: 50 °C for 2 min, 95 °C for 2 min, and 40 cycles of 95 °C for 15 s and 60 °C for 30 s. The genes corresponding to the different tags were then determined performing a Blastn on Pubmed (http://www.ncbi.nlm.nih.gov/pubmed/).

2.8 Isolation of midgut epithelium and perfusion apparatuses

Midguts isolated from 6th instar *S. frugiperda* larvae or 5th instar *B. mori* larvae, as reported above, were then mounted in two different apparatuses: the Ussing chambers (World Precision Instruments, Berlin, Germany) (figure 2.2) or a perfusion apparatus where the *in situ* shape and orientation are maintained (figure 2.3). The Ussing chamber allows to measure correctly the tissue and the shunt (paracellular) electrical resistance, and to determine the lumen to haemolymph flux of the molecules of interest. The shunt resistance is a useful parameter to evaluate the effect of compounds on the septate junctions permeability. The second perfusion apparatus offers the possibility to measure the flux of the molecules of interest in a condition more similar to that occurring *in vivo* and the surface of the tissue exposed to the bathing solution is larger then in Ussing chambers.

Midguts mounted in Ussing chambers were laid on a piece of thin cotton gauze and cut longitudinally. These procedures were performed at 4 °C to avoid the impairment of the

tissue. The cotton gauze, necessary to maintain the tissue extended, presented very large meshes and offered no restriction to the permeation of molecules. Dissected midguts were then mounted as a flat sheet between Ussing chambers separating two compartments, the luminal and the haemolymphatic one. The exposed surface of 19.6 mm^2 was bathed with the following buffer solutions, unless otherwise indicated: (in mM) 1 $CaCl_2$, 4.8 $MgSO_4$, 240 sucrose, 20 Kgluconate and 5 Tris adjusted to pH 7 in the haemolymph compartment (2.5 ml) or 5 CAPS adjusted to pH 10 in the luminal one (2.5 ml).

Solutions were circulated by gas influx (100% O_2) and maintained at 25 °C in water-jacketed reservoirs.

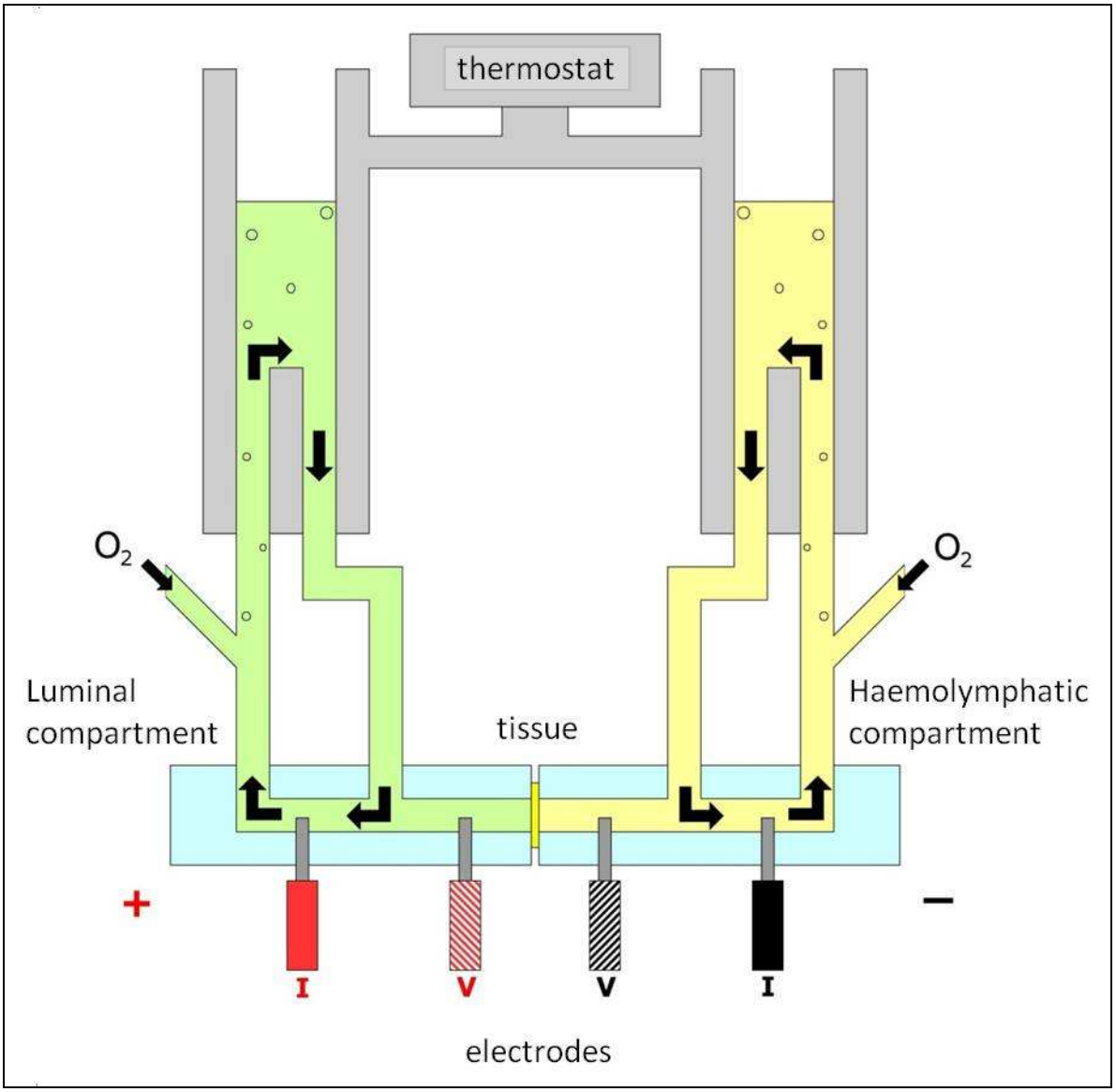

Figure 2.2: schematic representation of Ussing chambers connected to the reservoirs and to electrodes. V: voltage electrodes; I: current electrods.

Midguts to be mounted in the second apparatus, were isolated and rinses in a physiological solution (210 mM sucrose, 45 mM KCl, 10 mM Tris–HCl at pH 7) to eliminated the proteolytic enzymes present both in the endo- and ecto-peritrophic spaces. The internal chamber of the apparatus correspond to the luminal compartment and the external chamber to the haemolymphatic compartment. The region of the midgut exposed to the bathing solutions (0.5 cm^2) correspond to the middle part (Giordana *et al*., 1998), because the anterior part is too short and the posterior one too fragile to be mounted on the experimental apparatus. The bathing buffers had the following composition (in mM): 5 K_2SO_4, 4.8 $MgSO_4$, 1 $CaCl_2$, 10 KCitrate, 10 L-alanine, 10 L-glutamine, 10 glucose, 190 sucrose, 5 Tris, pH 8.3 in the luminal compartment and adjusted with HCl to pH 7 in the haemolymphatic one. Buffers present in the luminal and haemolymphatic compartments were continually oxygenated and stirred by bubbling pure O_2.

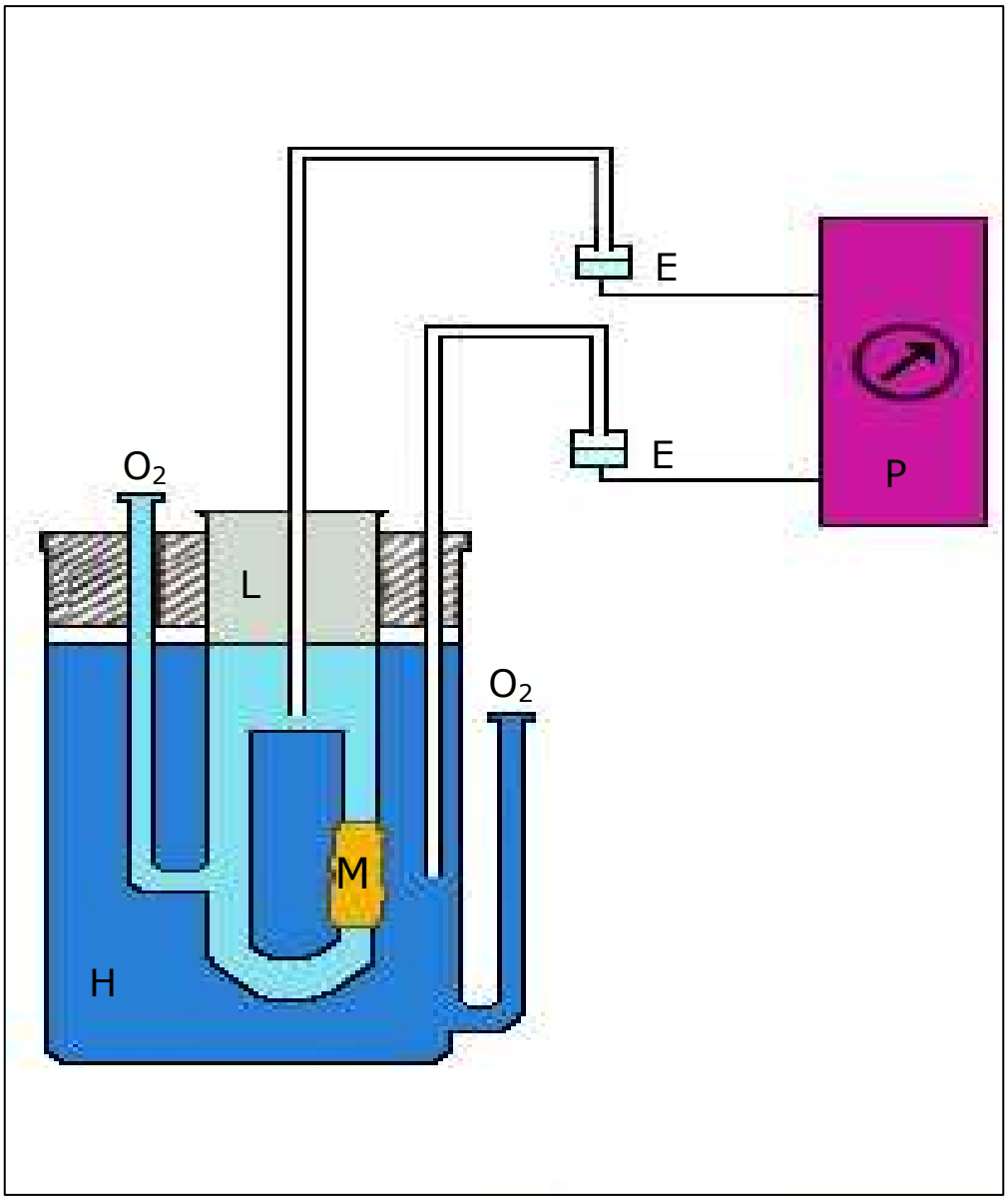

Figure 2.3: scheme of the apparatus used for transepithelial flux measurements (modified from Nedergaard and Harvey, 1968). M: midgut, L: luminal chamber, H: haemolymphatic chamber, O_2: oxygen inlet; E: electrodes; P: potentiometer.

To monitor the viability of the midgut epithelium, the transepithelial electrical potential difference (TEP) was recorded by a Keithley microvoltmeter, with calomel electrodes connected via agar–KCl (3 M) bridges to the solutions bathing both sides of the midgut (Casartelli *et al*., 2007).

2.9 Mechanisms involved in *Jc*DNV entry into columnar cells

To study the mechanism involved in *Jc*DNV entry into midgut cells, midgut tissues isolated by *S. frugiperda* larvae were mounted in Ussing chambers and preincubated for 30 min in the absence or in the presence of different drugs that interfere with endocytic processes: dynasore (DYN, 400 µM) that inhibits clathrin-coated vesicle formation blocking the GTPase dynamine, the sterol-sequestring drug methyl β cyclodextrine (MβCD, 60 µM) that inhibits lipid raft-dependent endocytosis, and the fungal toxin wortmannin (WTN, 10 mM) that inhibits the early events of receptor mediated endocytosis. Virus (0.1 ng/µl) was then added to the luminal compartment for 10 min. At the end of the incubation time, tissues were fixed with 4% parafolmaldehyde for 15 min, incubated for 15 min in IPS containing 1% BSA and permeabilized for 15 min with saponine in IPS (1 mg/ml). Midguts were then incubated for 1 h in IPS added with a mouse polyclonal antibody anti-*Jc*DNV (1:1000). The antibody recognizes the viral particle 4 (VP4), the major protein of the capsid. Tissues were then washed in IPS containing 1% BSA and incubated for 1 hour in the same buffer added with Cy3-conjugated goat anti-mouse IgG antibody (1:50) (Jackson) and with fluorescein isothiocynate (FITC)-phalloidin (2 µg/ml) to visualize actin filaments. Nuclei were labelled with Hoechst (5 µg/ml). Coverslips were then mounted in ProLong Gold antifade reagent (Invitrogen) and samples were observed with the confocal microscope as reported in paragraph 2.21.

2.10 Characterization of *Jc*DNV trafficking within midgut cells

Midguts isolated from *S. frugiperda* larvae were mounted in Ussing chambers and incubated with *Jc*DNV (0.1 ng/µl) for 5 or 15 min to analyze possible colocalisation events with Rab-5 or Rab-7 GTPases, markers for early and late endosomes, respectively. At the end of the incubation, tissues were fixed with 4% paraformaldehyde, incubated for 15 min in IPS containing 1% BSA and permeabilized for 15 min with saponine in IPS (1 mg/ml). Tissues were then incubated for 1 h with a mouse polyclonal antibody anti-*Jc*DNV (1:1000)

against VP4 and with a rabbit polyclonal antibody anti-Rab 5 or anti-Rab 7 GTPases (1:50) (Santa Cruz Biotechnology). Midguts were then washed in IPS containing 1% BSA, and incubated for 1 hour in the same buffer added with Cy3-conjugated goat anti-mouse IgG (1:50) and with FITC-conjugated goat anti-rabbit IgG (1:50) (Jackson). Nuclei were labelled with Hoechst (5 µg/ml). Samples were then mounted in ProLong Gold antifade reagent (Invitrogen) and observed with the confocal microscope as described in paragraph 2.21.

2.11 Detection of Cy3-*Jc*DNV in isolated midgut tissue

In order to establish the localization of *Jc*DNV in whole-mount midgut, tissues isolated from last instar larvae of *S. frugiperda* were mounted as a flat sheet in Ussing chambers. Cy3-*Jc*DNV (0.1 ng/µl) was added to the luminal side and, after 10, 30 or 60 min of incubation, tissues were removed from the Ussing chamber, washed five times with the luminal solution and fixed for 30 minutes in 4% paraformaldehyde. Samples were then rinsed five times in IPS and then mounted in ProLong Gold antifade reagent (Invitrogen). The tissues, covered with cover-slips, were examined with the confocal microscope as reported in paragraph 2.21.

2.12 Detection of VP4 in midgut cells

In order to verify if virus-like-particles (VPLs) formed only the major structural protein VP4 are able to enter midgut cells similarly to fully-virus capside, midgut tissue mounted in Ussing chambers were incubated for 10 min with VP4 in the luminal compartment.
At the end of the incubation time midguts were subjected to the immunofluorescence assay as described in par. 2.9 “Mechanism involved in *Jc*DNV entry into columnar cells” and observed with the confocal microscope as reported in the paragraph 2.21.

2.13 Quantification of the transepithelial passage of *Jc*DNV

To determine the amount of virus able to cross the midgut epithelial barrier after different time of incubation, isolated midguts of *S. frugiperda* larvae were mounted in Ussing chambers and incubated for 10 or 30 min with *Jc*DNV (0.1 ng/µl) added to the luminal compartment of the perfusion apparatus. At the end of the incubation the luminal and the haemolymphatic solution were withdrawn to quantify by qPCR the amount of virus (expressed as a ratio of viral DNA present in the haemolymphatic compartment and that present in both compartments) able to cross the midgut barrier. Viral DNA was purified with Wizard Genomic DNA Purification Kit (Promega). Viral sense 5'-GGAGGAGGCAACACTTCAGG-3' and antisense 5'-TCTGCCATGGAATTTCAGCC-3' primers were designed by Primer Express software (Applied Biosystem). A 200-bp fragment was amplified from position 1710 to 1911 of the viral genome located within open reading frame 1 encoding the Viral Protein 4 (VP4), the major capsid protein. Reactions were carried out using Platinum SYBR Green qPCR Super Mix kit (Invitrogen) as described in paragraph 2.7 "Transcriptomic analysis". A standard curve was generated after 40 cycles of PCR using five serial 10-fold dilutions of a plasmid containing the viral genome.

2.14 Effects of C10 on the lumen-to-haemolymphatic flux of fluorescein and rhodamine-proctolin

To measure the transepithelial passage of two organic molecules, fluorescein and rhodamine-proctolin (rh-proctolin), in the absence or in the presence of C10, isolated midgut of 5^{th} instar *B. mori* larvae were mounted in Ussing chambers. Midguts were bathed with the following buffer solutions (in mM): 20 Kgluconate, 212 or 252 sucrose for incubation in the presence or in the absence of C10 (20 mM), respectively, and 5 CAPS-TMAOH, pH 9.8 in the luminal compartment; 20 Kgluconate, 5 $CaCl_2$, 24 $MgSO_4$, 190 sucrose and 5 TRIS-HCl, pH 7.2 in the haemolymphatic compartment. The first solution lacks Ca^{2+} and Mg^{2+} to avoid the formation of the precipitates after the addition of C10.

To determine the amount of fluorescein able to cross the midgut epithelium, the fluorescent molecule was added to the luminal compartment of the perfusion apparatus at the concentration of 3 mM. Midguts were incubated in the absence or in the presence of C10 (20 mM) and the incubations lasted 120 or 180 min. At the end of the incubation time, 2 ml of haemolymphatic solution were withdrawn and the amount of fluorescein able to cross the epithelium was quantify with a spectrofluorimeter (excitation wavelength 509 nm, emission wavelength 521 nm). After subtraction of the background fluorescence, determined on samples collected from midguts incubated in the absence of fluorescein, the amount of protein transported was calculated by using a calibration curve produced with known amounts of the molecule dissolved in the haemolymphatic buffer.

Using the same perfusion apparatus we also measured the lumen-to-haemplymph passage of rh-proctolin (130 µM) in the absence or in the presence of C10. Incubations lasted 120 min. To avoid the possible degradation of proctolin, an endogenous molecule, by the peptidases present on the apical membrane of midgut cells, a peptidase inhibitor cocktail was added both in the luminal and in the haemolynphatic solutions. The composition (in mM) was: 1 phenanthroline, 0.01 bestetin, 0.01 amastatin. As reported for fluorescein, the amount of rh-proctolin able to reach the haemolymphatic solution was measured using a spectrofluorimeter (excitation wavelength 567 nm, emission wavelength 582 nm). At the end of the incubation time, midguts incubated with rh-proctolin were removed from the Ussing chamber and immediately observed with the confocal microscope as reported in paragraph 2.21.

2.15 CPPs internalisation in isolated midgut

Midguts of *B. mori* larvae were mounted in Ussing chambers to study the internalization of different Cells Penetrating Peptides (CPPs). The bathing solution had the following composition (in mM): 5 K_2SO_4, 4.8 $MgSO_4$, 1 $CaCl_2$, 10 K Citrate, 10 L-alanine, 10 L-glutamine, 10 glucose, 190 sucrose, 5 Tris. This solution was adjusted to pH 7 in the haemolymphatic compartment and to pH 8.3 in the luminal one. Incubations were carried

out in the presence of FITC-Tat, L- or D-eightarginine (R8 and r8, respectively) labeled with FITC, added to the luminal compartment at a final concentration of 200 µM. After 10 min, 30 min, 1 h or 3 h of incubation, midguts were removed from the perfusion apparatus and washed several times in rinsing buffer (20 mM K_2SO_4, 14.4 mM $MgSO_4$, 3 mM $CaCl_2$, 200 mM sucrose, 5 mM Tris-HCl, pH 7) to avoid unspecific binding of the peptides to midgut cell plasma membranes. Tissues were fixed for 30 min in 4% paraformaldehyde, washed five times in IPS, permeabilised with 0.1% Triton-X100 in IPS for 12 min and subjected to five additional washes. Nuclei were labeled incubating the tissue for 30 min with 0.5 µg/ml Hoechst. After one wash in rinsing buffer, the tissue samples were mounted in ProLong Gold antifade reagent (Invitrogen) and, after coverslip application, were examined with the confocal microscope as described in the paragraph 2.21.

To identify the process involved in FITC-Tat internalization, midgut tissue of *B. mori* larvae, mounted in Ussing chambers, were preincubated in the absence or in presence of an inhibitor of clathrin-mediated endocytosis, chlorpromazine (60 mM). Midguts were then incubated with FITC-Tat (200 µM) for 3 h. Samples were treated as described above and observed with the confocal microscope as described in the paragraph 2.21.

2.16 eGFP and Tat-eGFP transepithelial transport

To analyze the transepithelial flux of eGFP and Tat-eGFP, midguts of *B. mori* larvae were mounted on the perfusion apparatus that maintains the *in situ* shape and orientation. As reported in paragraph 2.2, eGFP and Tat-eGFP production and purification were performed in the laboratory of Prof. R. Rao (University of Naples “Federico II”).To evaluate if the CPP Tat enhances eGFP transepithelial transport, incubations were carried out in the presence of 1.5 µM eGFP or 1.5 µM Tat-eGFP in the luminal compartment. After 3 h of incubation, samples were collected from the haemolymphatic compartment and centrifuged at 12000 x g for 10min. The fluorescence of the supernatant (1 ml) was measured in a spectrofluorimeter (excitation wavelength 488 nm, emission wavelength 511 nm). After subtraction of the background fluorescence, determined on samples collected from

midguts incubated in the absence of eGFP and Tat-eGFP, the amount of protein transported was calculated by using a calibration curve produced with known amounts of the fluorescent proteins dissolved in the haemolymphatic buffer.

2.17 Transport of albumin in midgut tissue

In order to evaluate if the inhibition of lysosomal activity with specific molecules (NH_4Cl and cloroquine) increases the amount of albumin transported through the midgut epithelium of *B. mori* larvae, midgut tissues were mounted on the perfusion apparatus that maintains the *in situ* shape and orientation. Midguts were pre-incubated for 30 min in the absence (control) or in the presence of NH_4Cl (100 µM) or CQ (100 µM). FITC-albumin (14.2 µM) was added in the luminal compartment and after 2 h of incubation, the amount of protein transported was calculated as described in the previous paragraph. In this case excitation wavelength was 500 nm, emission wavelength was 520 nm.

2.18 Measurements of the shunt resistance

The transepithelial voltage (V_t) across midgut tissues isolated in Ussing chamber was measured continuously using a videographic voltmeter (Camille Bauer AG, Switzerland) connected to the bath solutions via Ag–AgCl voltage electrodes in series with agar bridges (3 M KCl, 5.5% Agar). All V_t measurements were performed assuming the lumen side as the positive pole. Solutions were connected also to a current pulse generator *via* current electrodes. Variations of V_t (ΔV_t) induced by a 1 s current pulse of 714.3 µA/cm^2 (I) were recorded and the transepithelial electrical resistance (R_t) was calculated by the Ohm law $\Delta V_t/I$ ratio ($\Omega \cdot cm^2$). In order to operate in experimental conditions in which the main component of the tissue resistance was represented by the paracellular resistance, the shunt resistance (R_{sh}) (Pannabecker *et al.,* 1992), the electrogenic V-ATPase was inactivated by incubating the midguts in the absence of K^+ (Fiandra *et al*., 2006). Since the voltage electrodes are inserted in the luminal and haemolymphatic compartments of the

Ussing chamber at a distance of 0.5 cm from the midgut, the resistance values recorded were corrected by subtraction of the solution resistance ($R_{sol}= \Delta V_t/I$).

2.19 Effects of C10 and *Jc*DNV on the paracellular electrical resistance

Larval midguts isolated from *B. mori* or *S.frugiperda* were mounted in Ussing chambers to evaluate the effect induced by sodium decanoate (C10) or by *Jc*DNV on the paracellulal electrical resistance.

When midgut were incubated with C10 the composition of the solution in the haemolymphatic compartment was (in mM): 280 sucrose, 4.8 $MgSO_4$, 1 $CaCl_2$, 5 TRIS-HCl, pH 7. The composition of the luminal solution was (in mM): 283 sucrose, 5 CAPS-TMAOH, pH 9.8. Variations of V_t (ΔV_t) induced by a 1 s current pulse were registered as described in the paragraph 2.18 "Measurements of the shunt resistance" and the electrical resistance (R_t) was calculated by the Ohm law. After 60 min, when the R_{sh} became constant, C10 (20 mM) was added to the luminal compartment of the perfusion apparatus and ΔV_t was registered for 120 min after the addition of the molecule. The R_{sh} was also calculated in midguts incubated in the absence of C10 (control).
The same experimental approach was used to evaluate if *Jc*DNV (0.1 ng/µl), added to the luminal compartment of Ussing chambers, caused a variation of the paracellular permeability in midguts isolated from *S. frugiperda* larvae. In these experiment a registration of ΔV_t across the tissue was performed for 60 min after the addition of the virus.

2.20 *Jc*DNV production and purification

To prepare *Jc*DNV stock virus, 100 *S. frugiperda* larvae were injected with *Jc*DNV and then left to grow for 7–10 days on the diet. Dead larvae were collected and virus extraction and

purification were performed on a renographine salt continuous density gradient and then dialysed as described in Jousset *et al*. (1990). Subsequently, virus was aliquoted and maintained at −20 °C until use. To verify the quality of the stock, cell supernatants were deposited on carbon-coated grids and negatively contrasted with 2% (w/v) sodium phosphotungstate, pH 7 and observed at transmission electron microscope at 50 kV (figure 2.4).

Viral lethal dose triggering 50% (LD50) was determined by infection of *S.frugiperda* cohorts with *Jc*DNV serial dilutions as described in Mutuel *et al* (2010).

*Jc*DNV particles were labelled with Cy3 using the FluoroLink Cy3 Reactive Dye 5-pack (GE Healthcare) following the manufacturer's instructions.

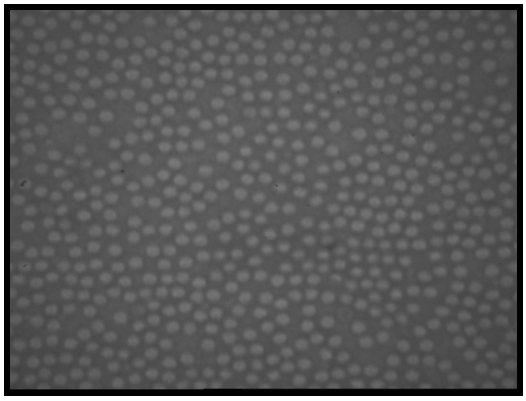

Figure 2.4: electron microscope images of *Jc*DNV negatively stained with sodium phosphotungstate.

2.21 Fluorescence acquisition and analysis

Fluorescence was acquired by using a confocal microscope CLSM TCS SP2 AOBS (Leica Microsystems Heidelberg GmbH, Germany) A 63X or 40X Leica oil immersion plan apo (NA1, 4) objective were used for the observations. FITC and eGFP were excited at 488 nm and the emitted fluorescence was collected between 500 and 560 nm; Cy3 was excited at 543 nm and the emitted fluorescence was collected between 550 and 620 nm; rhodamine was excited at 561 nm and the emitted fluorescence was collected between 570 and 600 nm Hoechst was excited at 405 nm and the emitted fluorescence was collected between

410 and 430 nm. To compare different experimental conditions (for example cells incubated with Tat-eGFP in the presence of various drugs), fluorescence acquisitions were always performed with the same hardware settings (laser intensity, sampling, acquisition rate, pinhole, and photomultiplier settings).

Results and Discussion

3.1 Strategies adopted by a densovirus to cross the midgut epithelium

Densoviruses (DNVs) are parvoviruses highly pathogenic for arthropods, mostly insect at larval stages, including agronomical pest and insect vector borne disease. They have limited host range and are not pathogenic to vertebrates, characteristics that make them particularly interesting as potential pest control agents alternative to chemical pesticides. We studied the interaction of *Junonia coenia* Densovirus (*Jc*DNV) with its host *Spodoptera frugiperda*. After oral ingestion, the virus crosses the intestinal barrier to reach the host haemocoel and replicate in the target tissues (tracheae, hemocytes, visceral muscles and epidermis) (Mutuel *et al*., 2010), but how *Jc*DNV passes through the midgut is totally unknown. Previous studies performed in my laboratory with isolated midgut cells from *S. frugiperda* larvae showed that *Jc*DNV enters specifically columnar cells, but not stem and goblet cells and that the mechanism involved in its penetration is markedly temperature-dependent, indicating the involvement of an energy-dependent process in the virus internalization (Casartelli, unpublished data).

During my PhD, we studied the mechanism adopted by *Jc*DNV to cross the midgut epithelium.

First we decided to identify the mechanism involved in *Jc*DNV internalisation in midgut cells of *S. frugiperda* larvae. Midgut tissues, mounted in Ussing chambers, were preincubated for 30 min in the absence or in the presence of three drugs able to inhibit specific endocytic pathways: dynasore that inhibits clathrin-mediated endocytosis, methyl-

β-cyclodextrine that inhibits lipid rafts-dependent endocytosis and the fungal toxin wortmannin that inhibits the early events of receptor mediated endocytosis. The virus was then added to the luminal compartment and the incubation lasted 10 min. At the end of the incubation midgut tissues were removed from the perfusion apparatus and prepared for confocal microscope observations. The images reported in figure 3.1 show that midguts incubated with the drugs did not present virus particles into the cell cytoplasm or, however, in a less amount compared to control, a clear indication that *Jc*DNV was internalized by endocytic mechanisms. Since the drugs used in these experiments interfere with different endocytic pathways, the virus probably crossed the apical membrane of columnar cells by different mechanisms. This is not a completely unexpected result. Although most parvoviruses, virus belonging to the same family of densoviruses, are known to use clathrin-mediated endocytosis (Cotmore and Tattersall, 2007; Harbison *et al,.* 2008), it has been demonstrated that this endocytic mechanism is not the only pathway involved in their internalization. The adeno-associated virus type 5 (AAV5), uses both clathrin- and caveolae-mediated endocytosis to enter D7 human embryo fibroblast (Bantel-Schaal *et al*., 2009) and the porcine parvovirus (PPV), one of the major causative agent of reproductive failure in swine, uses both clathrin-mediated endocytosis and macropinocytosis pathway to gain access into porcine test fibroblast (Boisvert *et al,.* 2010). The mechanism involved in the internalization of *Jc*DNV has been also characterized in a permissive lepidopteran cell line, *Lymantria dispar* 652 ovarian cells (Vendeville *et al* ., 2009). Treatments of the cells with methyl-β-cyclodextrine or Nystatin, which specifically inhibit lipid raft- and caveolae-dependent endocytosis, respectively, had no effect on *Jc*DNV entry. On the contrary, dynasore and chlorpromazine, two inhibitors of clathrin-dependent endocytosis, affected *Jc*DNV internalization, a clear indication that in these cells clathrin-mediated endocytosis is the main mechanism involved in *Jc*DNV internalization. Our results and those obtained by Vendeville and co-workers are in contrast, but it must be highlighted that the experiments has been performed in two different cell types, the permissive lepidopteran cell line, *Lymantria dispar* 652 ovarian cells and midgut cells, where the virus does not replicate.

For a complete picture of the early events involved in *Jc*DNV internalization, it would be essential to identify the membrane protein(s) acting as receptors for the virus. The receptor has been characterised for a few vertebrate parvoviruses (Brown *et al*., 1993) (Palermo *et al*., 2003), while no virus receptor has been yet identified for densoviruses. Recently it has been showed that two mutations on the capsid surface of *Jc*DNV were detrimental for midgut crossing but not for infection of other tissues, suggesting that these 2 residues are involved in the specific entry into midgut cells (Multeau and Ogliastro, personal communication). These findings will be of primary importance for future work aiming at identifying *Jc*DNV receptors and clarifying the mechanism of infection of this virus.

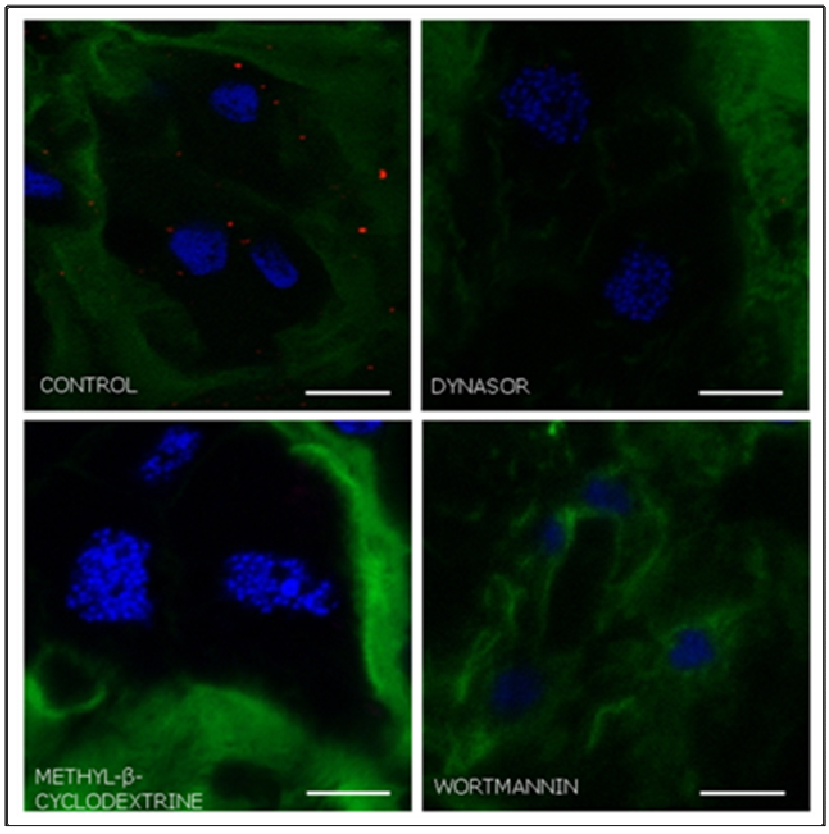

Figure 3.1: confocal laser-scanning micrographs (single optical sections) of midgut tissues preincubated for 30 min in the absence (control) or in the presence of drugs able to inhibit different endocytic mechanisms and incubated for 10 min with *Jc*DNV (red). Actin filaments (green) were labelled with FITC-phalloidin and nuclei (blue) with Hoechst. Bars: 20 µm

Once established that different endocytic mechanisms are involved in *Jc*DNV entry into midgut cells, we studied the intracellular pathway followed by the virus analyzing the time-dependent colocalisation events with two specific endocytic tracers: Rab 5- and Rab 7-GTPaes, markers of early and late endosomes, respectively (Hutagalung and Novick, 2011).

We incubated midgut tissues, mounted in Ussing chambers, with *Jc*DNV added to the luminal compartment for 5 min and then the tissues were stained with an anti-Rab-5 GTase. In figure 3.2.A is clearly visible that early endosomes (green) colocalized (yellow) with virus particles (red).

To evaluate if the virus follows the degradative pathway, we incubated the tissue, mounted in Ussing chambers, with *Jc*DNV added to the luminal compartment for 15 min and then the tissues were stained with an anti-Rab-7 GTPase. Figure 3.2.B shows that *Jc*DNV (red) colocalized (yellow) with late endosomes (green), suggesting that, after the internalization, the virus follows the degradative pathway.

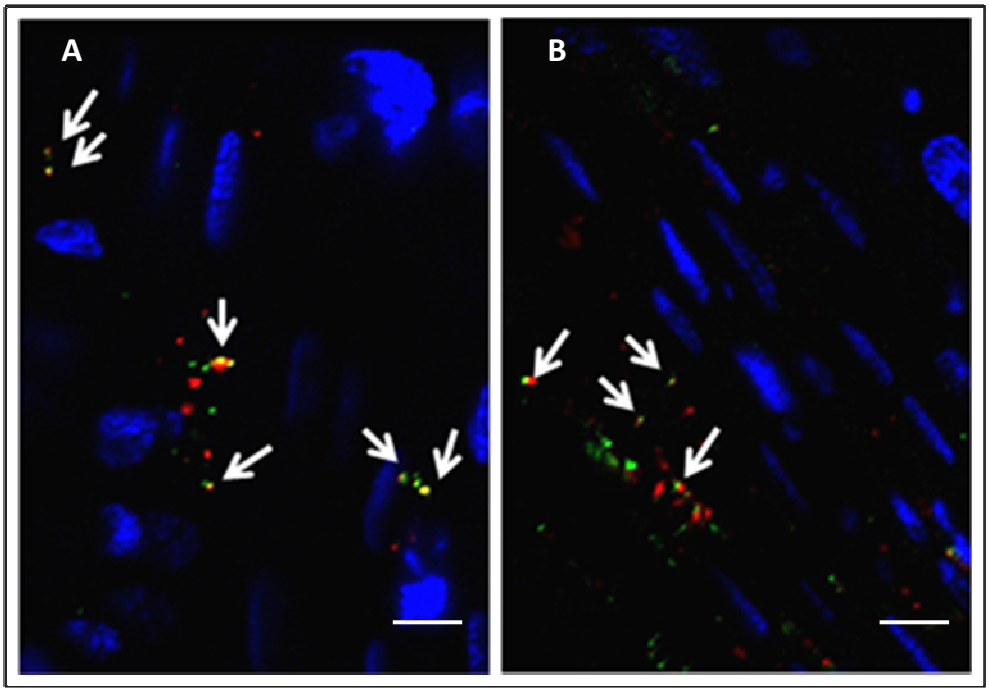

Figure 3.2: confocal laser-scanning micrographs (single optical section) of midgut tissues incubated for 5 (A) or 15 min (B) with *Jc*DNV (red). Arrows indicate the colocalization events (yellow) between the virus and Rab-5 (A) or Rab-7 GTPases (B) (green), markers of early and late endosomes, respectively. Nuclei (blue) were labelled with Hoechst. Bars: 20 µm.

Also in the permissive lepidopteran cell line, *Lymantria dispar* 652 ovarian cells, *Jc*DNV follows the degradative pathway (Vendeville *et al.*, 2009). The authors demonstrated that after 30 min of incubation with *Jc*DNV, 50% of the virus was present in early/recycling endosomes and 20% in late endosomes. Moreover, incubating the cells with two drugs known to raise the pH in endosomes and lysosomes, chloroquine and ammonium chloride, they demonstrated that *Jc*DNV productive infection required transit through late endocytic compartments. It has also been shown that endosomal acidification is essential for parvovirus infection, triggering capsid structural rearrangements and escape of the virus from endosomes into the cytoplasm (Douar *et al*., 2001; Mani *et al*., 2006). Since *Jc*DNV does not replicate in midgut cells, the presence of the virus in the acidic organelles (figure 3.2) is probably not necessary for its replication. In midgut cells of *S. frugiperda* larvae the presence of *Jc*DNV in early and late endosomes simply indicates that the virus, after internalization, is directed to the degradative pathway. This finding opens the question of how the virus is able to cross the gut barrier and reach the internal target tissues.

Taking into account that after internalization by midgut cells *Jc*DNVs are directed to the intracellular degradative pathway (figure 3.2), to clarify how the virus crosses the midgut barrier we decided to evaluate its localization in whole-mount midgut after different time of incubation. Midgut tissues of *S. frugiperda* larvae were mounted in Ussing chambers and incubated for 10, 30 or 60 min with Cy3-*Jc*DNV added to the luminal side of the perfusion apparatus. At the end of the incubation, tissues were removed from the apparatus and prepared for confocal microscope observations. The confocal images of whole-mount midguts show that after 10 min virus particles were already detectable in the enterocytes' cytoplasm (figure 3.3.A, arrows). After 30 min, the virus appeared in the intercellular spaces (figure 3.3.B, arrows) and a more intense paracellular signal was observed after one hour of incubation (figure 3.3.C).

The localization of *Jc*DNV in the intercellular space of the epithelium could be due to the ability of the virus to affect the permeability of the paracellular pathway. To test this hypothesis a registration of the paracellular electrical resistance or Shunt resistance (R_{sh}) has been performed in midgut tissue isolated in Ussing chambers in the absence or in the presence of the virus added to the luminal compartment. The decrease of R_{sh} indicates an

increase of the septate junction permeability, so that ions move more rapidly through the aqueous channels formed by the intercellular junctions. Figure 3.3.D shows that in 10 min the virus induced a significant decrease of R_{sh}, which further declined with longer time of exposition.

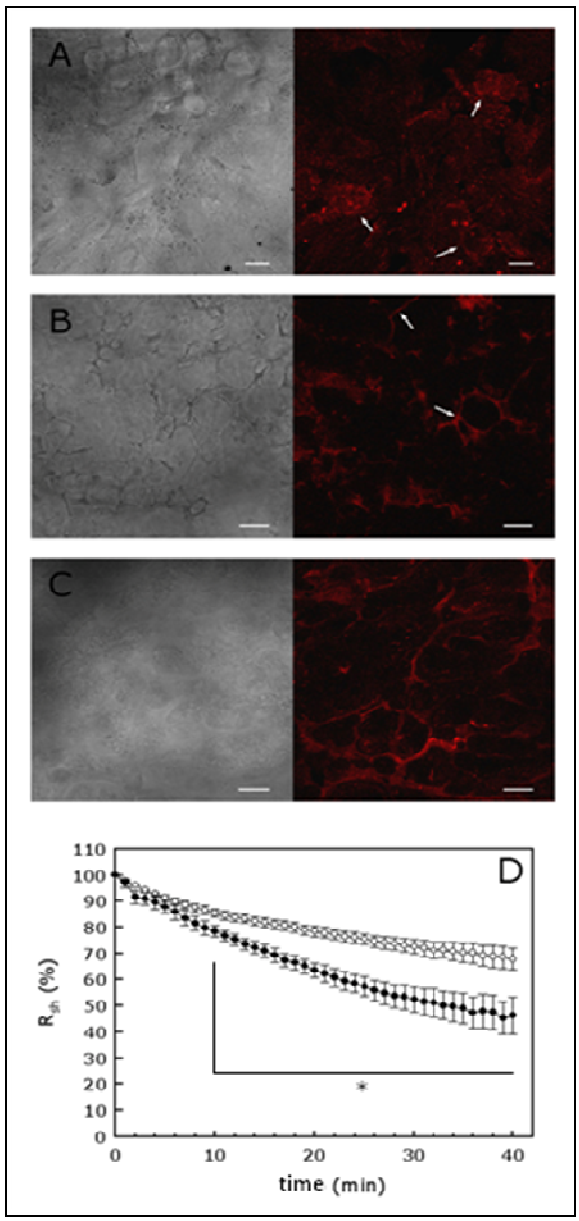

Figure 3.3: Brightfield (left) and confocal laser scanning micrographs (single optical section) (right) of whole-mount midguts after 10 (A), 30 (B) or 60 (C) minutes of incubation in the presence of Cy3-*Jc*DNV in the luminal compartment. Bars: 10 µM (A and B) and 20 µm (C). D: Shunt resistance values (R_{sh}) with time in the presence (close circle) or in the absence (open circle) of *Jc*DNV. R_{sh} values are expressed as % of the initial value (12.5 ± 3.5 Ω·cm^2 or 9.9 ± 2.5 Ω cm^2, in the absence or in the presence of *Jc*DNV, respectively. The values are means ± s.e. of three different experiments). Student's *t* test: *$P < 0.05$

These results indicate that the interaction of *Jc*DNV with the receptors and/or its internalization into midgut cells cause an alteration of the paracellular permeability. Considering the small size of the densoviruses capsid (20-26 nm), the enlargement of the paracellular route induced by the virus itself can be sufficient to allow the passage of *Jc*DNV through this pathway. It can be feasible that the increase of the paracellular permeability induced by the virus is a strategy adopted by the virus itself to promote its permeation through this route. Since *Jc*DNV, after internalization into midgut cells, is directed to the degradative pathway (figure 3.2), the paracellular pathway represents the main route followed by the virus to reach the haemocoel and therefore its target tissues.

The ability of viruses to cause changes in the permeability of the paracellular route has been already reported in literature. Golebiewski *et al.* (2011), showed that infection of polarized MDCK cells with the avian influenza NS1 ESEV virus causes the functional disruption of the tight junction (TJ), as demonstrated by the altered localization of the junctional proteins ZO-1 and Occludin, by the decrease of the transepithelial electrical resistance (TER), and by the increase of the diffusion of the paracellular tracer inulin across the polarized cell monolayer. Nava *et al.* (2004) demonstrated that the rotavirus protein VP8 is capable of disrupting the TJs in MDCK cells in a reversible, time and dose dependent manner. VP8 alters both the gate and fence function of intercellular TJs: in the presence of the protein a decrease of TER and an increase of the paracellular permeability to non-ionic tracers were recorded.

Our results demonstrate that also *Junonia coenia* densovirus causes an increase of the paracellular permeability in the larval midgut tissue of *S. frugiperda*, probably causing an alteration of the structural organization and/or an alteration of the functional properties of the septate junctions (SJ). The increase of the paracellular permeability allows the free diffusion of the virus through this pathway, that can thus cross the intestinal barrier and reach the internal target tissue.

It has been recently demonstrated in lepidopteran larval midgut that a modulation of cytosolic Ca^{2+} concentration induces a decrease of the paracellular permeability (Fiandra *et al*., 2006). To evaluate if the binding of *Jc*DNV to the plasma membrane and/or its

internalization into columnar cells of *S. frugiperda* larvae could trigger a cascade of signals which stimulates an increase of this intracellular mediator, we used Fluo-3AM, a cell permeant Ca^{2+}-sensitive fluorescent dye. Midgut cells obtained by enzymatic disaggregation of *S. frugiperda* larval midgut were loaded with Fluo-3AM, incubated for 10 min in the absence (control) or in the presence of *Jc*DNV and immediately observed with a fluorescent microscope (figure 3.4). It is evident that a large number of fluorescent cells were present in the sample incubated with the virus. 200 cells were observed for each experimental condition: in control sample the percentage of fluorescent columnar cells was 22 ± 1%, whereas in *Jc*DNV-treated sample the percentage raised to 73 ± 3% (means ± s.e. of three different experiments, $P < 0.001$, Student's *t*-test). The fluorescence intensity measured in the two conditions was also significantly different: in control fluorescent columnar cells we quantified a value of 1.88 ± 0.13 (a.u) and in those incubated with *Jc*DNV a value of 2.80 ± 0.08 (a.u.) (means ± s.e. of at least 100 cells, $P < 0.001$, Student's *t*-test).

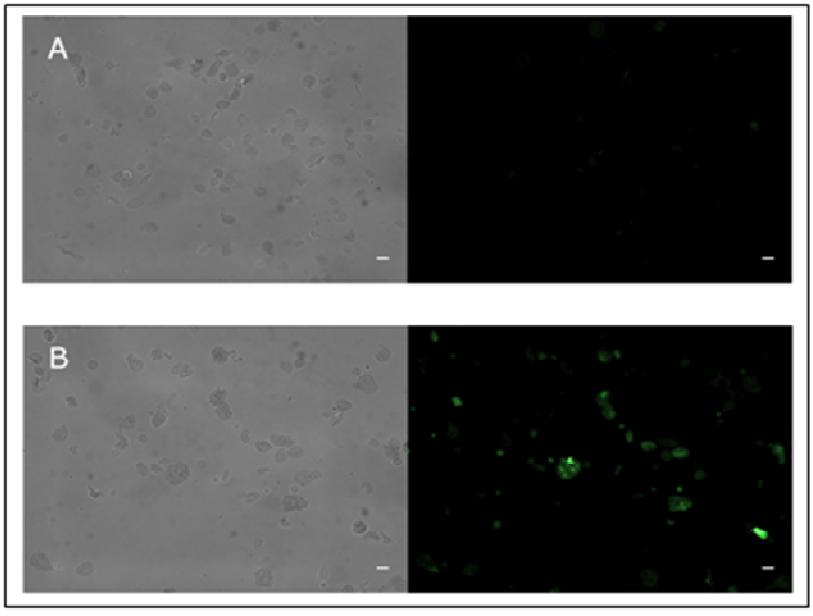

Figure 3.4: Brightfield (left) and fluorescent (right) micrographs of midgut cells obtained by enzymatic disaggregation and incubated in the absence (A) or in the presence (B) of *Jc*DNV for 10 min. Intracellular Ca^{2+} level was evaluated using the cell permeant Ca^{2+}-sensitive fluorescent dye Fluo-3AM. Bars: 20 µm

Our results indicate that *Jc*DNV modulates the permeability of the paracellular pathway by increasing the cytosolic calcium concentration.

But a question remains open: how can *Jc*DNV cause an increase of intracellular calcium concentration? It is becoming increasingly apparent that there are significant functional interactions between calcium and redox species, and that these interactions modify a variety of proteins that participate to signaling transduction pathways and other fundamental cellular functions. In particular, variations in ROS concentrations can affect cellular calcium-signaling pathways by modulating the activity of calcium pumps and by stimulating calcium release from internal stores (reviewed in Hidalgo and Donoso, 2008). In this context, reactive oxygen species have a physiological role as second messengers and are not toxic to cells. Alterations of redox condition occurs in a cell because of either an inhibition of anti-oxidant enzyme activities or an increased production of oxidants. Modifications of the oxidative status after a viral infection have been observed in mammalian cells (Akaike and Maeda, 2000; Schweizer and Peterhans, 1999), but also in the insect cell lines Sf-9 and Tn-5B1-4, infected with *Autographa californica* multiple nucleopolyhedrovirus (*Ac*MNPV) (Wang *et al*., 2001).

Taking into account these evidences, to verify if the raise of intracellular calcium concentration in midgut cells could be caused by an alteration of redox condition, we measured superoxyde dismutase (SOD) activity in cells incubated for 10 min in the absence or in the presence of *Jc*DNV. This enzyme is involved in the detoxification from pro-oxidants also in Lepidoptera (Wang *et al*., 2001; Krishnan and Kodrik, 2006). The cells exposed to the virus presented a significantly lower SOD specific activity compared to control. The values, expressed in mU/mg of protein, were 58.16 ± 3,58 (means ± s.e. of 7 determination) and 47.09 ± 3.58 (means ± s.e. of 8 determination), respectively ($P < 0.05$, Student's *t*-test). Our results and the recent evidences on the involvement of alterations in redox condition in the generation and modulation of physiological calcium signals suggest that the rise of intracellular Ca^{2+} concentration in absorptive midgut cells is the consequence of the redox modification induced by the virus.

To evaluate the efficiency of *Jc*DNV transepithelial passage, we quantified the amount of virus crossing the midgut. Midguts were mounted in Ussing chambers and *Jc*DNV was added to the luminal compartment to evaluate the amount of viral particles able to cross the midgut from the luminal to the haemplymphatic compartment. Viral particles were recovered in each compartment, DNA was extracted and viral genomes quantified by qPCR. The efficiency was given after 10 and 30 min of incubation as the ratio of viral genomes found in the haemolymphatic content on the total amount of virus estimated in both compartments. Figure 3.5 shows that after 10 min of incubation the amount of virus able to cross the epithelium was significantly lower compared to that measured after 30 min. After 10 min of incubation the lumen to haemolymph flux of the virus (expressed as viral genomes in haemolymphatic compartment/viral genomes in (haemolymphatic compartment + luminal compartment)/min) was $6.77 \times 10^{-6} \pm 0.80 \times 10^{-6}$, a value significantly lower than that calculated after 30 min of incubation, $2{,}17 \times 10^{-6} \pm 1.41 \times 10^{-6}$ ($P < 0{,}05$, Student's *t* test).

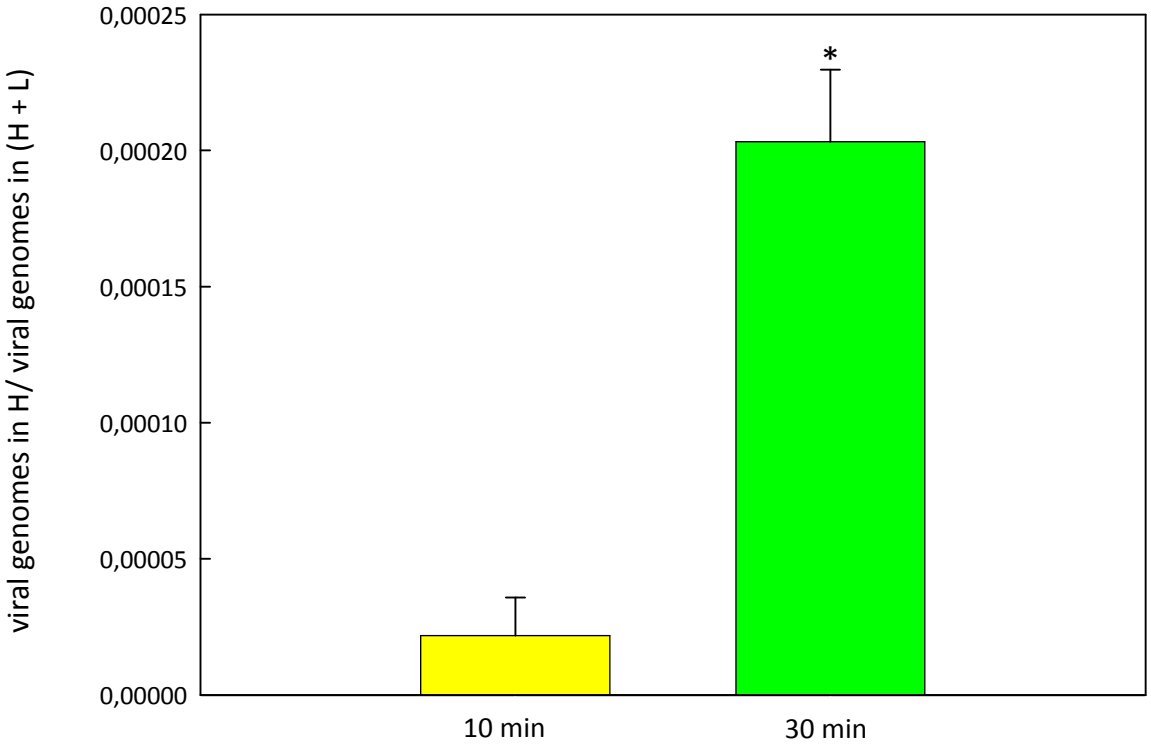

Figure 3.5: quantification of the lumen(L)-to-haemolymph(H) passage of *Jc*DNV after 10 or 30 min of incubation. The values are means ± s.e. of three different experiments. Student's *t* test: $*P < 0.05$.

These results are in agreement with the time-dependent effect of *Jc*DNV on the paracellular permeability and with the time-dependent localization of the virus in the intercellular space of the epithelium reported in figure 3.3. A significant *Jc*DNV transepithelial flux is observable only when the permeability of the paracellular route increases as a consequence of virus challenge.

Therefore, the mechanism by which *Jc*DNV sets in motion its delivery strategy can be summarized in the following steps:

- *Jc*DNV is internalized into columnar cells by different endocytic mechanisms;
- the interaction of the virus with its receptors and/or its internalization cause a modification of the cell oxidative status;
- the variation of the oxidative status affects calcium signaling pathways and causes the increase of intracellular Ca^{2+} concentration;
- the increased concentration of this intracellular mediator causes a raise of the paracellular permeability;
- *Jc*DNVs cross the midgut epithelium in a massive amount through the paracellular route, avoiding the intracellular degradation;
- the virus reaches the internal target tissues.

The first step of *Jc*DNV infection is its interaction with the receptors expressed on apical membrane of midgut cells. To shed light on this fundamental event, it is essential to establish which viral capsid protein is involved. Considering that *Jc*DNV capsid is composed of four structural proteins (VP) and VP4 represents about 60% of the total proteins, we evaluate the role of this structural protein in *Jc*DNV internalization. Moreover, it has been recently shown that virus-like-particles (VLP) containing only the major structural protein VP4 are able to enter *L. dispar* 652 ovarian cells similarly to fully-virus-capsid (Vendeville *et al.*, 2009). Midgut tissues mounted in Ussing chambers were incubated with VP4-VLP for 10 min. At the end of the incubation tissues were removed from the perfusion apparatus, subjected to an immunofluorescence assay and examined at the confocal microscope. In contrast with what reported in Vendeville *et al.* (2009), VP4-VLP are not able to enter

columnar cells after 10 min of incubation, revealing an important role for the other three viral structural proteins in the cell membrane attachment and/or in the infectious routing of viral particles (figure 3.6).

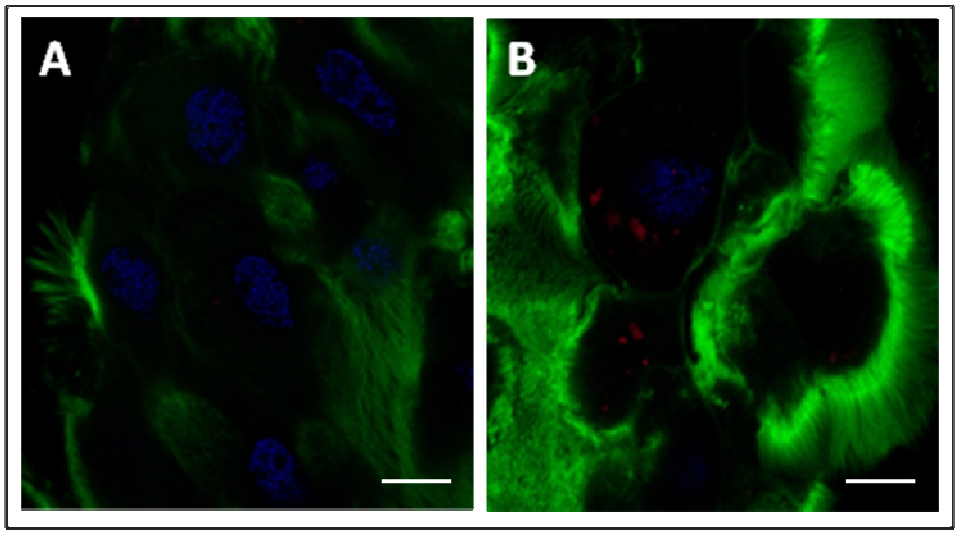

Figure 3.6: confocal laser-scanning micrographs (single optical section) of midgut tissues incubated with VP4-VLP (A) or with *Jc*DNV (B) for 10 min. VP4-VLP and *Jc*DNV are visible in red. Actin-filaments are labeled with phalloidin-FITC (green) and nuclei with Hoecst (blue). Bars: 20 µm

During the second year of my PhD I spent six months at the "Laborotoire de Biologie Integrative et Virologie des Insect" INRA-UMII (Institute National de la Researche Agronomique, Montpellier, France) under the supervision of Dr. Mylène Ogliastro. During my stay I continued the study on the interaction between *Jc*DNV and the permissive host *S. frugiperda.* To study the global change in gene expression in midgut cells induced by *Jc*DNV infection, I have performed a global transcriptomic analysis by Serial Analysis of Gene Expression (SAGE) and I validated the results by quantitative PCR (qPCR).

SAGE is an approach that allows the rapid and detailed analysis of thousands of transcripts (Velculescu *et al*., 1995).

Three principles underlie the SAGE methodology:

1. A short sequence tag (10-14bp) contains sufficient information to uniquely identify a transcript, considering that the tag is obtained from a unique position within each transcript;
2. Sequence tags can be linked together to from long serial molecules that can be cloned and sequenced, revealing the identity of multiple tags simultaneously;
3. The expression pattern of any population of transcripts can be quantitatively evaluated by determining the abundance of individual tags and identifying the gene corresponding to each tag.

In our study, SAGE libraries were generated from midgut cells of virally infected or control larvae of *S. frugiperda* at 24 or 72 hours post infection (pi). At 24 h pi the viral replication is not initiated in tissues where the replication occurs, by 72 h pi, viral genome amplification is clearly observed in target tissues and became exponential at 4 days pi (Mutuel *et al*., 2009). The protocol used in SAGE libraries preparation can be summarized in the following steps:

- larvae were infected individually by feeding with 1 mm^3 of diet contaminated with *Jc*DNV (control larvae were fed with 1 mm^3 of non-contaminated diet);
- infected and not infected larvae were then fed with fresh food for 1 or 3 days;
- larvae were sacrificed, the midguts were isolated and mature columnar cells were obtained by enzymatic disaggregation of the tissue;
- total RNA was purified from the two cells populations and used in SAGE library construction, made by the Skuldtech (Montpellier).

Each library from virus-infected larvae was compared with the corresponding library from control larvae to determine differentially expressed genes. Our results showed that 6318 tags were significantly regulated at 24 h post infection and 8586 tags were regulated at 72 h post infection.

One of the objective of my stay in the Dr. Mylène Ogliastro's laboratory was the validation of the SAGE method by qPCR. Based on the results obtained by SAGE analysis, we selected

four not regulated genes and we performed a qPCR using the total RNA extracted from the midgut cells of infected and non infected larvae. We demonstrated that effectively these genes were not regulated by *Jc*DNV infection, confirming the validity of the SAGE analysis.

Two of the four tags utilized in the analysis correspond to unknown genes, one is the Eukaryotic translation initiation factor 4E-binding protein 2 and the last is the Ccr4-associated factor, an evolutionary conserved protein complex that plays an important role in the control of transcription and mRNA decay.

The characterization of differentially up-regulated or down-regulated genes is on going in the Dr. Ogliastro's laboratory in Montpellier. Preliminary data indicate that some of the genes regulated in midgut cells of *S. frugiperda* larvae infected by *Jc*DNV are involved in apoptosis process (Gosslen, personal communication).

Barat-Houari *et al.* (2006) developed a cDNA microarray to analyze the gene transcription profile of the lepidopteran pest *S. frugiperda* in response to haemocoel injection of *Jc*DNV. They demonstrated that the transcript levels of 8 genes (0.51% of the arrayed cDNAs) displayed a significant increase (up to 5.8-fold) in *S. frugiperda* fat body 24 hours after injection of *Jc*DNV. Among the regulated genes, some are involved in the insect humoral response, for example lysozyme, a widely distributed ubiquitous enzyme involved in self-defense from bacterial infection. Also genes encoding proteins putatively involved in the insect cellular immune response and/or non-self recognition were regulated. This study was performed in the fat body of *S. frugiperda*, a tissue where *Jc*DNV replicates. It could be interesting to verify whether the genes regulated in the midgut, where the replication does not occur, are the same or whether they are involved in endocytosis, intracellular trafficking, or signal transduction (Brault *et al*., 2010), three important steps in the internalisation and transport of viruses.

Development of such global approaches will allow a better understanding of the strategies employed by viruses to manipulate their host physiology, and will permit the identification of potential targets of *Jc*DNV.

3.2 Strategy to enhance the permeability of the paracellular route

The reduction of chemical insecticide use is one of the major issues for safe food production. The importance of this objective in modern agriculture has fostered significant research efforts towards the development of innovative technologies based on the use of biological control agents (Bale *et al*., 2008), natural insecticides, which include peptide or protein toxins, deriving from plants and insect natural antagonists (Whetstone and Hammock, 2007). For an effective oral delivery of these potential bioinsecticides it is crucial to develop strategies to facilitate their passage through the insect midgut barrier. They can reach the haemocoel either though the cellular pathway, crossing the two polarized plasma membranes of the epithelial cells, or through the paracellular pathway along the aqueous channel formed by the junctional complexes, according to the physico-chemical and biological properties of each molecule. The insect midgut, paracellular pathway is particularly interesting for the delivery of bioinsecticides with a low molecular weight targeting haemocoelic receptors. Moreover in our laboratory it has been recently demonstrated that the permeability of this route can be modulated: in lepidopteran larval midgut, an increment of cAMP or Ca^{2+} concentration in the cytosol induces the opening of the septate junction (SJ) and the increase of the paracellular permeability (Fiandra *et al.,* 2006). It is now important to identify the signaling pathway(s) that may lead to the increase of these intracellular mediators and clarify how these molecules can modulate the permeability of the junction.

To study one of the signaling pathway(s) that may lead to the intracellular release of Ca^{2+} responsible for the increase of the junction permeability, we took advantage of sodium caprate (C10), a medium-chain fatty acid (MCFA) known to modulate the mammalian tight junction (TJ) by activation of a Ca^{2+} ions-mediated intracellular signaling pathway (Cano-Cebrian *et al*., 2005). In mammalian intestine, several sodium salts of MCFAs are known to cause a consistent increase of TJ permeability (Lindmark *et al*., 1995).

As above mentioned, it has been proposed (Cano-Cebrian *et al.,* 2005), on the bases of different experimental evidences, that C10 enhances the paracellular route by triggering

the IP_3-dependent signaling cascade: Ca^{2+} release from the intracellular stores and activation of myosin light chain kinase (MLCK) are followed by myosin phosphorylation and contraction of the perijunctional actin-myosin ring connected to the tight junction.

Therefore, we decided to verify whether C10 could modulate the permeability of the paracellular route also in insect. To this end, we incubated for 180 min isolated midgut from *B. mori* larvae in Ussing chambers and we registered the possible variation in the paracellular resistance or Shunt resistance (R_{Sh}) in the absence (control) or in the presence of C10, added to the luminal compartment after 1 h of incubation. The graph reported in figure 3.7 shows paracellular resistance values (R_{sh}) with time in midguts incubated in the two experimental conditions. R_{sh} values are expressed as percentage of the value recorded 90 min after the start of the incubation. These values are: 60.21 ± 2.58 Ω·cm^2 and 59.87 ± 2.19 Ω cm^2, in the absence and in the presence of C10, respectively (means ± s.e. of five different experiments). Time 0 in the graph represents the thirtieth min after the addition of C10 in the luminal compartment and, in control sample, the ninetieth min from the beginning of the incubation. We have not reported in the graph the values calculated in the first 90 min of incubation since no variation of R_{sh} are observed in the two experimental conditions. The data reported in figure 3.7 show that in 45 min (fifteenth min in the graph) C10 induces a significant decrease of R_{sh}, which further declines with longer times of exposition. It is possible to conclude that C10 causes, also in midgut epithelium of *B. mori* larvae, a decrease of the transepithelial shunt resistance, i.e. an increase of the junction ion conductance.

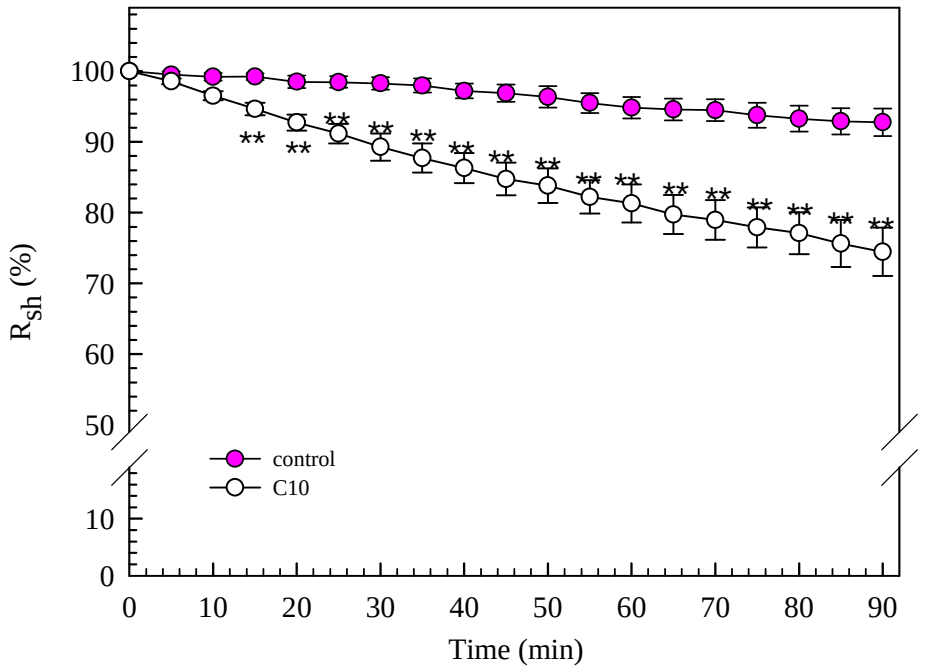

Figure 3.7: paracellular resistance values with time in midgut of *B. mori* larvae in the absence (white circle) or in the presence (pink circle) of C10, 20 mM. (The values are means ± s.e. of five different experiments. Student's *t* test: $^{**}P < 0.01$.

To verify the ability of C10 to increase the permeability of the paracellular route not only to ions but also to organic molecules, midgut tissues, mounted in Ussing chambers, were incubated with proctolin labeled with rhodamine (rh-proctolin) (649 Da) or fluorescein (332 Da). The amount of the molecules able to cross the midgut epithelium was calculated in the absence or in the presence of C10.

Proctolin is a neuropeptide identified in the nervous system of different orders of insects and it has been proposed as a possible pest control agent (Bavoso *et al*., 1995; Fiandra *et al*., 2010). This peptide crosses the lepidopteran midgut barrier only through the paracellular pathway (Fiandra *et al*., 2009), for this reason it can be used to evaluate the effect of C10 on the permeability of the paracellular route. Midgut tissues were mounted in Ussing chambers and incubated for 120 min with rh-proctolin added to the luminal compartment, in the absence (control) or in the presence of C10. At the end of the incubation time the amount of rh-proctolin in the haemolymphatic solution was quantify

with a spectrofluorometer. The amount of rh-proctolin able to cross the midgut barrier was significantly higher in midgut incubated in the presence of C10 compared to the control (figure 3.8).

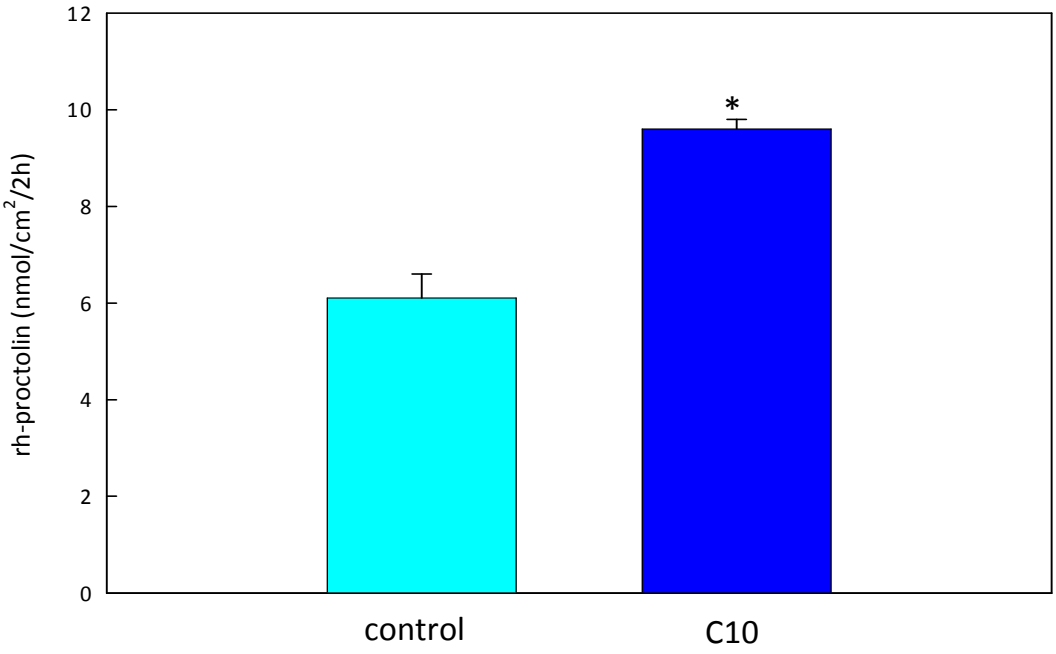

Figure 3.8: lumen-to-haemolymph flux of rh-proctolin (130 µM) after 120 min of incubation in the absence (control) or in the presence of C10 (20 mM). Mean values ± e.s. of 3 different experiments. Student's *t* test *P<0.05.

At the end of the incubation time, midguts were removed from the Ussing chambers and observed with a confocal microscope. In midgut tissues incubated in the absence of C10 (control), the fluorescent signal due to the presence of rh-proctolin in the intercellular spaces was rather weak, indicating that the permeability of the SJ to the peptide is extremely low (figure 3.9). On the contrary, in samples incubated in the presence of C10, rh-proctolin can abundantly diffuse in the intercellular spaces (figure 3.9), confirming the ability of the fatty acid to increase the permeability of the septate junction to organic molecules.

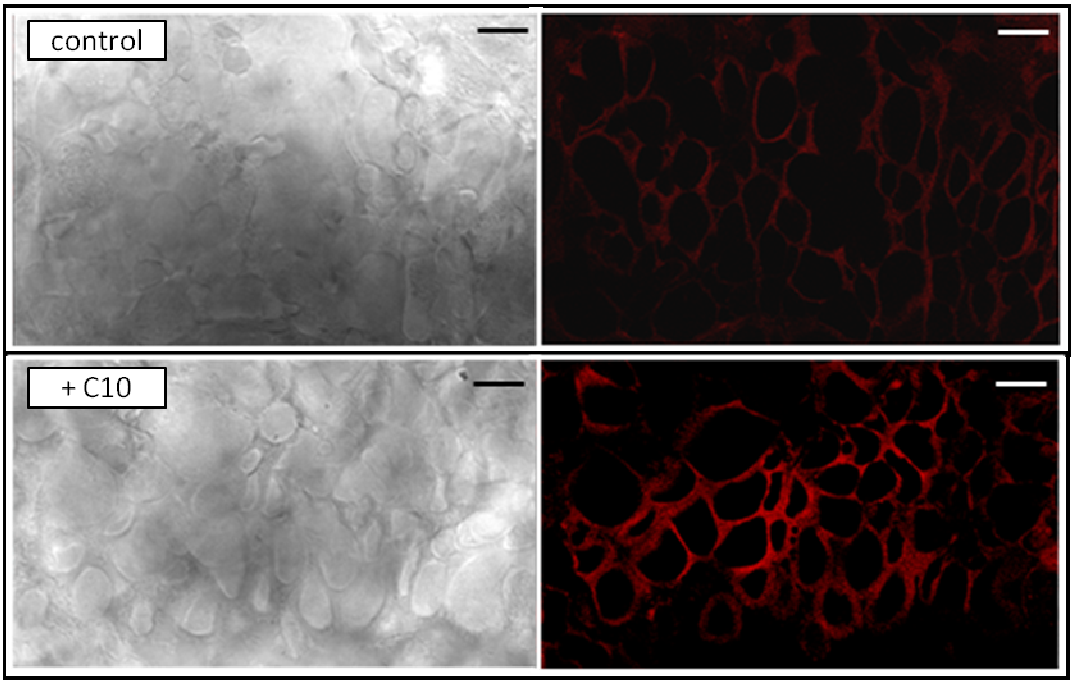

Figure 3.9: brightfield and confocal laser-scanning micrographs (single optical section) of midgut tissues incubated with rh-proctolin (130 µM) in the absence or in the presence of C10 (20 mM). Bars: 20 µm

The ability of C10 to increase the permeability of the paracellular route to organic molecules was also demonstrated measuring the flux of fluorescein. Fluorescein is not able to cross the plasma membrane of intestinal epithelial cells of *B. mori* larvae (Casartelli, unpublished data). Therefore fluorescein, like proctolin, is a good tracer of the SJ permeability and suitable for evaluating the effect of C10 in midgut tissue of lepidopteran larvae. Moreover, the apparent permeability coefficient of fluorescein through the gut epithelium of *B. mori* larvae is low (Fiandra *et al*., 2009). Midguts were incubated for 120 or 180 min with fluorescein added to the luminal solution in the absence (control) or in the presence of C10. Figure 3.10 shows the amount of fluorescein able to cross the midgut epithelium in the two experimental condition after the different time of incubation. Fluorescein passage was significantly increased after three hours of exposure to C10. After 120 min, the passage of the fluorescent molecule in the presence of C10 is greater than in control midgut, even though the values are not significantly different.

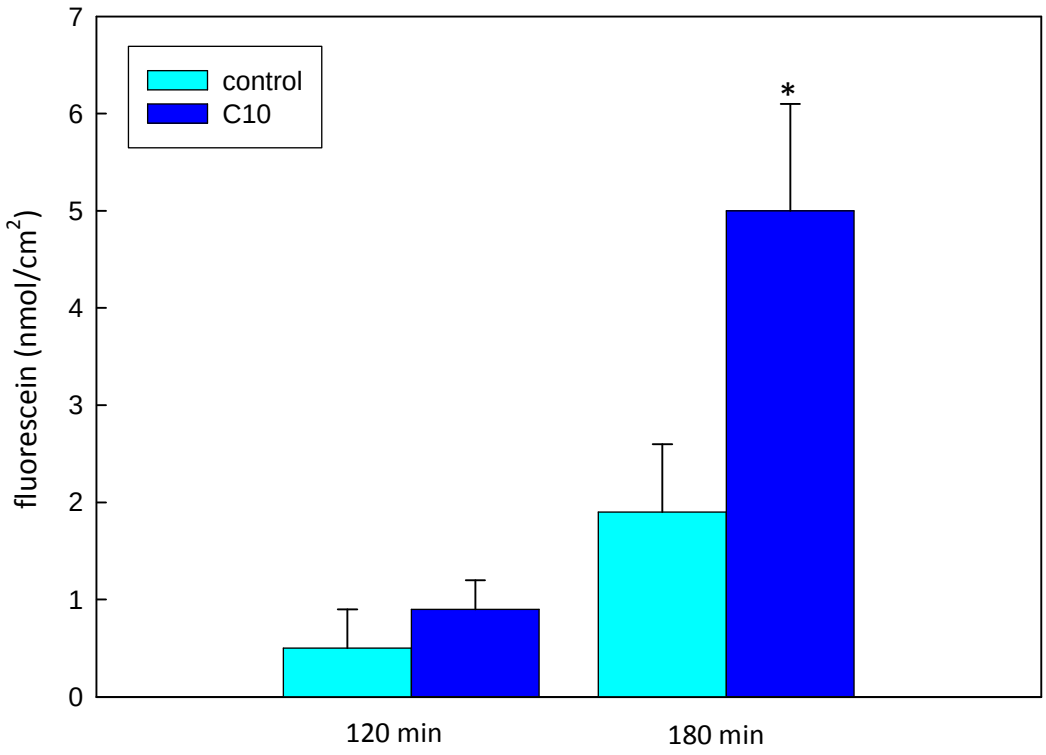

Figure 3.10: lumen-to-haemolymph flux of fluorescein (3 mM) after 120 or 180 min of incubation in the absence or in the presence of C10 (20 µM). Mean values ± e.s. of 3 different experiments. Student's *t* test * P <0.01.

These data clearly demonstrate the ability of C10 to increase the permeability of the paracellular route to ions and organic molecules, and show that C10 requires at least 45 min of incubation to affect the paracellular permeability to ions (figure 3.7) and at least 2 h to affect the paracellular permeability to organic molecules (figure 3.8) in the midgut epithelium of lepidopteran larvae. On the contrary, in mammals, the effect induced by C10 on the permeability of the thigh junction is much faster (Chao *et al*., 1999). This difference could be due to the different organization of the occluding junctions of vertebrates (tight junctions) and invertebrates (septate junction) (Beyenbach *et al.,* 2009). TJs are located at the most apical region of epithelial cells and they extend into the paracellular pathway for only a short distance, less than 1 micron. Moreover, TJs are points of contact between neighboring cells that are formed by the interaction of the extracellular loops of the integral membrane proteins, claudin and occludin (Furuse *et al*., 1998). Interactions of

these extracellular loops obliterate the extracellular space and give the appearance of the focal fusion of the plasma membranes of neighboring cells. Beyond the less than 1 µm region of the vertebrate TJ, the lateral interstitial space accounts for more than 95% of the length of the paracellular pathway. In contrast, SJs span the whole height of the epithelial cells from apical to basal poles over the length of many microns. Ladder-like septa appear to make sure that the lateral plasma membranes of adjacent cells do not fuse. They are kept approximately 10-20 nm apart. What forms the rungs of the paracellular ladder is unknown. The constitution of the electron-dense material in the space between septa is also unknown. In the view of the wide paracellular space (10-20 nm) and the small diameters of ions and some organic molecules, like glucose, it follows that the solutes can occupy the intercellular septate junctional space, unless septa prevent access. Preventing access may account for the barrier function of septate junctions. By contrast, a reversible, zipper-like opening of the septa would provide access, thereby increasing the paracellular permeability. Taking into account the SJs span nearly the whole lateral membrane of epithelial cells, such an increase could require a certain time.

In vertebrate, claudins and occludins provide the barrier and permselectivity properties of the tight junctions. Moreover, claudins display a stunning spontaneous breaking and resealing (Sasaki *et al*., 2003). Similarly, the opening and closing of septa-forming proteins could regulate the permeability and conductance of sepate junction (Beyenbach *et al*., 2009). The finding of claudin-like proteins, such as sinuous and megatrachea in SJ (Behr *et al*., 2003; Wu *et al*., 2004), raises the intriguing question of whether SJ also undergo spontaneous turnover and remodeling. Cytoskeletal elements that interact directly or indirectly with these proteins play a fundamental role in their organization, so a destabilization and/or reorganization of cytoskeletal elements can be essential to modulate the paracellular permeability. The discovery of molecules able to modulate the paracellular permeability and the identification of the molecular mechanisms involved are of primary importance to define appropriate strategy to increase the paracellular permeability to small organic molecules with an insecticide activity targeting haemocoelic receptors. The demonstration that C10 is an enhancer of the paracellular permeability in

the midgut of lepidopteran larvae and the identification of the molecular actors involved in the pathway activated by this fatty acid is a first step in this direction.

Since in midgut tissue of *B. mori* larvae, the permeability of the paracellular pathway can be modulated by a fine regulation of cytosolic Ca^{2+} concentration (Fiandra *et al.,* 2006), and the raise of Ca^{2+} concentration is a fundamental step in the IP_3-dependent signaling cascade induced by C10 in mammals (Cano-Cebrian *et al*., 2005), we decided to evaluate whether the signal cascade trigged by C10 involves Ca^{2+} release from the intracellular stores also in Lepidoptera. Free cytosolic calcium was measured using the cell permeant Ca^{2+}-sensitive fluorescent dye Fluo-3AM. Midgut cells obtained by enzymatic disaggregation of the tissue were loaded with Fluo-3 AM and then incubated in the absence (control) or in the presence of C10 (2 mM) and immediately observed for 15 min with a fluorescence microscope. Cells incubated in the absence of C10 showed a very weak fluorescent signal that did not vary during the incubation time, as shown by the images in figure 3.11 A and C. On the contrary, in cells incubated with C10 a transient increase of cytosolic calcium concentration was observed with a maximum after 5 min of incubation (figure 3.11 B). After 10 minutes of incubation in the presence of C10 the fluorescent signal drastically decreases (Figure 3.11 D). Therefore, we can conclude that C10 causes a transient increase of intracellular Ca^{2+} in midgut cells of lepidopteran larvae, similar to that observed in Caco-2 mammalian cells (Kimura *et al*., 2001).

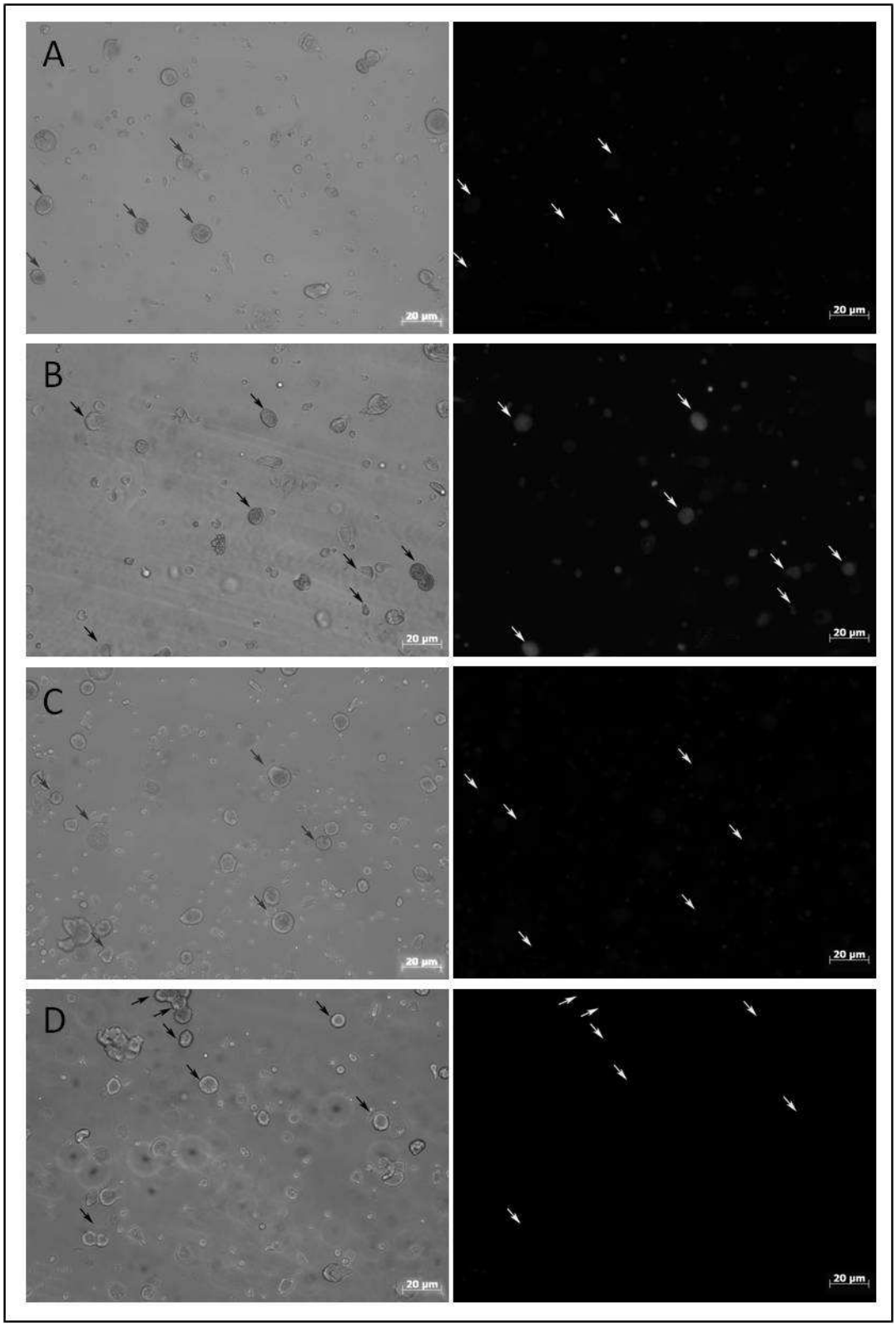

Figure 3.11: brightfield and fluorescence micrograph of *B. mori* midgut cells obtained by enzymatic disaggregation of the tissue incubated in the absence (A and C) or in the presence (B and D) of C10 (2mM) after 5 or 10 min of incubation.

The modulation of the paracellular permeability has been widely studied in insect Malpighian tubules. Beyenbach *et al*. (2009), on the basis of different experimental evidences, proposed a model to explain the mechanism of action of diuretic neuropeptides in causing the increase of the paracelluler permeability in *Aedes aegypti* Malpighian tubules. These neuropeptides, after binding of their specific receptors, activate phospholipase C which converts phosphatidylinositol (4,5)-bisphosphate into two intracellular messengers: membrane associated diacylglycerol (DAG) and cytoplasmic inositol (1,4,5)-trisphosphate (IP3). The binding of IP3 to receptors at the endoplasmic reticulum opens Ca^{2+} channels, allowing the entry of Ca^{2+} into the cytoplasm. As the Ca^{2+} concentration in the cytoplasm rises, the rapid fall of the Ca^{2+} concentration in the endoplasmic reticulum triggers the opening of Ca^{2+} channels in the plasma membrane by means of a "store-depletion mechanism". Ca^{2+} enters the cell, raising the intracellular Ca^{2+} concentration even more. Ca^{2+} binding to inactive protein kinase C (PKC) allows PKC to interact with DAG in the plasma membrane, thus targeting PKC to the membrane. When PKC binds to DAG, the kinase is activated. As the active PKC is now membrane bound, phosphorylations are limited to substrates in close proximity to the membrane and cytoskeleton. One known substrate of PKC is adducin (Matsuoka *et al*., 1998). Adducin is a membrane-skeletal protein found at the junctions of actin and spectrin that colocalize at sites of cell‑cell contact (Kaiser *et al*., 1993; Kaiser *et al*., 1989). The phosphorylation of adducin by PKC causes the appearance of a phosphorylated form of the protein in the cytosol and determines the destabilization and remodeling of the cytoskeleton with a consequent open of the paracellular route.

Also in mammals it has been demonstrated that calcium plays a central role in the modulation of paracellular permeability in absorptive cells (Pérez *et al*., 1997; Karczewski and Groot, 2000). As above mentioned, the medium chain fatty acid C10 modulates septate junctions permeability triggering a signaling cascade which involves an increase of cytosolic calcium concentration through the activation of phospholipase C (Cano Cebrian *et al*., 2005). In the molecular model proposed by these authors, the increase in calcium levels is followed by phosphorilation of myosin light chains by myosin light chian kinases

that causes the contraction of the perijunctional actin-myosin ring, resulting in an increased paracellular permeability.

Preliminary results obtained in my laboratory (Casartelli, unpublished data), indicate that in midgut cells of lepidopteran larvae the signaling pathway activated by C10 apparently follows the model proposed by Cano-Cebrian *et al*. (2005). How myosin light chain phosphorylation causes in midgut cells a rearrangement of the cytoskeletal elements connected to the numerous multi-domain scaffolding proteins which interact with SJ integral proteins (Wu and Beitel, 2004) and, as a consequence, an increase of the paracellular permeability is presently totally unknown.

3.3 Strategies to enhance the permeability of the transcellular route

One of the major problems using orally administered bioinsecticide proteins with a haemocoelic target is their delivery across the digestive system. These macromolecules can be degraded by digestive endo- and exo-peptidases and their movement across the gut epithelium can be insufficient to exert a biological activity. For an effective oral delivery, it will be crucial to study in depth the mechanisms involved in protein absorption and to develop strategies to facilitate their passage through the midgut barriers. Movement across the digestive system of orally delivered proteins has been largely demonstrated in numerous insect species (reviewed by Jeffers and Roe, 2008) and in our laboratory it has been demonstrated, in isolated midgut of *B. mori*, that the mechanism involved in the absorption of two model proteins, albumin and horseradish peroxidase, is trancytosis, a complex transcellular pathway (Casartelli *et al*., 2005, 2007). However, studies on the mechanisms involved in proteins absorption and on the development of delivery strategies to enhance protein movement across the insect digestive system are still limited. The results reported in the following sections aim at adding information in these fields of search.

3.3.1 Use of Cell Penetrating Peptides (CPPs)

As above mentioned, one of the main goal for the effective oral delivery of molecules with an insecticidal activity is the identification of potential enhancers of gut permeability.

To this end, in my laboratory, the use of Cell Penetrating Peptides (CPPs) has been considered. These peptides have the intriguing ability to penetrate cell membranes and accumulate in the nucleus, either alone or as conjugates with a range of cargos, such as proteins, peptides, oligonucleic acids. Despite the numerous studies performed in mammalian cells on the ability of cationic CPPs to act as vectors for macromolecule delivery through the plasma membrane, the precise mechanism of entry is still controversial and it has often been characterized by the contraposition between a direct translocation through the plasma membrane or a specific form of endocytosis. Independently from the mechanism involved, the first step is thought to be the strong ionic interaction between the CPPs' positively charged amino acid residues and the negatively charged plasma membrane constituents such as heparan sulfate, heparin, and chondroitin sulfate B (Gump and Dowdy, 2007).

To shed light on this important field of search, we characterized the process involved in the internalization of selected CPPs into the midgut cells of *B. mori* larvae.

One of the best known and more often used CPPs is Tat, a peptide containing the membrane translocation region 47-57 that is part of the transactivator protein of the human immunodeficiency virus type 1 (HIV-1). First, we decided to examine the time course of FITC-Tat internalization in isolated midgut of *B. mori* larvae mounted in Ussing chambers. The peptide was added to the luminal compartment of the perfusion apparatus and after 10 min, 30 min, 1 h or 3 h of incubation the tissues were removed, fixed and observed at the confocal microscope.

As shown in figure 3.12, after 10 and 30 min the peptide was not present within the cell cytoplasm, as demonstrated by the absence of the fluorescent signal. After 1 h of incubation a weak fluorescence was present inside the cells, but not in the nuclei. After 3 h a strong signal appeared uniformly distributed in the cell cytoplasm and in the nucleus.

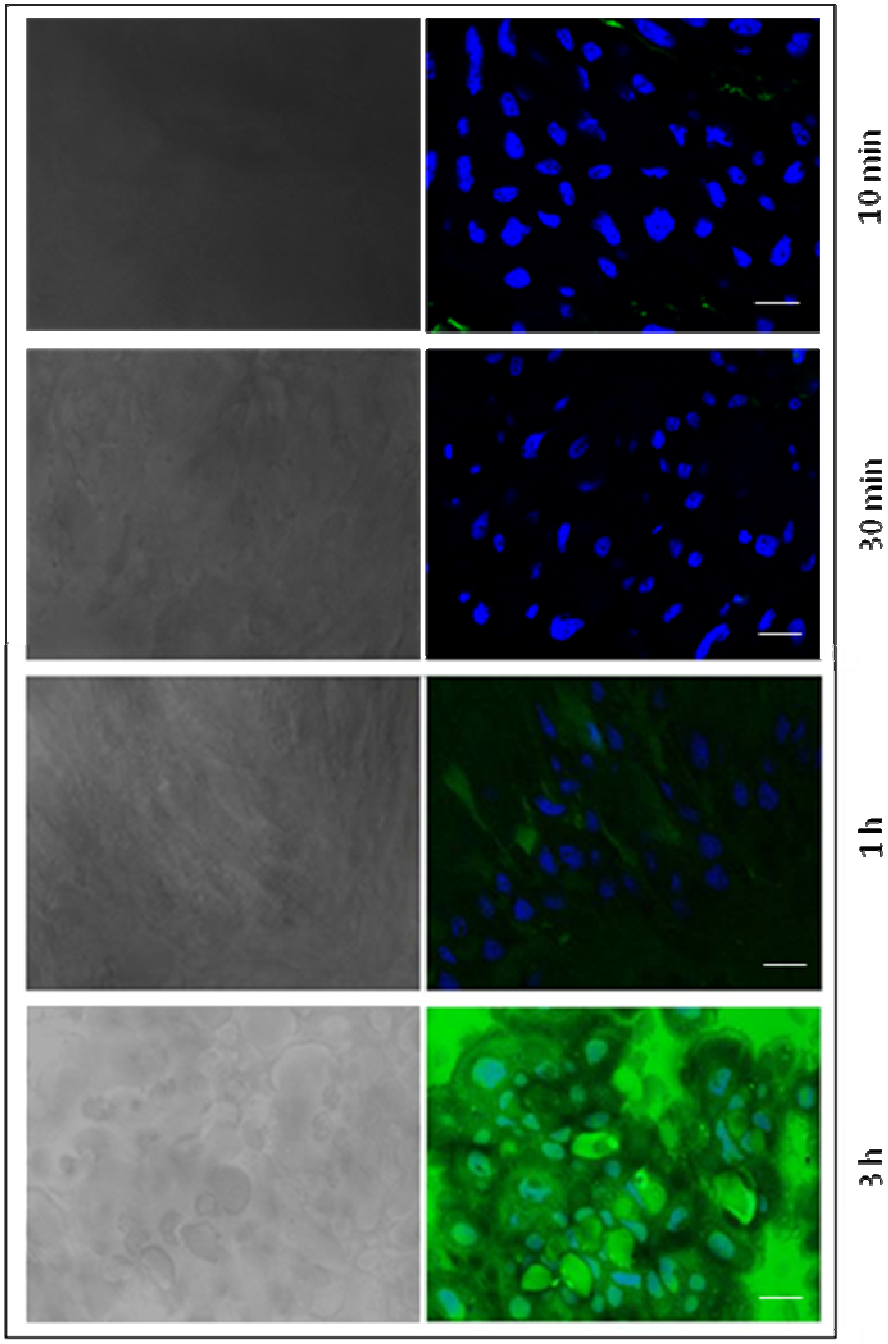

Figure 3.12: brightfield and confocal laser-scanning micrograph of *Bombyx mori* midgut tissue, incubated for different time intervals in the presence of 200 µM FITC-Tat. Bars: 20 µm.

To clarify if the mechanism involved in FITC-Tat internalization is an energy-dependent endocytic process or is an energy-independent mechanism (i.e a direct penetration through the plasma membrane), the internalization of the labelled peptide was evaluated after 3 h of incubation in midguts mounted in Ussing chambers and preincubated in the

absence or in the presence of chlorpromazine, an inhibitor of clathrin-mediated endocytosis. As reported in figure 3.13, a complete inhibition of Tat internalization is observed, a clear indication that an endocytic process is involved in its internalization.

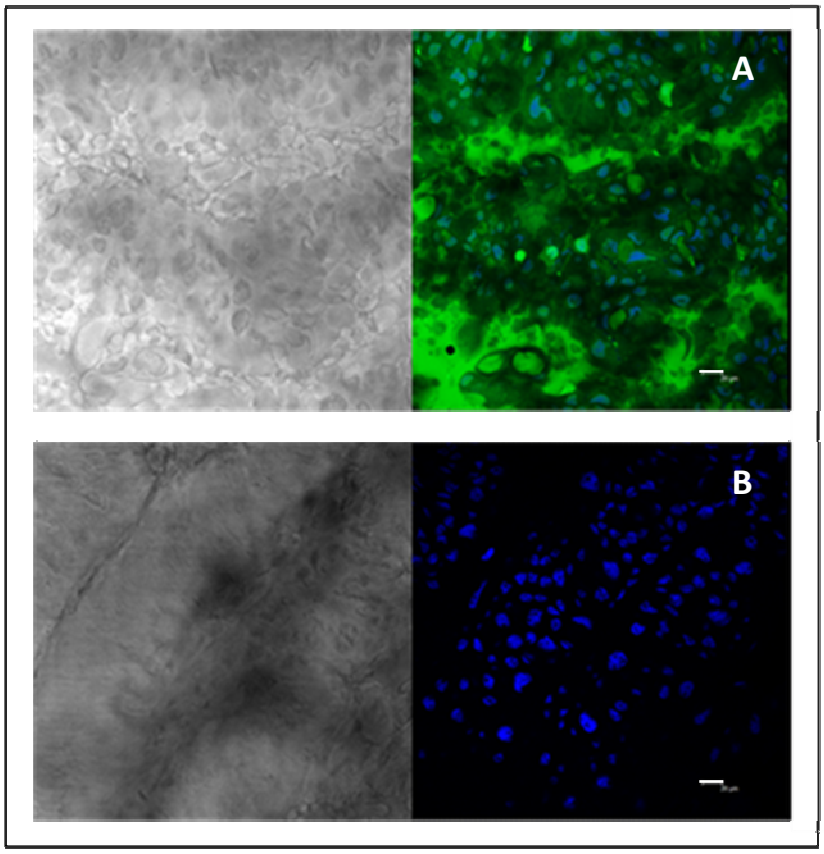

Figure 3.13: effect of chlorpromazine (60 µM) on FITC-Tat internalisation in *B. mori* midgut. Midguts were pre-incubated for 30 min in the absence (A) or in the presence (B) of the inhibitor of clathrin-mediated endocytosis and then incubated with 200 µM FITC-Tat for 3 h.

Recent studies performed in my laboratory evaluated the use of the CPP Tat as a delivery vector for proteins through the plasma membrane of midgut cells of lepidopteran larvae (Cermenati *et al*., 2011). It has been demonstrated that the recombinant fusion protein formed by the CPP Tat and eGFP (enhanced Green Fluorescent Protein) is internalized more efficiently than the recombinant eGFP alone, both by columnar cells in culture and midgut tissue of *B. mori* larvae, a clear indication that this peptide can act as a vector also in insect cells. Moreover, it has been demonstrated that the fluorescence due to Tat-eGFP

internalization is uniformly diffused inside the cytoplasm but not in the nucleus (Cermenati *et al*., 2011). This last result is apparently in contrast with that reported in figure 3.12, where a nuclear localization of the Tat peptide has been observed. On the other hand, it has been demonstrated in mammalian cells that CPPs accumulate in the cell nuclei after internalization. Nuclear accumulation of fluorescently labeled CPPs was initially shown in fixed cells (Futaki *et al*., 2001) and was later considered an artefact of cell fixation (Richard *et al*., 2003). Studies on living cells, however, confirmed CPPs nuclear localization (Duchardt *et al*., 2007; Potocky *et al*., 2003; Zaro and Shen, 2005; Ziegler *et al*., 2003, 2005), a property that can be exploited to deliver cargos whose biological activity is addressed to the nucleus, such as plasmid DNA or proteins regulating gene expression. Therefore, the results reported in figure 3.12 agree with the nuclear localization of labeled CPPs reported in literature for mammalian cells. To explain the different cellular localization between the fusion protein Tat-eGFP (Cermenati *et al*., 2011) and the Tat peptide labeled with FITC (figure 3.12) it is necessary to consider how molecules can reach the nucleus. While movement of ions, metabolites, and other small molecules through the nuclear pore complex (NPC) occurs by passive diffusion, the translocation of molecules larger than 40 kDa generally requires specific transport receptors (Cook *et al*., 2007; D'Angelo and Hetzer, 2008; Terry *et al*., 2007). Most of the cargos coupled to CPPs exceed the size limit for free diffusion and have to depend on active transport, which requires the presence of a nuclear localization signal (NLS) in the molecule that binds to the nuclear import machinery (Cook *et al*., 2007). Tat Peptide, like other CPPs that are derivatives of transcription factors, possesses the NLS in its sequence, and should, in principle, efficiently target cargos to the nucleus. The lack of nuclear localization observed in the experiments with Tat-eGFP (Cermenati *et al*., 2011) is in accordance with a study of the transduction kinetics of Tat-eGFP into cultured mice myoblasts and muscle tissue (Caron *et al*., 2001), where it is suggested that the NLS present in the Tat peptide was not sufficient for the nuclear localization of Tat-eGFP and that the unfolding of the cargo was also required. Since eGFP shows a high resistance to denaturation (Yang *et al*., 1996), the lack of its nuclear localization observed by Caron *et al*. (2001) and by Cermenati *et al*. (2011) can be

considered a consequence of this intrinsic property of the cargo and therefore not be dependent on the incapacity of the Tat peptide to deliver cargos to the nucleus.

As reported above, the CPP Tat acts as a delivery vector in insect midgut cells, enhancing the internalization of eGFP (Cermenati *et al.*, 2011). During my PhD we performed experiments to identify the mechanism involved in Tat-eGFP internalization in midgut cells. Cultured cells of *B. mori* larvae were preincubated for 30 min with two inhibitors of clathrin-mediated endocytosis, chlorpromazine and phenylarsine oxide. Cells were then incubated with 1.5 µM Tat-eGFP for 30 min. Afterwards, the cells were fixed and processed for confocal microscopy observations. As shown in figure 3.14, the drugs did not inhibit protein internalization, a clear indication that clathrin-mediated endocytosis is not involved in Tat-eGFP uptake.

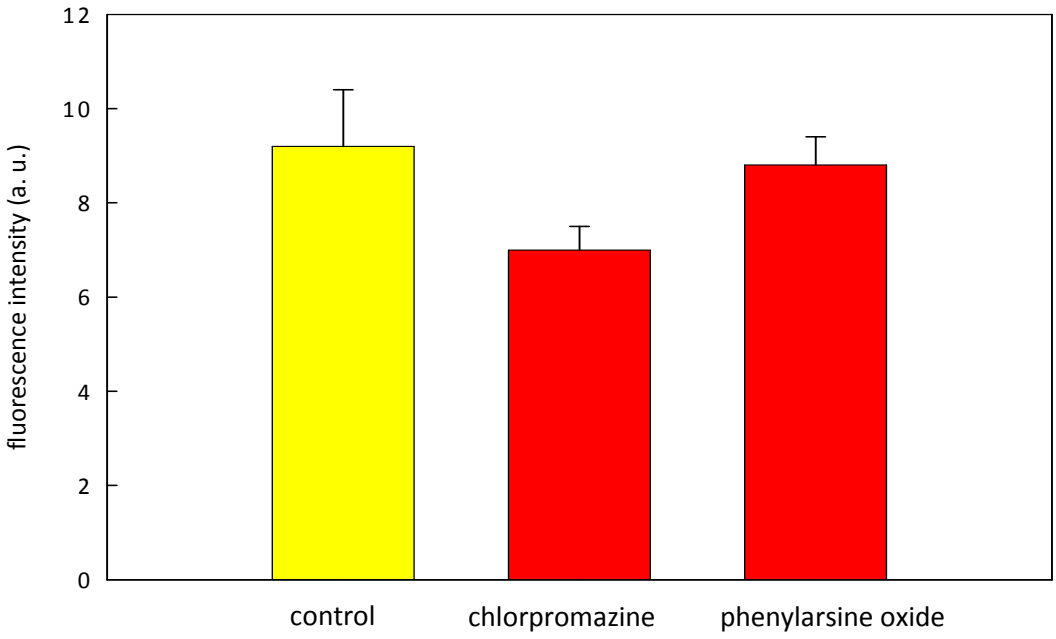

Figure 3.14: effect of inhibitors of clathrin-mediated endocytosis on Tat-eGFP internalization. Cells were pre-treated for 30 min with chlorpromazine (100 µM) or phenylarsine oxide (20 µM) and then incubated with 1.5 µM Tat-eGFP for 30 min. The quantification of the fluorescence intensity (a.u.) was performed in single optical section acquired in a middle focal plane of the cell, in which the nucleus was clearly evident, by confocal laser microscope. Region of interest (ROIs), precisely defining the cell cytoplasm, were drawn and the calculated mean gray values were used. Values are means ± s.e. of the fluorescence intensity recorded in at least 10 cells for each experimental conditions

To exclude the involvement of any other endocytic mechanism, we tested the effect of two metabolic inhibitors, dinitrophenol and sodium azide. Pretreatment of the cells with the two drugs did not reduce Tat-eGFP internalization by columnar cells (figure 3.15), revealing that the internalisation of the fusion protein is an energy-independent process. Therefore, the mechanism involved in the fusion protein Tat-eGFP and in FITC-Tat peptide internalization (figure 3.13) appears different. This is not an unexpected result since in mammalian cells it has been reported that different factors, included the cargo conjugated to the CPP, can influence the mechanism of CPP internalization (Patel *et al*., 2007).

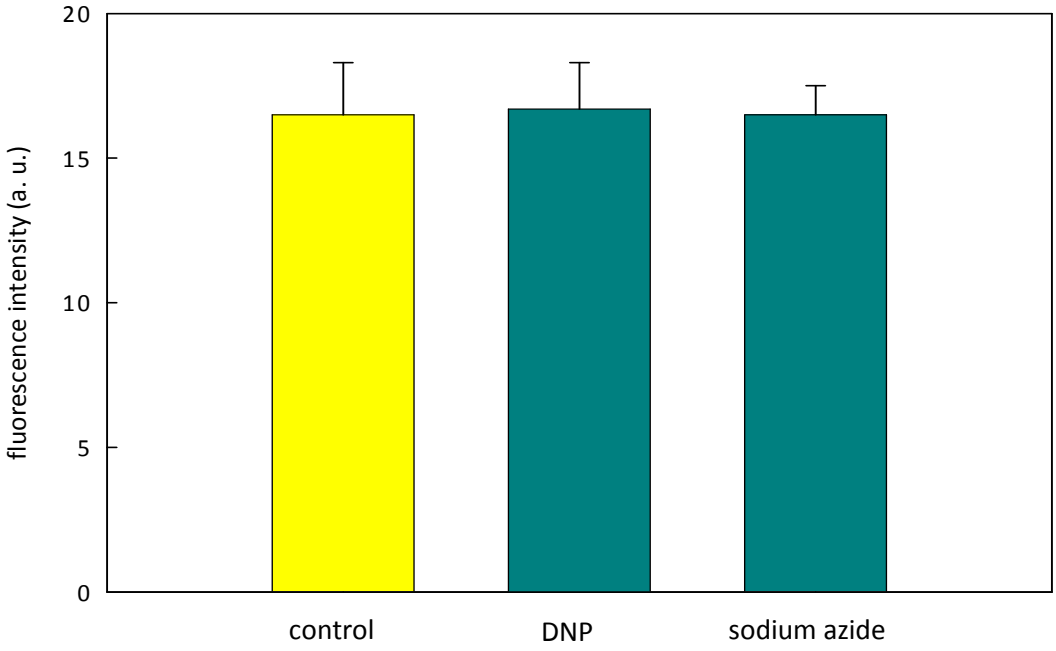

Figure 3.15: effect of metabolic inhibitors on Tat-eGFP internalization by columnar cells. Cells were pre-treated for 30 min with 2,4-dinitrophenol (DNP) (100 µM) or sodium azide (10 mM) and then incubated with 1.5 µM Tat-eGFP for 30 min. The quantification of the fluorescence intensity (a.u.) was performed in single optical section acquired in a middle focal plane of the cell, in which the nucleus was clearly evident, by confocal laser microscope. Region of interest (ROIs), precisely defining the cell cytoplasm, were drawn and the calculated mean gray values were used. Values are means ± s.e. of the fluorescence intensity recorded in at least 10 cells for each experimental conditions

Despite the numerous studies performed in mammalian cells on the ability of cationic CPPs to act as vectors for macromolecule delivery through the plasma membrane, the precise mechanism of entry is still controversial. The first step is thought to be the strong ionic interaction between the CPPs' positively charged amino acid residues and the negatively charged plasma membrane constituents (Gump and Dowdy, 2007). The subsequent events involved in the internalization process have been differently described in literature. The first studies suggested that CPPs' entry into cells was a receptor- and energy-independent process, leading to a destabilization of the lipid bilayer organization, with a possible formation of inverted micelles (Derossi *et al*., 1996; Futaki *et al*., 2001; Tung and Weissleder, 2003). This univocal view of the process was soon challenged and the involvement of endocytosis as the main pathway of internalization was proposed (Richard *et al*., 2003). Now, several experimental evidences reevaluate the energy-independent mechanism, but the scientific community working in this area agree with the idea that CPPs can follow different pathways (Duchardt *et al*., 2007; Mueller *et al*., 2008; Ziegler *et al*., 2005), depending on the CPP under investigation, the cell system used, the cargo coupled to the CPP and the experimental conditions (Patel *et al*., 2007; Schmidt *et al*., 2010). In our experimental system, the CPP Tat increases eGFP internalization by a mechanism that does not involve endocytosis, since no inhibition of the fusion protein uptake is exerted by drugs that interfere with the endocytic uptake (figure 3.14) and by metabolic inhibitors (figure 3.15). The energy-independent process implies the spontaneous penetration of CPPs through the plasma membrane. Recently, two possible energy-independent mechanisms have been proposed: the formation of pores (as a result of the penetration of multiple peptides into the bilayer, leading to the spontaneous formation of a transmembrane pore) (Ciobanasu *et al*., 2010; Herce *et al*., 2009) and micropinocytosis (due to a membrane curvature induced by the CPPs, ultimately leading to the formation of small vesicles) (Yesylevskyy *et al*., 2009). All these studies have been performed using pure artificial bilayers and simulation techniques, so they are still speculative and difficult to apply to cultured cells or isolated tissue. The definition of the precise mechanism of action of a CCP in a given experimental context is an important information to exploit the delivery properties of any arginine-rich peptide. Therefore,

further studies are necessary to shed light on this important point, in each experimental model system to be manipulated.

We also planned to evaluate whether an increase of eGFP internalization due to Tat peptide enhanced eGFP transepithelial transport. We measured the amount of protein able to cross the midgut barrier at a fixed protein concentration (1.5 µM), in the luminal compartment. The amount of protein transported to the opposite compartment was determined after 3 h of incubation. As shown in figure 3.16, the CPP Tat significantly enhances eGFP transepithelial transport, and nearly a five-fold increase of the flux was recorded. The ability of CPPs to enhance transepithelial transport has been reported also in mammalian tissues. CPPs have been used to deliver therapeutic drugs across a tight cell layer *in vivo* (Rothbard *et al*., 2000; Rousselle *et al*., 2000) and the CPP transportan, after internalization into Caco-2 cells, crossed the epithelial layer by a mechanism involving a transcellular pathway (Lindgren *et al*., 2004). The transepithelial transport across Caco-2-cell monolayer of the Tat-insulin fusion protein was six-fold higher than that of native insulin (Liang and Yang, 2005), and various types of CPPs improved the absorption of insulin by the rat intestine (Kamei *et al*., 2008; Morishita *et al*., 2007).

Cell membranes are effectively impermeable to hydrophilic compounds unless the permeation is facilitated by dedicated transport/receptor systems. Our previous studies demonstrated that proteins can be absorbed by transcytosis across the lepidopteran midgut epithelium (Casartelli *et al*., 2005, 2007). For albumin, a protein we used in these studies, we showed that its internalization was particularly efficient, since a receptor was involved in the process (Casartelli *et al*., 2008). Nevertheless, the amount of the protein crossing the midgut epithelium *in vitro* after 3 h of incubation was only approximately 1% of that present in the lumen compartment (Casartelli *et al*., 2005). We show here that eGFP was similarly transported across the midgut epithelium of lepidopteran larvae (figure 3.16) but, whatever the mechanism involved, the amount of eGFP that reached the hemolymphatic compartment was dramatically increased when the protein was fused to the CPP Tat: the percentage of eGFP transported through the epithelium raised from less than 1% to 4% of the amount of protein present in the luminal compartment. The fusion of

Tat peptide to eGFP alters the physiological plasma membrane permeability to this protein and, as a consequence, eGFP is more efficiently internalized in midgut cells and transported across the epithelium.

Our results clearly indicate that in insect midgut cells Tat peptide can be used to increase not only the internalization of a poorly permeable cargo molecule through the plasma membranes (Cermenati *et al*., 2011), but also its transepithelial transport. Therefore, these data open new perspectives for oral delivery of insecticide macromolecules hitting either endocellular midgut receptors or targets located in the hemocoel.

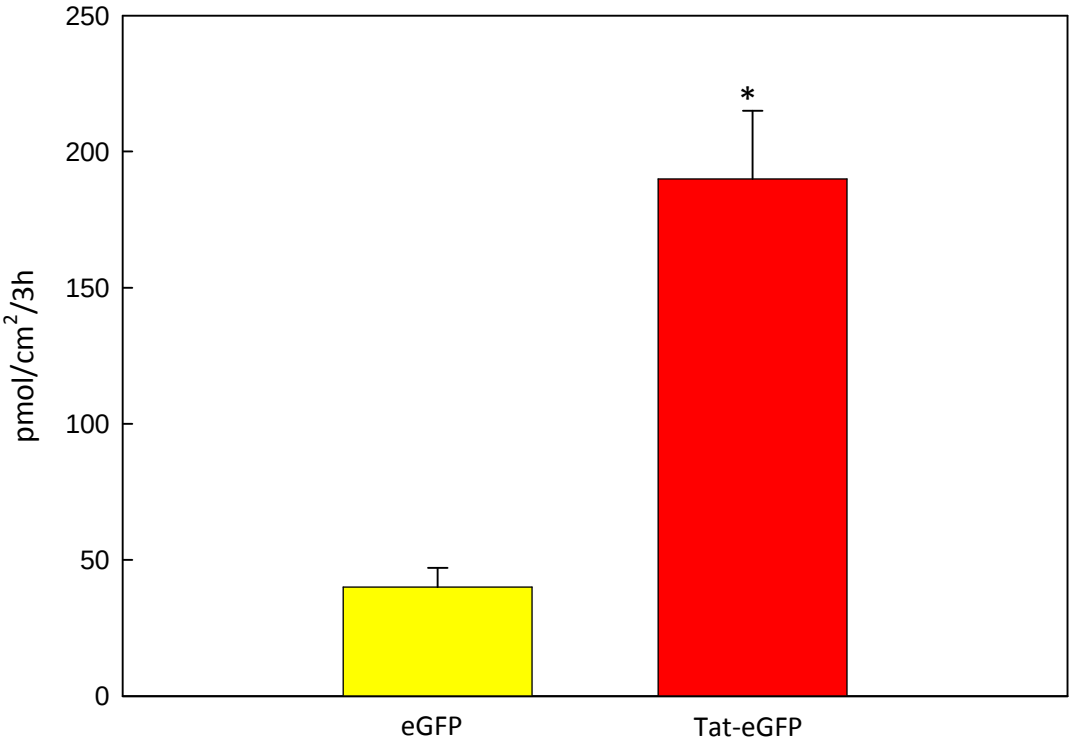

Figure 3.16: transepithelial transport of eGFP (1.5 µM) and Tat-eGFP (1.5 µM) after 3h of incubation. At time 0, the proteins were added to the physiological solution in the luminal compartment. The amount of eGFP and Tat-eGFP transported to the haemolymphatic compartment is reported. Each bar represents the mean ± s.e. of six experiments. Student's *t*-test * $P < 0.01$.

The use of cell-penetrating peptides as delivery vectors for molecules that otherwise do not cross the plasma membrane or that are poorly internalized is gaining significance in biomedicine (Jarver *et al*., 2010). Although different strategies are pursued for the optimization of CPP-based delivery, premature degradation of CPPs before they reach their target *in vivo* remains a common concern for therapeutic applications (Patel *et al*., 2007) and can represent an obstacle also in the perspective of using *in vivo* CPPs to efficiently deliver macromolecules with an insecticide activity. A common strategy used in mammals to overcome this problem is the use of CPPs consisting of D-amino acids (D-CPPs). The altered stereochemistry of peptides containing D-amino acids renders D-CPPs much more protease resistant than their L-amino acid counterparts (Elmquist and Langel, 2003; Pujals *et al*., 2007; Youngblood *et al*., 2007). The increased stability is not limited to peptides composed entirely of D-amino acids, but was also observed for partial D-amino acid substitutions at the termini in small peptides (Tugyi *et al*., 2005)

Different studies (Derossi *et al*., 1996; Mitchell *et al*., 2000; Elmquist and Langel, 2003; Fretz *et al*., 2007), performed in mammalian cells to evaluate if the chirality of CPPs is fundamental for their internalization, have led to the prevailing paradigm that cellular uptake of CPPs is a chirality independent process. On the contrary, Verdurmen *et al*. (2011) demonstrated a clear chirality dependence in the uptake of L- and D- form of different CPPs, with a preference for L-peptides.

Therefore, we decided to analyze the role of the chirality in the CPPs uptake in the larval midgut of *B. mori*. Midgut tissues were mounted in Ussing chambers and incubated with FITC-R8 (L-eight-arginine labelled with FITC) and FITC-r8 (D-eight-arginine labelled with FITC) for different time intervals. Samples were then observed with a confocal microscopy. Figure 3.17 shows that both peptides were not present inside the cell cytoplasm after 10 min of incubation, since no fluorescence was detected in midgut cells. After 30 min a weak fluorescence signal was detected only in midgut incubated with FITC-r8 and after 1 h of incubation both peptides are present inside the cells' cytoplasm, but only FITC-r8 appears clearly present in the nuclei. A part from the different efficiency of internalization and the apparently different intracellular localization, the presence of both peptides inside the

midgut is a clear indication that chirarity is not critical for CPP internalization in midgut cells of *B. mori* larvae.

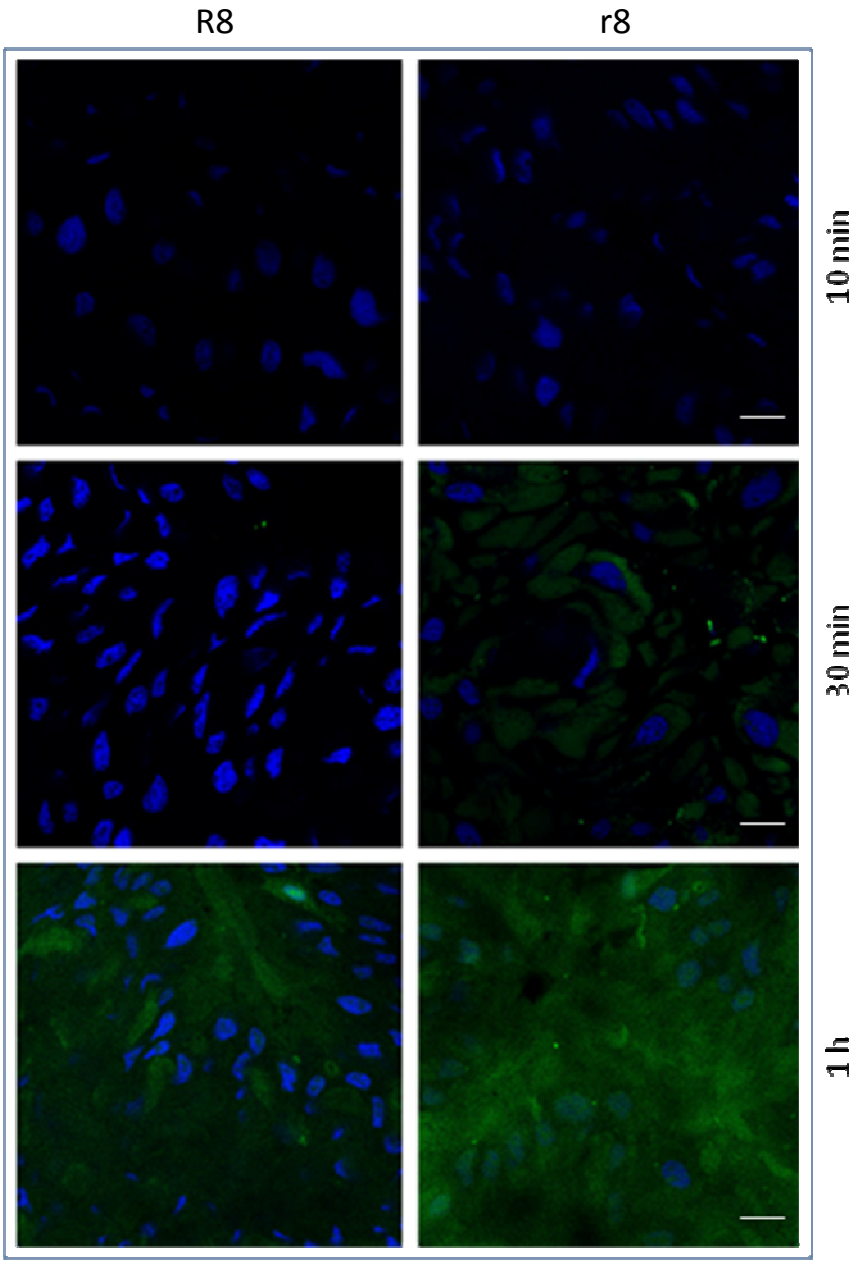

Figure 3.17: confocal laser-scanning micrograph of *B. mori* midgut tissue, incubated for different time intervals in the presence of 200 µM FITC-R8 and FITC-r8. Bars: 20 µm

These results is particularly interesting in the perspective of an *in vivo* application of CPPs as a tool to increase the delivery of macromolecules with potential insecticide activity,

avoiding the possible degradation of the peptide due to proteases present in the midgut lumen.

3.3.2 Inhibition of the intracellular degradative pathway

It has been demonstrated in our laboratory that the model protein albumin crosses the insect midgut epithelium of *B. mori* larvae by transcytosis (Casartelli *et al.*, 2005). The uptake is clathrin-dependent and mediated by a megalin-like multiligand receptor (Casartelli *et al.*, 2008). After internalization, albumin was found in early endosomes, but only a small amount of the protein was directed to the basolateral membrane, to be transferred to the haemocoel. The major part of albumin was delivered to lysosomes, suggesting a relative rapid degradation (Casartelli *et al*, unpublished data). We tried to increase the amount of the protein that follows the transcellular route by blocking the intracellular degradative pathway with specific drugs, chloroquine (CQ) and ammonium chloride (NH_4Cl). The isolated midguts of fifth instar *B. mori* larvae were mounted in a suitable apparatus maintaining the *in situ* shape and orientation to measure the amount of protein able to cross the midgut barrier in tissue preincubated in the absence (control) or in the presence of CQ and NH_4Cl. In the graph reported in figure 3.18 it is evident that the passage of albumin through the midgut epithelium preincubated with CQ is not significantly different compared to that measured in midguts incubated in the absence of the drug (Student's *t* test). The same result was obtained in midguts preincubated with NH_4Cl, the other inhibitor used to block the degradative pathway (figure 3.19)

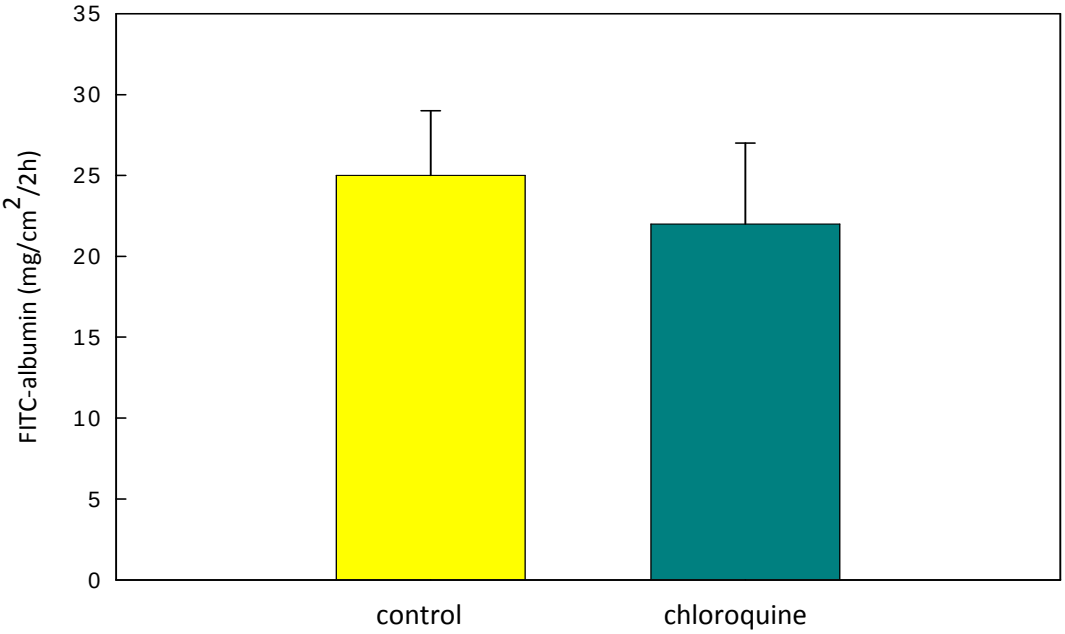

Figure 3.18: lumen-to-haemolymph flux of FITC-albumin (14.2 µM) through the midgut epithelium of *B. mori* larvae after 2 h of incubation. The tissues were preincubated for 30 min in the absence (control) or in the presence of chloroquine (100 µM). Each bar represents the mean ± s.e. of ten experiments.

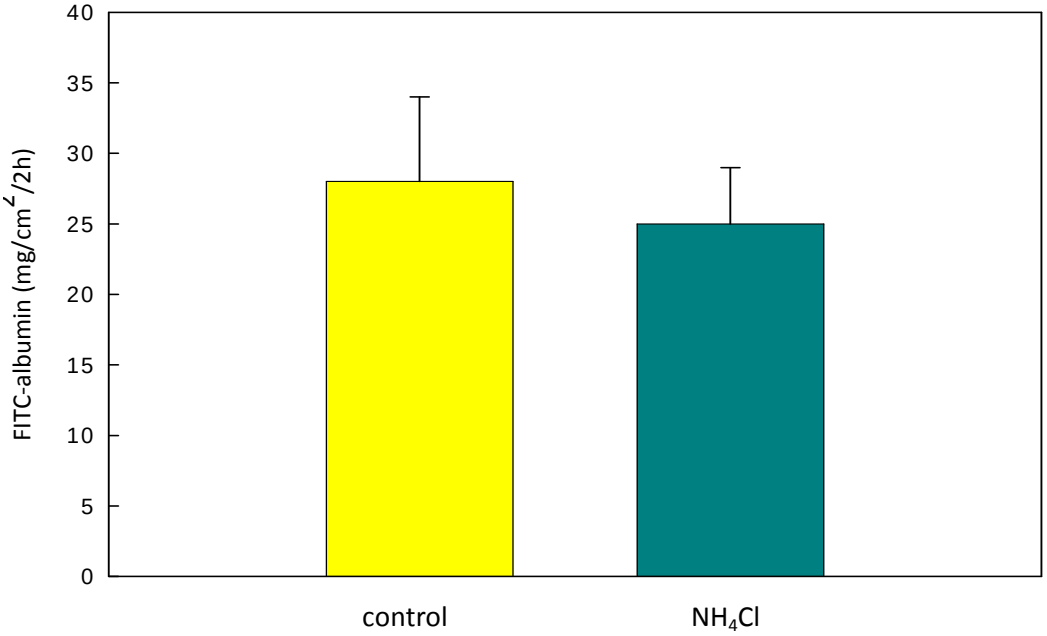

Figure 3.19: lumen-to-haemolymph flux of FITC-albumin (14.2 µM) through the midgut epithelium of *B. mori* larvae after 2 h of incubation. The tissues were preincubated for 30 min in the absence (control) or in the presence of NH_4Cl (100 µM). Each bar represents the mean ± s.e. of ten experiments.

Our results indicate that the inhibition of lysosomal activity do not increase the amount of albumin directed to the transcellular route. We cannot exclude that the concentration of the drugs used for these experiments was inadequate to reduce significantly the lysosomal activity, although data reported in literature indicate that these concentrations are effective in inhibiting the intracellular degradation. Alternatively, it is possible that, despite the degradation pathway is inhibited by the selected drugs, the amount of protein directed to the transcytotic pathway do not increase. In mammalian absorptive epithelia it has been observed that, after internalization by endocytic mechanism, proteins can follow different pathways: they can be transported by transytosis across the epithelium, recycled to the same domain of membrane where endocytosis occurred or can be delivered to lysosomes for degradation (Apodaca, 2001). As reported above, in our laboratory it has been demonstrated in isolated midgut of *B. mori* larvae that albumin, after internalization, is massively directed to the degradative pathway and that only a small amount of the internalized protein crosses undegraded the basolateral membrane (Casartelli *et al*., 2005). No information is available about a possible recycling of the protein to the apical membrane domain, where endocytosis occurred. Therefore, we can not exclude that the inhibition of the degradative intracellular pathway causes an increase of the amount of albumin directed to the recycling pathway.

Even though this first attempt to manipulate the intracellular pathways followed by a protein internalized by endocytosis to obtain an increase in the amount of protein directed to the transcellular route did not give positive results, it is mandatory to continue the study on the molecular mechanisms mediating their absorption. Only a complete picture of the mechanisms will contribute to develop suitable strategy to enhance protein absorption.

References

;

Akaike T., Maeda H. (2000). Nitric oxide and virus infection. *Immunology.*101:300-8;

Anderberg E.K., Lindmark T., Artursson P. (1993). Sodium caprate elicitis dilatations in human instestinal tight junctions and enhances drug absorption by the paracellular route*. Pharmaceutical Research*. 10:857-64;

Anderson E., Harvey W.R. (1966). Active transport by the cecropia midgut. II. Fine structure of the midgut epithelium. *Juornal of Cell Biology.* 31:107-34;

Apodaca G. (2001). Endocytic Traffic in Polarized Epithelial Cells: Role of the Actin and Microtubule Cytoskeleton *Traffic*. 2:149–59;

Bailey, K. L., Boyetchko, S. M. & Langle, T. (2010) Social and economic drivers shaping the future of biological control: a Canadian perspective on the factors affecting the development and use of microbial biopesticides. *Biological control.* 52:221–29;

Bailon, P., Won, C.-Y. (2009). PEG-modified biopharmaceuticals. *Expert Opinion on Drug Delivery.* 6:1–16;

Baldwin K.M., Hakim R.S. (1991). Growth and differentiation of the midgut epithelium. *Tissue Cell.* 23:411-22;

Bale J.S., van Lenteren J.C., Bigler F.(2008). Biological control and sustainable food production. *Philosophical Transactions of the Royal Society B: Biological Sciences***.** 363:761-76;

Bantel-Schaal U., Braspenning-Wesch I., Kartenbeck J. (2009). Adeno-associated virus type 5 exploits two different entry pathways in human embryo fibroblasts. *Journal of General Virology.* 90:317-22;

Barat-Houari M., Hilliou F., Jousset F.X., Sofer L., Deleury E., Rocher J., Ravallec M., Galibert L., Delobel P., Feyereisen R., Fournier P., Volkoff A.N. (2006). Gene expression profiling of

Spodoptera frugiperda hemocytes and fat body using cDNA microarray reveals polydnavirus-associated variations in lepidopteran host genes transcript levels. *BMC Genomics*. 7:160;

Bavoso A., Falabella P., Giacometti R., Halane A.J., Ostuni A., Pennacchio F. and Tremblay E. (1995). Intestinal absorption of proctolin in *Helicoverpa armigera* (Lepidoptera, Noctuidae) larvae. *REDIA* 78:173–85;

Behr M., Riedel D., Schuh R. (2003). The claudin-like Megatrachea is essential in septate junctions for the epithelial barrier function in Drosophila. *Developmental Cell*. 5:611-20;

Belloncik S. (1990). Potential use of densonucleosis virus as biological control agents of insect pests. *In CRC Handbook of Parvoviruses (Tijssen, P., ed.)*, pp. 29–39, CRC Press Inc, Boca Raton, FL;

Bement W. M., Mooseker M. S., (1996). The cytoskeleton of the intestinal epithelium. In *The Cytoskeleton* (ed. J. E. Hesketh and I. F. Pryme) Vol. 3. pp. 359- 404. Greenwich: JAI Press;

Bergoin M., Tijssen P. (2008). Parvoviruses of arthropods. *Encyclopedia of Virology*, 4: 76-85;

Beyenbach K.W., Baumgart S., Lau K., Piermarini P.M., Zhang S. (2009). Signaling to the apical membrane and to the paracellular pathway: changes in the cytosolic proteome of Aedes Malpighian tubules. *Journal of Experimental Biology.* 212:329-40;

BIOPESTICIDES 92 page report published May 01, 2008 http://www.alacrastore.com/storecontent/markintel/GLOBAL_INDUSTRY_ANALYSTS_SMALL_PRIVATE_PLAYERS-50230556

Boisvert M., Fernandes S., Tijssen P. (2010). Multiple pathways involved in porcine parvovirus cellular entry and trafficking toward the nucleus. *Journal of Virology.* 84:7782-92;

Bonfanti P., Colombo A., Heintzelman M.B., Mooseker M.S., Camatini M. (1992). The molecular architecture of an insect midgut brush border cytoskeleton. *European Journal of Cell Biology.* 57:298-307.

Bradford M.M. (1976). A rapid and sensitive method for the quantitation of microgram quantities of protein utilizing the principle of protein-dye binding*. Analytical Biochemistry*. 72:248-54;

Brault V., Tanguy S., Reinbold C., Le Trionnaire G., Arneodo J., Jaubert-Possamai S., Guernec G., Tagu D. (2010). Transcriptomic analysis of intestinal genes following acquisition of pea enation mosaic virus by the pea aphid Acyrthosiphon pisum. *Journal of General Virology*. 91:802-8;

Brown K.E., Anderson S.M., Young N.S. (1993). Erythrocyte P antigen: cellular receptor for B19 parvovirus. *Science*, 262: 114-17;

Brown R.E. (1998). Sphingolipid organization in biomembranes: what physical studies of model membranes reveal. *Journal of Cell Science.*111:1-9;

Bruemmer A., Scholari F., Lopez-Ferber M., Conway J.F., Hewat E.A. (2005). Structure of an Insect Parvovirus (Junonia coenia Densovirus) Determined by Cryo-electron Microscopy. *Journal of Molecular Biology.* 347:791-801;

Cano-Cebriàn M.J., Zornoza T., Granero L., Polache A. (2005). Intestinal absorption enhancement via the paracellular route by fatty acids, chitosan and other: a target for drug delivery. *Current Drug Delivery.* 2:9-22;

Cappellozza L., Cappellozza S., Saviane A., Sbrenna G. (2005) Artificial diet rearing system for silkworm *Bombyx mori* (Lepidoptera Bombycidae): effect of vitamin C deprivation on larval growth and cocoon production*. Applied Entomology and Zoology*. 40: 405-12;

Caron N.J., Torrente Y., Camirand G., Bujold M., Chapdelaine P., Leriche K. (2001). Intracellular delivery of a Tat-eGFP fusion protein into muscle cells. *Molecular Therapy.* 3:310–8;

Casartelli M., Cermenati G., Rodighiero S., Pennacchio F., Giordana B. (2008). A megalin-like receptor is involved in protein endocytosis in the midgut of an insect (*Bombyx mori*, Lepidoptera). *American Journal of Physiology.* 295:1290–300;

Casartelli M., Corti P., Cermenati G., Grimaldi A., Fiandra L., Santo N., Pennacchio F., Giordana B. (2007). Absorption of horseradish peroxidase in *Bombyx mori* larval midgut. *Journal of Insect Physiology.* 53: 517-25;

Casartelli M., Corti P., Leonardi M.G., Fiandra L., Burlini N., Pennacchio F., Giordana B. (2005). Absorption of albumin by the midgut of a lepidopteran larva. *Journal of Insect Physiology*, 51: 933-40;

Casartelli M., Leonardi M.G., Fiandra L., Parenti P., Giordana B. (2001) Multiple transport pathways for dibasic amino acids in the larval midgut of the silkworm *Bombyx mori. Insect Biochemistry and Molecular Biology*. 31:621-32;

Casida JE, Quistad GB (1998) Golden age of insecticide research: past, present, or future? *Annual Review of Entomology.* 43: 1–16.

Cermenati G., Corti P., Caccia S., Giordana B, Casartelli M. (2007). A morphological and functional characterization of *Bombyx mori* larval midgut cells in culture. *Invertebrate Survival Journal*, 4:119-26;

Cermenati G., Terracciano I., Castelli I., Giordana B., Rao R., Pennacchio F., Casartelli M. (2011). The CPP Tat enhances eGFP cell internalization and transepithelial transport by the larval midgut of Bombyx mori (Lepidoptera, Bombycidae). *Journal of Insect Physiology.* 57:1689-97;

Chao A.C., Nguyen J.V., Broughall M., Griffin A., Fix J.A., Daddona P.E. (1999). *In vitro* and *in vivo* evaluation of effects of sodium caprate on enteral peptide absorption and on mucosal morphology*. International Journal of Pharmaceutics.* 191:15-24;

Chiu Y.L., Ali A., Chu C.Y., Cao H., Rana T.M. (2004). Visualizing a correlation between siRNA localization, cellular uptake, and RNAi in living cells. *Chemistry & Biology.* 11:1165-75;

Christensen E.I., Birn H. (2002). Megalin and cubilin: multifunctional endocytic receptors. Nat. Rev. Mol. Cell. Bio. 3:258-68;

Ciobanasu C., Siebrasse J.P., Kubitscheck U. (2010). Cell-penetrating HIV1 TAT peptides can generate pores in model membranes. *Biophysical Journal.* 99:153–62;

Cioffi M. (1979). The morphology and fine structure of the larval midgut of a moth (*Manduca sexta*) in relation to active ion transport. *Tissue Cell.* 11: 467-79;

Conner S.D, Schmid S.L. (2003) Regulated portals of entry into the cell. *Nature* 422: 37-44;

Cook A., Bono F., Jinek M., Conti E. (2007.) Structural biology of nucleocytoplasmic transport. *Annual Review of Biochemistry* 76:647–71;

Cotmore S.F., Tattersall P. (2007). Parvoviral host range and cell entry mechanisms. *Advances in Virus Research*, 70: 183-232;

Croizier L., Jousset F., Veyrunes J.C., Lopez-Ferber M., Bergoin M., Croizier G. (2000). Protein requirements for assembly of virus-like particles of *Junonia coenia* densovirus in insect cells. *Journal of General Virology.* 81:1605–13;

D'Angelo M.A., Hetzer M.W.(2008). Structure, dynamics and function of nuclear pore complexes. *Trends in Cell Biology.* 18:456–66;

Deli M.A. (2009). Potential use of tight junction modulators to reversibly open membranous barriers and improve drug delivery. 1788:892-10;

Derossi D., Calvet S., Trembleau A., Brunissen A., Chassaing G., Prochiantz A. (1996). Cell internalization of the third helix of the Antennapedia homeodomain is receptor-independent. *The Journal of Biological Chemistry* 271, 18188– 93.

Douar A.M., Poulard K., Stockholm D., Danos O. (2001). Intracellular trafficking of adeno-associated virus vectors: routing to the late endosomal compartment and proteasome degradation. *Journal of Virology.* 75:1824-33;

Dow J.A.T. (1992). pH gradients in lepidopteran midgut. *Journal of Experimental Biology*. 172:355–75;

Dow J.A.T., Peacock J.M. (1989). Microelectrode evidence for the electrical isolation of goblet cell cavities in *Manduca sexta* middle midgut. *Journal of Experimental Biology*. 143:101–14;

Dow JAT. (1986). Insect midgut formation *Advances in Insect Physiology*. 19:187-328;

Duchardt F., Fotin-Mleczek M., Schwarz H., Fischer R., Brock R. (2007). A comprehensive model for the cellular uptake of cationic cell-penetrating peptides. *Traffic.* 8:848–66;

Duchardt F., Ruttekolk I.R., Verdurmen W.P., Lortat-Jacob H., Bürck J., Hufnagel H., Fischer R., van den Heuvel M., Löwik D.W., Vuister G.W., Ulrich A., de Waard M., Brock R. (2009). A cell-penetrating peptide derived from human lactoferrin with conformation-dependent uptake efficiency. *Journal of Bilogical Chemistry.* 284:36099-108;

Dumas B., M. Jourdan, A. M. Pascaud, and M. Bergoin. (1992). Complete nucleotide sequence of the cloned infectious genome of *Junonia coenia* densovirus reveals an organization unique among parvoviruses. *Virology* 191:202–222;

Elmquist A., Langel U. (2003). *In vitro* uptake and stability study of pVEC and its all-D analog. *Biological Chemistry.* 384:387-93;

El-Sayed A., Futaki S., Harashima H. (2009). Delivery of macromolecules using **arginine**-rich cell-penetrating peptides: ways to overcome endosomal entrapment. *AAPS Journal*. 11:13-22;

European Parliament. 2010 Pesticides: framework for Community action to achieve a sustainable use of pesticides. http://www.europarl.europa.eu/oeil/file.jsp

Fawell S., Seery J., Daikh Y., Moore C., Chen L.L., Pepinsky Barsoum B. (1994) Tatmediated delivery of heterologous proteins into cells. *Proceedings of the National Academy of Sciences of the United States of America.* 91: 664–68;

Fernàndez-Carneado J., Kogan M.J., Pujals S., Giralt E. (2004) Amphipathic Peptides and Drug Delivery. *Peptide Science zob. Biopolymers*. 76: 196–203;

Fiandra L., Casartelli M., Cermenati G., Burlini N., Giordana B. (2009). The intestinal barrier in lepidopteran larvae: permeability of the peritrofic membrane and of the midgut epithelium to two biologically active peptides*. Journal of Insect Physiology.* 55:10-8;

Fiandra L., Casartelli M., Giordana B. (2006). The paracellular pathway in the lepidopteran larval midgut and its modulation by intracellular mediators. *Comparative Physiology and Biochemistry*. 144:464- 73;

Fiandra L., Terracciano I., Fanti P., Garonna A., Ferracane L., Fogliano V., Casartelli M., Giordana B., Rao R., Pennacchio F. (2010). A viral chitinase enhances oral activity of TMOF. *Insect Biochemistry and Molecular Biology*. 40:533-40;

Fitches E., Audsley N., Gatehouse J.A., Edwards J.P. (2002). Fusion proteins containing neuropeptides as novel insect control agents: snowdrop lectin delivers fused allatostatin to insect haemolymph following oral ingestion. *Insect Biochemistry and Molecular Biology*. 32:1653– 61;

Fitches E., Edwards M.G., Mee C., Grishin E., Gatehouse A.M.R., Edwards J.P., Gatehouse J.A. (2004) Fusion protein containing insect-specific toxins as pest control agents: snowdrop lectin delivers fused insecticidal spider venom toxin to insect haemolymph following oral ingestion. *Journal of Insect Physiology*. 50: 61–71;

Fitches E.C., Bell H.A., Powell M.E., Back E., Sargiotti C., Weaver R.J., Gatehouse J.A. (2010). Insecticidal activity of scorpion toxin (ButaIT) and snowdrop lectin (GNA) containing fusion proteins towards pest species of different orders. *Pest Management Science.* 66:74-83;

Flower N.E., Filshie B.K. (1975). Junctional structures in the midgut cells of lepidopteran caterpillars*. Journal of Cell Science*. 17:221-39;

Fonseca S.B., Pereira M.P., Kelley SO. (2009) Recent advances in the use of cell-penetrating peptides for medical and biological applications. *Advanced Drug Delivery Reviews*. 61: 953-64;

Fotin A., Cheng Y., Sliz P., Grigorieff N., Harrison S.C., Kirchhausen T., Walz T. (2004). Molecular model for a complete clathrin lattice from electron cryomicroscopy. *Nature*. 432:573–79;

Fretz M.M., Penning N.A., Al-Taei S., Futaki S., Takeuchi T., Nakase I. Storm G., Jones A.T. (2007)**.** Temperature-, concentration- and cholesterol-dependent translocation of L- and D-octa-arginine

across the plasma and nuclear membrane of CD34+ leukaemia cells. *Biochemical Journal***.** 403:335–42;

Furuse M., Fujita K., Hiiragi T., Fujimoto K., Tsukita S. (1998). Claudin-1 and -2: novel integral membrane proteins localizing at tight junctions with no sequence similarity to occludin. *Journal of Cell biology.* 141:1539-50;

Futaki S., Nakase I., Tadokoro A., Takeuchi T., Jones A.T. (2007). Arginine-rich peptides and their internalization mechanisms. *Biochemical Society Transactions.* 35, 784–87;

Futaki S., Suzuki T., Ohashi W., Yagami T., Tanaka S., Ueda K., Sugiura Y. (2001). Arginine-rich peptides. *The Journal of Biological Chemistry.* 276:5836–40;

Giordana B., Leonardi M.G., Casartelli M., Consonni P., Parenti P. (1998). K(+)-neutral amino acid symport of Bombyx mori larval midgut: a system operative in extreme conditions. *American Journal of Physiology.* 274:1361-71;

Giordana B., Sacchi V.F., Hanozet G.M. (1982) Intestinal amino acid absorption in lepidopteran larvae*. Biochimica et Biophysica Acta.* 692:81-8;

Golebiewski L., Liu H., Javier R.T., Rice A.P.(2011) The avian influenza virus NS1 ESEV PDZ binding motif associates with Dlg1 and Scribble to disrupt cellular tight junctions. *Journal of Virology.* 85:10639-48;

Gump J.M., Dowdy S.F. (2007). TAT transduction: the molecular mechanism and therapeutic prospects. *Trends in Molecular Medicine.* 13:443-8;

Hajek, A. (2004) Natural enemies: an introduction to biological control. Cambridge, UK: Cambridge University Press;

Hand A.R., Gobel S. (1972). The structural organization of the septate and gap junctions of Hydra. *Journal of Cell Biology.* 52:397-408;

Hansen M., Kilk K., Langel U., (2008). Predicting cell-penetrating peptides. *Advanced Drug Delivery Reviews.* 60:572–79;

Harbison C.E., Chiorini J.A., Parrish C.R. (2008). The parvovirus capsid odyssey: from the cell surface to the nucleus. *Trends in microbiology*. 16:208-14;

Herce H.D., Garcia A.E., Litt J., Kane R.S., Martin P., Enrique N., Rebolledo A., Milesi V. (2009). Arginine-rich peptides destabilize the plasma membrane, consistent with a pore formation translocation mechanism of Cell-Penetrating Peptides. *Biophysical Journal.* 97:1917–25;

Hidalgo C., Donoso P. (2008). Crosstalk between calcium and redox signaling: from molecular mechanisms to health implications. *Antioxid Redox Signal.* 10:1275-312

Hilder V.A., Powell K.S., Gatehouse A.M.R., Gatehouse J.A., Gatèhouse L.N., Shi Y., Hamilton W.D.O., Merryweather A., Newell C., Timans J.C., Peumans W.J., Van Damme E.J.M., Boulter D. (1995) Expression of snowdrop lectin in transgenic tobacco plants results in added protection against aphids. *Transgenic Research.* 4**:** 18-25;

Hinshaw J.E., Schmid S.L. (1995). Dynamin self assembles into rings suggesting a mechanism for coated vesicle budding. *Nature* 374:190-2;

Hutagalung A.H., Novick P.J. (2011). Role of Rab GTPases in membrane traffic and cell physiology. *Physiological Review.* 91:119-49;

Ishizawa T., Hayashi M., Awazu S. (1987). Enhancement of jejunal and colonic absorption of fosfomycin by promoters in the rat. *Journal of Pharmacy and Pharmacology*. 39:892-95;

Ito K., Kidokoro K., Sezutsu H., Nohata J., Yamamoto K., Kobayashi I., Uchino K., Kalyebi A., Eguchi R., Hara W., Tamura T., Katsuma S., Shimada T., Mita K., Kadono-Okuda K. (2008). Deletion of a gene encoding an amino acid transporter in the midgut membrane causes resistance to a Bombyx parvo-like virus. *Proceedings of the National Academy of Sciences of the United States of America.* 105:7523-7;

Jarver P., Mager I., Langen U. (2010). *In vivo* biodistribution and efficacy of peptide mediated delivery. *Trends in Pharmacological Sciences.* 31:528–35;

Jeang K.T., Xiao H., Rich E.A. (1999) Multifaceted activities of the HIV-1 transactivator of transcription, Tat. *Journal of Biological Chemistry*. 274: 28837–40;

Jeffers L.A., Michael Roe R. (2008). The movement of proteins across the insect and tick digestive system. *Journal of Insect Physiology.* 54: 319-32;

Jousset F.X., Jourdan M., Compagnon B., Mialhe E., Veyrunes J.C., Bergoin M.(1990). Restriction maps and sequence homologies of two densovirus genomes. *Journal of General Virology.* 71:2464-6;

Kaiser H.W., Ness W., O'Keefe E., Balcerkiewicz A., Kreysel H.W. (1993). Localization of adducin in epidermis. *Journal of Investigative Dermatology.* 101:783-8;

Kaiser H.W., O'Keefe E., Bennett V. (1989). Adducin: Ca^{++}-dependent association with sites of cell-cell contact. *Journal of Cell biology.*109:557-69;

Kamei N., Morishita M., Eda Y., Ida N., Nishio R., Takayama K. (2008). Usefulness of cell-penetrating peptides to improve intestinal insulin absorption. *Journal of Controlled Release*. 132:21–5;

Kamm W., Jonczyk A., Jung T., Luckenbach G., Raddatz P., Kissel T. (2000). Evaluation of absorption enhancement for a potent cyclopeptidic α_{υ}, β_3- antagonist in a human intestinal cell line (Caco-2). *European Journal of Pharmaceutical Sciences.* 10:205-14;

Kang, J.S., De Luca, P.P., Lee, K.C. (2009). Emerging PEGylated drug. *Expert Opinion on Emerging Drugs.* 14:363–380;

Karczewski J., Groot J. (2000). Molecular physiology and pathophysiology of tight junctions III. Tight junction regulation by intracellular messengers: differences in response within and between epithelia. *American Journal of Physiology*. 279:660–65.

Kimura Y., Hosoda Y., Yamaguchi M., Nagano H., Shima M., Adachi S., Matsuno R. (2001). Effects of medium-chain fatty acids on intracellular calcium levels and the cytoskeleton in human intestinal (Caco-2) cell monolayers. *Bioscience Biotechnology & Biochemistry.* 65:743-51;

Krishnan N., Kodrík D. (2006). Antioxidant enzymes in Spodoptera littoralis (Boisduval): are they enhanced to protect gut tissues during oxidative stress? *Journal of Insect Physiology.* 52:11-20;

Kukulies J., Komnick H. (1983). Plasma membranes, cell junctions and cuticle of the rectal chloride epithelia of the larval dragonfly *Aeshna cyanea. Journal of Cell Science*. 59:159-82;

Lajoie P., Nabi I.R. (2010). Lipid rafts, caveolae, and their endocytosis. *International Review of Cell and Molecular Biology.* 282:135-63;

Lane N.J., Flores V. (1988). Actin filaments are associated with the septate junctions of invertebrates. *Tissue Cell.* 20:211-17;

Leonardi M.G., Casartelli M., Parenti P., Giordana B. (1998) Evidence for a low-affinity, high-capacity uniport for amino acids in *Bombyx mori* larval midgut. *American Physiological Society.* 363:6119-98;

Liang J.F., Yang V.C. (2005). Insulin-cell penetrating peptide hybrids with improved intestinal absorption efficiency. *Biochemical and Biophysical Research Communications.* 335:734–38;

Lindgren M.E., Hallbrink M.M., Elmquist A.M., Langel U. (2004). Passage of cell penetrating peptides across a human epithelial cell layer *in vitro*. *Biochemical Journal.* 377:69–76;

Lindmark T., Kimura Y., Artursson P. (1998). Absorption enhancement through intracellular regulation of tight junction permeability by medium chain fatty acids in Caco-2 cells. *Journal of Pharmacology and Experimental Therapeutics*. 284:362-369;

Lindmark T., Nikkila T., Artursson P. (1995). Mechanism of absorption enhancement by medium chain fatty acids in intestinal epithelial Caco-2 cell monolayers. *Journal of Pharmacology and Experimental Therapeutics*. 275:958-64;

Lo Y.L., Huang J.D. (2000). Effects of sodium deoxycholate and sodium caprate on the transport of epirubicin in human intestinal epithelial Caco-2 cell layers and everted gut sacs of rats. *Biochemical Pharmacology.* 59:665-72;

Loeb M.J., Martin P.A., Narang N., Hakim R.S., Goto S., Takeda M. (2001). Control of life, death and differentiation in cultured midgut cells of the lepidopteran *Heliothis virescens*. *In Vitro Cellular & Developmental Biology-Animal*, 37: 348-352;

Loeb MJ, Hakim RS (1996) Insect midgut epithelium *in vitro*: an insect stem cell system. *Journal of Insect Physiology.* 42:1103-11;

Lv X-Y., Li J., Zhang M., Wang C-M., Fan Z., Wang C., Chen L. (2010). Enhancement of Sodium Caprate on Intestine Absorption and Antidiabetic Action of Berberine. *AAPS PharmSciTech.* 11:372-82;

Mahera S., Kennelly R., Bzik V.A., Baird A.W., Wang X., Winter D., Braydena D.J. (2010). Evaluation of intestinal absorption enhancement and local mucosal toxicity of two promoters. I. Studies in isolated rat and human colonic mucosae. *European Journal of Pharmaceutical Sciences.* 38;291–300

Mani B., Baltzer C., Valle N., Almendral J.M., Kempf C., Ros C. (2006) Low pH-dependent endosomal processing of the incoming parvovirus minute virus of mice virion leads to externalization of the VP1 N-terminal sequence (N-VP1), N-VP2 cleavage, and uncoating of the full-length genome. *Journal of Virology*. 80:1015-24;

Marechal V., Prevost M.C., Petit C., Perret E., Heard J.M., Schwartz O. (2001) Human immunodeficiency virus type 1 entry into macrophages mediated by macropinocytosis. *Journal of Virology*. Nov:11166-77;

Marrone, P. G. 2007 Barriers to adoption of biological control agents and biological pesticides. CAB Reviews: perspectives in agriculture, veterinary science, nutrition and natural resources, vol. 2, no. 15. Wallingford, UK: CABI Publishing.

Marsh M., McMahon H.T. (1999) The structural Era of endocytosis. *Science* 285:215-20;

Martin M.M., Barbehenn R.V. (1997). Permeability of the peritrophic envelopes of herbivorous insects to dextran sulfate: a test of the polyanion exclusion hypothesis. *Journal of Insect Physiology*. 43:243–49;

Matsuoka Y., Li X., Bennett V. (1998). Adducin is an in vivo substrate for protein kinase C: phosphorylation in the MARCKS-related domain inhibits activity in promoting spectrin-actin complexes and occurs in many cells, including dendritic spines of neurons. *Journal of Cell Biology.* 142:485-97.

McMahon H.T. and Boucrot E. (2011). Molecular mechanism and physiological functions of clathrin-mediated endocytosis. *Nature Reviews Molecular Cell Biology*. 12:517-33

Mettlen M., Pucadyil T., Ramachandran R., Schmid S.L. (2009). Dissecting dynamin's role in clathrin-mediated endocytosis. *Biochemical Society Transactions.* 37:1022-6;

Mitchell, D.J., Kim, D.T., Steinman, L., Fathman, C.G., and Rothbard, J.B. (2000). Polyarginine enters cells more efficiently than other polycationic homopolymers. **Journal** *of Peptide Research*. 56:318–25;

Moffett D.F., Koch A. (1992). Driving forces and pathways for H+ and K+ transport in insect midgut goblet cells. *Journal of Experimental Biology*. 172:403–15;

Morishita M., Kamei N., Ehara J., Isowa K., Takayama K. (2007). A novel approach using functional peptides for efficient intestinal absorption of insulin. *Journal of Controlled Release.* 118:177–84;

Mostov K.E., Verges M., Altschuler Y. (2000) Membrane traffic in polarized epithelial cells. *Current Opinion in Cell Biology*. 12:483-90;

Mueller J., Kretzschmar I., Volkmer R., Boisguerin P. (2008). Comparison of cellular uptake using 22 CPPs in four different cell lines. *Bioconjugate Chemistry* 19:2363–74;

Musacchio T., Torchilin V.P. (2011). Recent developments in lipid-based pharmaceutical nanocarriers. *Fronters in Bioscience.* 16:1388-412;

Mutuel D, Ravallec M, Chabi B, Multeau C, Salmon JM, Fournier P, Ogliastro M. (2010). Pathogenesis of Junonia coenia densovirus in Spodoptera frugiperda: a route of infection that leads to hypoxia. *Virology*. 403:137-44.

Nachman R.J., Teal P.E.A., Strey, **A**. (2002). Enhanced oral availability/pheromonotropic activity of peptidase-resistant topical amphiphilic analogs of pyrokinin/PBAN insect neuropeptides. *Peptides*. 23:2035–43;

Nava P., López S., Arias C.F., Islas S., González-Mariscal L. (2004). The rotavirus surface protein VP8 modulates the gate and fence function of tight junctions in epithelial cells. *Journal for cell science.* 117:5509-19;

Noirot C., Noirot-Timothèe C. (1998). Cell Associations. *Microscopic Anatomy of Invertebrates.* 11A:27-49;

Oerke, E. C., Dehne, H. W., Schoenbeck, F. &Weber, A. (1994). Crop production and crop protection: estimated losses in major food and cash crops. Amsterdam, The Netherlands: Elsevier Science Publishers B.V.

Oshima K., Fehon R.G. (2011). Analysis of protein dynamics within the septate junction reveals a highly stable core protein complex that does not include the basolateral polarity protein Discs large. *Journal of Cell Science.* 124:2861-71;

Palade G.E. (1953) Fine structure of blood capillaries. *Journal of Applied Physiology*. 24:1424.

Palermo L.M., Hueffer K., Parrish C.R. (2003). Residues in the apical domain of the feline and canine transferrin receptors control host-specific binding and cell infection of canine and feline parvoviruses. *Journal of Virology*, 77: 8915-23;

Pannabecker T.L., Aneshansley D.J., Beyenbach K.W. (1992). Unique electrophysiological effects of dinitrophenol in Malpighian tubules. *American. Journal of Phisiology.* 263:609-14;

Patel L.N., Zaro J.L., Shen W. (2007) Cell Penetrating Peptides: Intracellular Pathways and Pharmaceutical Perspectives. *Pharmaceutical Research*. 24: 1977-92;

Pereira-Leal J.B., Seabra M.C. (2001). Evolution of the Rab family of small GTP-binding proteins. *Journal of Molecular Biology.* 313:889-901;

Pèrez M., Barber A., Ponz F. (1997). Modulation of intestinal paracellular permeability by intracellular mediators and cytoskeleton. *Canadian Journal of Physiology and Pharmacology*. 75:287-92;

Potocky T.B., Menon A.K., Gellman S.H. (2003). Cytoplasmic and nuclear delivery of a TAT-derived peptide and a beta-peptide after endocytic uptake into HeLa cells. *The Journal of Biological Chemistry.* 278:50188–94;

Pretty, J. (2008). Agricultural sustainability: concepts, principlesand evidence. *Philosophical Transactions of the Royal Society B*. 363:447–65.

Pujals S., Giralt E. (2008). Proline-rich, amphipathic cell-penetrating peptides. *Advanced Drug Delivery Reviews.* 60:473-84;

Reise Sousa C., Howard J.E., Hartley R., Earley F.G.P., Djamgoz M.B.A.(1993). An insect epidermal cell line (UMBGE-4): structural and electrophysiological characterization. *Comparative Biochemistry and Physiology.* 106:759-67;

Richard J.P., Melikov K., Vives E., Ramos C., Verbeure B., Gait M.J., Chernomordik L.V., Lebleu B. (2003) Cell-Penetrating Peptides. A reevaluation of the mechanism of cellular uptake. *Journal of Biological Chemistry*. 278: 585-90;

Ritter B., Blondeau F., Denisov A.Y., Gehring K., McPherson P.S. (2004) Molecular mechanisms in clathrin-mediated membrane budding revealed through subcellular proteomics. *Biochemical Society Transactions*. ;32:769–73;

Rivers C.F., and Longworth J.F. (1972). A non-occluded virus of *Junonia coenia (Nymphalidae: Lepidoptera). Journal of Invertebrate Pathology.* 20, 369-370;

Rothbard J.B., Garlington S., Lin Q., Kirschberg T., Kreider E., McGrane P.L. (2000). Conjugation of arginine oligomers to cyclosporin a facilitates topical delivery and inhibition of inflammation. *Nature Medicine*. 6:1253–57;

Rousselle C., Clair P., Lefauconnier J.M., Kaczorek M., Schermann J.M., Temsamani J. (2000). New advances in the transport of doxorubicin through the blood-brain barrier by a peptide vector-mediated strategy. *Molecular Pharmacology.* 57:679–86;

Ryan, S.M., Mantovani, G., Wang, X., Haddleton, D.M., Brayden, D.J. (2008). Advances in PEGylation of important biotech molecules: delivery aspects. *Expert Opinion on Drug Delivery*. 5:371–83;

Sakai M., Imai T., Ohtake H., Azuma H., Otagiri M. (1997). Effects of absorption enhancers on the transport of model compounds in Caco-2 cell monolayers: assessment by confocal laser scanning microscopy. *Journal of Pharmaceutical Science*. 86:779-85;

Salama NN, Eddington ND, Fasano A. (2006). Tight junction modulation and its relationship to drug delivery. *Advanced Drug Delivery Reviews* 58:15-28;

Sandvig K., Pust S., Skotland T., van Deurs B. (2011). Clathrin-independent endocytosis: mechanisms and function. *Current Opinion in Cell Biology.* 23:413-20;

Sasaki K., Yonebayashi S., Yoshida M., Shimizu K., Aotsuka T., Takayama K. (2003). Improvement in the bioavailability of poorly absorbed glycyrrhizin via various non-vascular administration routes in rats. *International Journal of Pharmaceutics.* 265:95-102;

Scherer P.E., Okamoto T., Chun M., Nishimoto I., Lodish H.F., Lisanti M.P. (1996). Identification, sequence, and expression of caveolin-2 defines a caveolin gene family. *Proceedings of the National Academy of Sciences of the United States of America*. 93:131-5;

Scherer P.E., Lewis R.Y., Volonte D., Engelman J.A., Galbiati F., Couet J., Kohtz D.S., van Donselaar E., Peters P., Lisanti M.P.(1997). Cell-type and tissue-specific expression of caveolin-2. Caveolins 1 and 2 co-localize and form a stable hetero-oligomeric complex *in vivo. Journal of Biological Chemistry.* 272:29337-46;

Schipper N.G.M., Varum K.M., Artursson P. (1996). Chitosan as absorption enhancers for poorly absorbable drugs.1: Influence of molecular weight and degree of acetylation on drug transport across human intestinal epithelial (Caco-2) cells. *Pharmaceuticl Res*earch 13:1686-92;

Schmidt N., Mishra A., Lai G.H., Wong G.C.L. (2010). Arginine-rich cell-penetrating peptides. *FEBS Letters*. 584:1806–13;

Schweizer M., Peterhans E. (1999). Oxidative stress in cells infected with bovine viral diarrhoea virus: a crucial step in the induction of apoptosis. *Journal of General Virology.* 80:1147-55;

Seabra M.C., Mules E.H., Hume A.N. (2002) Rab GTPases, intracellular traffic and disease. *Trends in Cell Biology.* 8:23-30;

Sever S., Muhlberg A.B., Schmid S.L. (1999). Impairment of dynamin's GAP domain stimulates receptor-mediated endocytosis. *Nature*. 398:481-6;

Shi Y.L., Xu Y.F., Zhang H. (1994). Effect of Pinellia ternata lectin on membrane currents of mouse motor nerve terminals. *Science in China Series B:Chemistry.* 37:448-53;

Simons K., Fuller S.D. (1985). Cell surface polarity in epithelia. *Annual Review Cell Biology.*1:243-88;

Simons K., van Meer G. (1988). Lipid sorting in epithelial cells. *Biochemistry.* 27:6197-202;

Simons K., Ikonen E. (1997). Functional rafts in cell membranes. *Nature.* 387:569-72;

Simons K., Toomre D. (2000). Lipid rafts and signal transduction. *Nature Reviews Molecular Cell Biology.* 1:31-9;

Skaer H., Le B., Maddrell S.H.P., Harrison J.B. (1987). The permeability properties of septate junction in Malpighian tubules of *Rhonius. Journal of Cell Science*. 88:251-67;

Smith J., Wood E., Dornish M. (2004). Effect of chitosan on epithelial cell tight junction. *Pharmaceutical Research.* 21**:** 43-9;

Söderholm J.D., Öman H., Blomquist J., Veen J., Lindmark T., Olaison G. (1998). Reversible increase in tight junction permeability to macromolecules in rat ileal mucosa *in vitro* by sodium caprate, a constituent of milk fat*. Digestive Disease and Science*. 43:1547-52;

Spies AG, Spence KD (1985) Effect of a sublethal *Bacillus Thuringensis* crystal endotoxin treatment on the larval midgut of a moth, *Manduca sexta*: a SEM study. *Tissue Cell* 17: 379-94;

Staehelin L.A. (1974). Structure and function of intercellular junctions. *International Review of Cytology*. 39:191-283.

Swanson J.A., Watts C. (1995). Macropinocytosis. *Trends in Cell Biology.* 5:424-8;

Takahashi K., Murakami T., Yumoto R., Hattori T., Higashi Y., Yata N. (1994). Decanoic acid induced enhancement of rectal absorption of hydrophilic compounds in rats. *Pharmaceutical Research.* 11:1401-04;

Tepass U., Tanentzapf G., Ward R., Fehon R. (2001). Epithelial cell polarity and cell junctions in *Drosophila Annual Review of Genetics.* 35:747-84;

Terra W. R., and Ferreira C.. (1994). Insect digestive enzymes: properties, compartmentalization and function. *Comparative Biochemistry and Physiology.* 109:1–62;

Terry L.J., Shows E.B., Wente S.R. (2007). Crossing the nuclear envelope: hierarchical regulation of nucleocytoplasmic transport. *Science.* 318:1412–16;

Tomita M., Hayashi M., Awazu S. (1995). Absorption-enhancing mechanism of sodium caprate and decanoyl carnitine in Caco-2 cells. *Journal of Pharmacology and Experimental Therapeutics*. 272:739-743;

Traub L.M. (2003). Sorting it out: AP-2 and alternate clathrin adaptors in endocytic cargo selection. *Journal of Cell Biology.* 163:203-8;

Trung N.P., Fitches E., Gatehouse J.A. (2006) A fusion protein containing a lepidopteran-specific toxin from the South Indian red scorpion (Mesobuthus tamulus) and snowdrop lectin shows oral toxicity to target insects. *BMC Biotechnology*. 6: 18–29;

Tugyi R., Uray K., Iva´ n D., Fellinger E., Perkins A., Hudecz F. (2005). Partial D-amino acid substitution: improved enzymatic stability and preserved Ab recognition of a MUC2 epitope peptide. *Proceedings of the National Academy of Sciences of the United States of America* 102:413–18;

Tuma P.L., Hubbard A.L. (2003) Transcytosis: crossing cellular barriers. *Physiological Review.* 83:871-32;

Tung C.-H., Weissleder R. (2003). Arginine containing peptides as delivery vectors. *Advanced Drug Delivery Reviews*. 55:281–94;

Turbeck B.O. (1974) A study of the concentrally laminated concretions, 'spherites', in theregenerative cells of the midgut of lepidopterous larvae. *Tissue Cell*. 6:627-40;

Uchiyama T., Sugiyama T., Quan Y.S., Kotani A., Okada N., Fujita T., Muranishi S., Yamamoto A. (1999). Enhanced permeability of insulin across the rat intestinal membrane by various absorption enhancers: their intestinal mucosal toxicity and absorption-enhancing mechanism of n-lauryl-β-D-maltopyranoside*. Pharmaceutical Research* 51:1241-50;

Van Emden H. F. & Service M. W. (2004) Pest and vector control. Cambridge, UK: Cambridge University Press;

Van Huis, A., & Meerman, F. (1997). Can we make IPM work for resourcepoor farmers in sub-Saharan Africa? *International Journal of Pest Management,* 43(4) 313-320;

Velculescu V.E., Zhang L., Vogelstein B., Kinzler K.W. (1995). Serial analysis of gene expression. *Science.* 270:484-7;

Vendeville A., Ravallec M., Jousset F.X., Devise M., Mutuel D., López-Ferber M., Fournier P., Dupressoir T., Ogliastro M. (2009). Densovirus infectious pathway requires clathrin-mediated endocytosis followed by trafficking to the nucleus. *Journal of Virology.* 83:4678-89;

Verdurmen W.P., Bovee-Geurts P.H., Wadhwani P., Ulrich A.S., Hällbrink M., van Kuppevelt T.H., Brock R. (2011). Preferential uptake of L- versus D-amino acid cell-penetrating peptides in a cell type-dependent manner. *Chemistry & Biology.* 18:1000-10*;*

Vives E., Brodin P., Lebleu B. (1997) A truncated HIV-1 Tat protein basic domain rapidly translocated through the plasma membrane and accumulates in the cell nucleus. *Journal of Biological Chemistry* 272: 16010-17;

Wakeham D.E., Chen C.Y., Greene B., Hwang P.K., Brodsky F.M. (2003). Clathrin self-assembly involves coordinated weak interactions favorable for cellular regulation. *EMBO Journal.* 22: 4980-90;

Wang Y., Oberley L.W., Murhammer D.W. (2001). Evidence of oxidative stress following the viral infection of two lepidopteran insect cell lines. *Free Radical Biology and Medicine*.31:1448-55;

Warnock D.E., Schmid S.L. (1996). Dynamin GTPase, a force-generating molecular switch. *Bioessays*. 18:885-93. Review;

Way M-, Parton R.G. (1995). M-caveolin, a muscle-specific caveolin-related protein. *FEBS letters*. 376:108-12;

Whetstone P.A., Hammock B.D. (2007). Delivery methods for peptide and protein toxins in insect control. *Toxicon.* 49:576-96;

Wieczorek H., Weerth S., Schindlbeck M., Klein U. (1989) A vacuolar-type proton pump in a vesicle fraction enriched with potassium transporting plasma membranes from tobacco hornworm midgut. *Journal of Biological Chemistry*. 264:11143-48;

Wigglesworth V.B. (1943). The fate of haemoglobin in Rhodnius prolixus (Hemiptera) and other blood-sucking arthropods. *Proceedings of the Royal Society of London: Biological Sciences* 131:313–39;

Wigglesworth V. (1972). The principles of insect physiology. London: Chapman and Hall, pp. 488-89;

Woods D.F., Hough C., Peel D., Callaini G., Bryant P.J. (1996). Dlg protein is required for junctions structure, cell polarity and proliferation control in *Drosophila epithelia. Journal of Cell Biology.* 134:1469-82;

Wu M.V., Schulte J., Hirschi A., Tepass U., Beitel G.J. (2004). Sinuous is a Drosophila claudin required for septate junction organization and epithelial tube size control. *Journal of Cell Biology.* 164:313-23;

Wu V.M., Beitel G.J. (2004). A junctional problem of apical proportions: epithelial tube-size control by septate junctions in the Drosophila tracheal system. *Current Opinion in Cell Biology.* 16:493:9;

Yang F., Moss L.G., Phillips Jr G.N. (1996). The molecular structure of green fluorescent protein. *Nature Biotechnology.* 14:1246–51;

Yesylevskyy S., Marrink S.-J., Mark A.E. (2009). Alternative mechanisms for the interaction of the Cell-Penetrating Peptides Penetratin and the TAT peptide with lipid bilayers. *Biophysical Journal*. 97;40–9;

Youn Y.S., Chae S.Y., Lee S., Jeon J.E., Shin H.G., Lee K.C. (2007). Evaluation of therapeutic potentials of site-specific PEGylated glucagon-like peptide-1 isomers as a type 2 anti-diabetic treatment: Insulinotropic activity, glucose-stabilizing capability, and proteolytic stability. *Biochemical Pharmacology.* 73:84-93;

Youngblood D.S., Hatlevig S.A., Hassinger J.N., Iversen P.L., Moulton H.M. (2007). Stability of cell-penetrating peptide-morpholino oligomer conjugates in human serum and in cells. *Bioconjugate Chemestry*.18:50-60;

Zaro J.L., Shen W.-C. (2005). Evidence that membrane transduction of oligoarginine does not require vesicle formation. *Experimental Cell Research.* 307:164–73;

Zerial M., McBride H. (2001). Rab proteins as membrane organizers. *Nature Reviews Molecular Cell Biology.* 2:107-17;

Zhu W., Vandingenem A., Huybrechts R., Vercammen T., Baggerman G., De Loof A., Poulos C.P., Valentza A., Breuer M. (2001). Proteolitic breakdown of the Neb trypsin modulating oostatic

factor (Neb-TMOF) in the Haemolymph of different insects and its gut epithelial transport. *Journal of Insect Physiology.* 16:1193-202;

Ziegler A., Blatter X.L., Seelig A., Seelig J. (2003). Protein transduction domains of HIV-1 and SIV TAT interact with charged lipid vesicles. Binding mechanism and thermodynamic analysis. *Biochemistry*. 42:9185–94;

Ziegler A., Nervi P., Durrenberger M., Seelig J. (2005). The cationic cell-penetrating peptide CPP TAT derived from the HIV-1 protein TAT is rapidly transported into living fibroblast: optical, biophysical, and metabolic evidence. *Biochemistry.* 44:138–48;

Zorko M., Langel U. (2005). Cell-penetrating peptides: mechanism and kinetics of cargo delivery. *Advanced Drug Delivery Reviews*. 57:529–45;

Zornoza T., Cano M.J., Polache A., Granero L. (2003). Pharmacology of acamprosate: an overview. *CNS Drug Reviews.* 9:359-64;